COMBUSTION PROPERTIES OF RECLAIMED USED ENGINE LUBRICATING OIL BLENDED WITH SALMON FISH OIL AND WOODY PYROLYSIS OIL

By Daniel Alacoque

A Thesis submitted to the School of Graduate Studies in partial fulfillment of the requirements for the degree of

Master of engineering (M. Eng.) in Process Engineering

Faculty of Engineering and Applied Science
Memorial University of Newfoundland
St. John's, Newfoundland and Labrador

October 2018

ABSTRACT

Biofuels from animals and plants are being investigated as substitutes for petroleum fuel. In remote locations, fish and wood waste are recycled into biofuel and used engine lubricating oil (UELO) is recycled as fuel when re-refining is unavailable. This work focused on blending reclaimed UELO (R-UELO) with unrefined salmon oil from fishmeal process and pyrolysis oil from fast pyrolysis of woody biomass. Physical, chemical, and thermal properties were determined for nine mixtures of R-UELO, fish oil, and pyrolysis oil to screen blends for combustion. R-UELO/fish oil blends showed promising miscibility, viscosity, and heating values. R-UELO/pyrolysis oil blends showed poor miscibility, high water content, and low heating values. R-UELO, fish oil, and a 50% R-UELO/fish oil blend were combusted in a pilot-scale multi-fuel furnace and demonstrated straightforward ignition and combustion. Emissions were analyzed with GC-TCD. Implications of this study are optimistic for UELO generators in proximity to fish processing plants.

ACKNOWLEDGEMENTS

This research was made possible with the help of several people. First and foremost, I would like to thank my supervisor Dr. Kelly Hawboldt of Memorial University (MUN) for her guidance and encouragement. Dr. Hawboldt allowed me to lead my own research but steered me in the right direction when needed. Although Dr. Lesley James only co-supervised for one year, her support was appreciated until the very end. I would like to thank my father, Hubert Alacoque, who supported me with his expertise and advice as well as partially funded my research with his company Newfoundland Energy Services Limited (NESL). Jerome Gushue, manager of the Pit Crew Drive Thru, happily gave advice on everything practical and helped with UELO reclamation. Wade Murphy, Sheila Trenholm, and Julia Pohling in the Marine Bioprocessing Facility at the Marine Institute kindly walked me through fish oil production process. Part of this research was made possible by Dennis Cramm at MUN Technical Services who custom-built the pilot-scale multi-fuel furnace with his team. His guidance throughout furnace design, construction, and commissioning was a welcome addition to graduate school. Support from Peter Fransham at Abritech and Dmitry Chebotarenko at Nortec about the furnace was also greatly appreciated. I would like to give special thanks to my fellow grad students and work term students Anke Krutof, Jing Jing Cai, Sadegh Papari, Ibraheem Adioti, Chanciee Ossihou, and Joachim Urbanek who helped me with everything from laboratory knowledge to having fun. Finally, I would like to sincerely thank my friends, family, and partner Sarah Jane Johnson for providing me with unfailing support, continuous encouragement, and healthy distractions throughout my research.

TABLE OF CONTENTS

ABSTRACT ii

ACKNOWLEDGEMENTS iii

TABLE OF CONTENTS iv

LIST OF TABLES x

LIST OF FIGURES xiii

LIST OF ABREVIATIONS xvii

LIST OF SYMBOLS xix

LIST OF APPENDICES xx

1 INTRODUCTION 1

1.1 Background 1

1.2 Research objectives and scope 2

1.3 Contribution of the thesis 3

1.4 Thesis organization 4

PART 1 – LITERATURE REVIEW 5

2 USED ENGINE LUBRICATING OIL (UELO) 5

2.1 Background of used oil 5

2.2 Composition and properties of virgin engine lubricating oil 11

2.3 Composition and properties of UELO 15
2.4 UELO recycling 19
2.4.1 Acid/clay process 22
2.4.2 Vacuum distillation process 24
2.4.3 Solvent de-asphalting or solvent extraction process 25
2.4.4 Thin film evaporation process 30
2.4.5 Thermal de-asphalting process 31
2.4.6 Modern UELO recycling technologies 33
2.4.7 Comparison of UELO recycling options 34
3 FISH OIL FROM PROCESSING PLANT WASTE 40
3.1 Background of fish oil 40
3.2 Composition and properties of fish oil 42
3.3 Recovering fish oil from fish waste 47
4 PYROLYSIS OIL FROM WOODY BIOMASS 51
4.1 Background of pyrolysis oil 51
4.2 Composition and properties of pyrolysis oil 53
4.3 Pyrolysis of woody biomass 57
5 UELO, FISH OIL, AND PYROLYSIS OIL AS FUEL 61

5.1 Fuel properties 61

5.1.1 Density 62

5.1.2 Viscosity 63

5.1.3 Water and sediment content 63

5.1.4 Cold temperature performance 64

5.1.5 Sulfur content 64

5.1.6 Heating value 65

5.1.7 Thermal degradation and ash content 65

5.1.8 Flash point 66

5.2 Combustion and emission characteristics 67

5.3 UELO as fuel 68

5.4 Fish oil as fuel 74

5.5 Pyrolysis oil as fuel 79

5.6 Blends of UELO with fish oil or pyrolysis oil 81

PART 2 – BLENDING AND COMBUSTION EXPERIMENTS 83

6 EXPERIMENTAL METHODOLOGY 83

6.1 Production of reclaimed UELO 85

6.2 Production of pyrolysis oil from woody biomass 88

6.3 Production of fish oil from salmon fish waste 89
6.4 Blending 96
6.5 Physical properties 97
6.5.1 Density (specific gravity) 97
6.5.2 Kinematic viscosity 98
6.6 Chemical properties 100
6.6.1 Water content 100
6.6.2 Elemental analysis and sulfur content 101
6.7 Thermal properties 102
6.7.1 Heating value 102
6.7.2 Thermo-gravimetric analysis (TGA) and ash content 105
6.7.3 Flash point 107
6.8 Pilot-scale multi-fuel furnace experiments 108
7 RESULTS AND DISCUSSION 118
7.1 Blending 118
7.2 Physical properties 120
7.2.1 Density 120
7.2.2 Kinematic viscosity 124

7.3 Chemical properties 127
7.3.1 Water content 127
7.3.2 Elemental analysis and sulfur content 128
7.4 Thermal properties 129
7.4.1 Heating value 129
7.4.2 Thermo-gravimetric analysis (TGA) and ash content 131
7.4.3 Flash point 136
7.5 Pilot-scale multi-fuel furnace experiments 137
7.5.1 Selection of blends to proceed to furnace experiments 137
7.5.2 Combustion observations and measurements 139
7.5.3 Theoretical exhaust gas calculations 142
7.5.4 Micro GC analysis 146
8 CONCLUSIONS AND RECOMMENDATIONS 157
8.1 Conclusions 157
8.2 Recommendations for future work 159
9 REFERENCES 161
10 APPENDICES 176
10.1 Kinematic viscosity results 176

10.2 TGA data 177

10.3 Chamber and stack temperatures 187

10.4 Adiabatic flame temperature calculation 190

10.5 Theoretical combustion calculations 192

10.5.1 Combustion calculations with 0% excess air (stoichiometric) 193

10.5.2 Combustion calculations with 15% excess air 194

10.6 Micro GC results 195

LIST OF TABLES

Table 2-1: Categorization of European lubricating oil and used oil [16] 9

Table 2-2: Origin of main contaminants in UELO [10] 16

Table 2-3: Concentration of PAHs in a UELO sample from a 1993 study [29] 17

Table 2-4: Physical properties of UELO from various samples [10] 18

Table 2-5: Comparison of existing commercialized re-recycling processes [10, 16] 21

Table 2-6: Technologies, economics and operational requirements for various re-refining processes [17] 36

Table 2-7: Environmental aspects of various re-refining processes [17] 37

Table 3-1: Average composition of fish waste [6] 40

Table 3-2: Water and lipid composition of unrefined salmon fish oil [3] 42

Table 3-3: Thermal properties of unrefined fish oils [6] 43

Table 3-4: Viscosity measurements of various fish oils [4, 61] 45

Table 4-1: Chemical composition of pyrolysis oil [67, 69] 54

Table 4-2: Requirements for Grade G and D pyrolysis oil from ASTM D7544 55

Table 4-3: Process parameters and yields of slow and fast pyrolysis [67] 58

Table 5-1: Comparison of required properties for various fuel types 62

Table 5-2: Comparison of properties for diesel, heavy fuel, and UELO [10] 70

Table 5-3: Contamination of UELO, virgin engine oil, and heating fuels [21] 71

Table 5-4: Emission testing from diesel fuel and UELO [21] 72

Table 5-5: Comparison of fish oil properties from various studies [60, 83, 84] 74

Table 5-6: Difference of emissions of fish oil blends compared to diesel fuel [60, 84] 77

Table 6-1: Specific gravity of various components of UELO [10] *87*

Table 6-2: R-UELO and fish oil blends *96*

Table 6-3: R-UELO and pyrolsis oil blends *96*

Table 6-4: Division of groups of matter as per ASTM E1131 ..... *105*

Table 6-5: Setup parameters for Micro GC columns *117*

Table 7-1: Phase separation of R-UELO/fish oil and R-UELO/pyrolysis oil blends *118*

Table 7-2: Kinematic viscosities of the neat oil mixtures *124*

Table 7-3: Water content of neat fuels using Karl Fischer *127*

Table 7-4: Elemental analysis results for R-UELO, fish oil, and pyrolysis oil *128*

Table 7-5: HHV results of neat fuels *129*

Table 7-6: TGA results for R-UELO and fish oil blends (wt. %) *134*

Table 7-7: TGA results for R-UELO and pyrolysis oil blends (wt. %) *135*

Table 7-8: A summary of physical, chemical, and thermal properties *138*

Table 7-9: Burner settings and combustion properties for each fuel *140*

Table 7-10: Exhaust gas concentration from theoretical calculations *143*

Table 7-11: Adiabatic flame temperature of each fuel *144*

Table 7-12: Thermal conductivity of various gases [98] *147*

Table 7-13: Calibration data for Micro GC Column 1 ..... *148*

Table 7-14: Micro GC Column 1 PoraPLOT U results *151*

Table 7-15: Micro GC Column 2 CP-Sil 5 CB results *154*

Table 10-1: viscosity data from Brookfield rheometer with statistical analysis *176*

Table 10-2: Experimental purge gas data for TGA *177*

Table 10-3: Temperatures X, Y, and Z used in TGA analysis *177*

Table 10-4: Micro GC EZChrom Software integration results *195*

LIST OF FIGURES

Figure 2-1: Comparison of used oil collection and lost to environment [1] 6

Figure 2-2: Comparison of burned and re-refined used oil in selected regions [1] 8

Figure 2-3: Schematic diagram of the acid/clay process 24

Figure 2-4: Schematic diagram of the distillation process 25

Figure 2-5: Schematic diagram of the solvent de-asphalting process 29

Figure 2-6: Schematic diagram of the TFE process 31

Figure 2-7: Schematic diagram of the TDA process 32

Figure 3-1: Extraction of fish oil within the fishmeal production process [6] 48

Figure 4-1: Simple flow chart of pyrolysis process [65] 57

Figure 4-2: Fast pyrolysis of biomass into bio-char, bio-gas, and bio-oil [76] 59

Figure 6-1: Flow diagram of UELO reclamation process at the Pit Crew 85

Figure 6-2: Flow diagram of UELO centrifugal separation at the Pit Crew 86

Figure 6-3: Process flow diagram of fish waste processing procedure 89

Figure 6-4: Hobart grinder model 4146 at the MI bio-processing facility 90

Figure 6-5: GROEN jacked mixing kettle model RA at the MI bio-processing facility 91

Figure 6-6: Cooked fish waste pressed at the MI bio-processing facility 92

Figure 6-7: Press liquor placed in containers designed for the Beckman centrifuge 93

Figure 6-8: The Beckman centrifuge at MI bio-processing facility 94

Figure 6-9: Separation funnel at the MI bio-processing facility 94

Figure 6-10: Crude fish oil produced at the MI bio-processing facility 95

Figure 6-11: Gay-Lussac pycnometer filled with pyrolysis oil *97*

Figure 6-12: Rheometer and water bath circulator *99*

Figure 6-13: The custom-built pilot-scale multi-fuel furnace *109*

Figure 6-14: 20-L day tank equipped with two ball valves *110*

Figure 6-15: Gear pump with disposable fuel filter *111*

Figure 6-16: Nortec WB 40 burner *112*

Figure 6-17: Testo 325-1 flue gas analyzer (testo.com) *113*

Figure 6-18: Gas Alert MicroClip XT (gasalertmicroclipxt.com) *114*

Figure 6-19: 4-Channel Omega Handheld Thermometer (omega.com) *115*

Figure 6-20: Sample gas cylinder used to capture emission gases *116*

Figure 7-1: 50/50 vol. % blend of R-UELO and fish oil *119*

Figure 7-2: 3:1 by mass of pyrolysis oil:R-UELO *119*

Figure 7-3: Density measurements for all mixtures for three different temperatures *121*

Figure 7-4: Densities of R-UELO/fish oil mixtures at different volume fractions *122*

Figure 7-5: Densities of R-UELO/pyrolysis oil mixtures at different volume fractions *123*

Figure 7-6: Kinematic viscosity of R-UELO/fish oil mixtures at various temperatures *125*

Figure 7-7: Kinematic viscosity of R-UELO/pyrolysis oil mixtures at various temperatures *125*

Figure 7-8: Heating value (HHV) of R-UELO/fish oil and R-UELO/pyrolysis oil blends *130*

Figure 7-9: TGA analysis of fish oil and R-UELO blends under nitrogen and air atmosphere *132*

Figure 7-10: TGA analysis of pyrolysis oil and R-UELO blends under nitrogen and air atmosphere *133*

Figure 7-11: Column 1 results for diesel fuel *149*

Figure 7-12: Column 1 results for R-UELO *149*

Figure 7-13: Column 1 results for 50/50% R-UELO/fish oil blend *150*

Figure 7-14: Column 1 results for 100% fish oil *150*

Figure 7-15: Column 2 results for diesel fuel *152*

Figure 7-16: Column 2 results for R-UELO *153*

Figure 7-17: Column 2 results for 50/50% R-UELO/fish oil blend *153*

Figure 7-18: Column 2 results for 100% fish oil *154*

Figure 10-1: TGA curve of R-UELO with indicators of volatiles and ash content *178*

Figure 10-2: TGA curve of fish oil with indicators of volatiles and ash content *179*

Figure 10-3: TGA curve of pyrolysis oil with indicators of volatiles and ash content *180*

Figure 10-4: TGA analysis of F20 ..... *181*

Figure 10-5: TGA analysis of F50 ..... *182*

Figure 10-6: TGA analysis of F80 ..... *183*

Figure 10-7: TGA analysis of P20 ..... *184*

Figure 10-8: TGA analysis of P50 ..... *185*

Figure 10-9: TGA analysis of P80 ..... *186*

Figure 10-10: Temperature measurements for combustion of R-UELO and 100% fish oil *188*

Figure 10-11: Temperature measurements for combustion of R-UELO and 50% R-UELO/fish oil *189*

Figure 10-12: Column 1 results for diesel fuel *197*

Figure 10-13: Column 1 results for R-UELO *198*

Figure 10-14: Column 1 results for 50/50% R-UELO/fish oil blend *199*

Figure 10-15: Column 1 results for 100% fish oil *200*

Figure 10-16: Column 2 results for diesel fuel *201*

Figure 10-17: Column 2 results for R-UELO *202*

Figure 10-18: Column 2 results for 50/50% R-UELO/fish oil blend *203*

Figure 10-19: Column 2 results for 100% fish oil *204*

LIST OF ABREVIATIONS

A	Argon
APCR	Air Pollution Control Regulations
API	American Petroleum Institute
ASTM	American society for testing and materials
BDT	Bone dry tones
CFC-113	Trichloro-trifluoro-ethane
CH_4	Methane
CHNO	Carbon, hydrogen, nitrogen, and oxygen
CO	Carbon monoxide
CO_2	Carbon dioxide
DSC	Differential scanning calorimetry
EPA	Environmental Protection Agency
EU	European Union
FAO	Food and Agriculture Organization
FFA	Free fatty acid
FTIR	Fourier transform infrared spectroscopy
GC	Gas chromatography
GC-FID	Gas chromatography - Flame ionization detector
GC-MS	Gas chromatography - Mass spectrometry
GC-TCD	Gas chromatography - Thermal conductivity detector
GCV	Gross calorific value
H_2	Hydrogen
H_2S	Hydrogen sulfide
HC	Hydrocarbon
HCl	Hydrochloric acid
HHV	Higher heating value
HRMS	High-resolution mass spectrometry
HWMR	Hazardous Waste Management Regulations
KET	Ketone
KOH	Potassium hydroxide
KTI	Kinetics Technology International
LC	Liquid chromatography
LHV	Lower heating value
LPG	Liquefied petroleum gas
MEK	Methyl-ethyl-ketone
MI	Marine Institute

MP	Microwave pyrolysis
MUN	Memorial University of Newfoundland
N_2	Nitrogen
N_2O	Nitrous oxide
NaCl	Sodium chloride
NCV	Net calorific value
NESL	Newfoundland Energy Services Limited
NIR	Near-infrared spectroscopy
NL	Newfoundland and Labrador
NM2P	N-methyl-2-pyrrolidone
NMR	Nuclear magnetic resonance
NO	Nitric oxide
NO_x	Nitrogen oxides
O_2	Oxygen
PAH	Polycyclic aromatic hydrocarbons
PAO	poly-α-olefins
PCB	Polychlorinated biphenyl
PCT	Polychlorinated terphenyl
PM	Particulate matter
PUFA	Polyunsaturated fatty acid
R-11	Trichloro-trifluoro-methane
RFC	Recycled fuel for commercial boilers
RFO	Reprocessed fuel oil
R-UELO	Reclaimed used engine lubricating oil
SFA	Saturated fatty acid
SO_x	Sulfur oxides
SP	Stabilized petroleum
TAG	Triaclyglycerol
TBHQ	Tertary butylhydroquinone
TCD	Thermal conductivity detector
TDA	Thermal de-asphalting
TFE	Thin-film evaporation
TGA	Thermo-gravimetric analysis
UELO	Used engine lubricating oil
UF	Ultrafiltration
USA	United States of America
VI	Viscosity index
VOC	Volatile organic compound
WE	Wax ester

LIST OF SYMBOLS

ΔU_{BA}	Heat of combustion of benzoic acid calorimetry standard
$\Delta U_{capsule}$	Heat of combustion of calorimetry gelatin capsule
ΔU_g	Gross heat of combustion of calorimetry sample
ΔU_n	Net heat of combustion of calorimetry sample
ΔU_{wire}	Heat of combustion of calorimetry nichrome wire
e_1	Calorimetry correction for heat of formation of nitric acid
e_2	Calorimetry correction for heat of formation of sulfuric acid
e_3	Calorimetry correction for heat of combustion of nichrome wire
H	Mass percentage of hydrogen in calorimetry sample
m	Mass
m_{BA}	Mass of benzoic acid calorimetry standard
$m_{capsule}$	Mass of calorimetry gelatin capsule
m_{wire}	Mass of combusted calorimetry nichrome wire
T1	Pre-heat temperature 1 in preliminary fuel heating box
T2	Pre-heat temperature 2 in preliminary fuel heating box
ν	Settling velocity
V	Volume
ν	Kinematic viscosity
W	Energy equivalent of calorimeter
μ	Dynamic viscosity
ρ	Density
ω	Angular velocity

LIST OF APPENDICES

1	Kinematic viscosity results
2	TGA data
3	Chamber and stack temperatures
4	Adiabatic flame temperature calculation
5	Theoretical combustion calculations
5.1	Combustion calculations with 0% excess air (stoichiometric)
5.2	Combustion calculations with 15% excess air
6	Micro GC results

1 INTRODUCTION

1.1 Background

The quantity of used engine lubricating oil (UELO) generated per year is substantial, representing both an economic cost and environmental risk associated with transport, handling and storage, and disposal. For every one liter of lubricating oil purchased and used approximately 0.5 L of used oil is produced. For instance, of the 4.5 million tonnes of lubricating oil used in the USA in 2005, 2.6 million tonnes of used oil were generated [1]. There are two basic approaches to recycling UELO, as a fuel in combustion or in a re-refining process where base oil (mineral or synthetic) is recovered. For use as fuel, UELO must be reclaimed to meet fuel standards and/or combustion devices must be fit with pollution control. Re-refining processes require enormous UELO feedstock and include technologies such as acid/clay, vacuum distillation, solvent de-asphalting or solvent extraction, thin-film evaporation, and thermal de-asphalting.

Newfoundland Energy Services Limited (NESL) reclaims UELO into low quality heating fuel at two local oil change retail facilities that generate 120,000 L/year of UELO. The reclamation process is based on physical and thermal separation processes and creates a fuel product referred to as reclaimed UELO (R-UELO). UELO is heated to improve flow and separation and remove water and gasoline before being centrifuged and filtered.

Bio-oils are sourced from biomass and produced using pyrolysis, fermentation,

hydrolysis, and physical or chemical extraction processes, or made from synthetic oils to meet specific biodegradation and toxicity standards. Plant matter, animal waste, agricultural crops and residues, municipal waste, and industrial effluents are all possible feedstocks for deriving bio-oils [2]. Many vegetable and waste oils (tallow, cooking, and animal processing waste oils) can be used neat or in blends with minimal processing as a heating oil.

At Memorial University (MUN) we are investigating two bio-oils; oils extracted from fish processing waste and bio-oil from the pyrolysis of forestry residues (saw chips, bark and dust). Our work indicates theses bio-oils have very good flow and thermal properties [3, 4]. The overall objective of our work is to develop processing systems to recover value from waste, accounting for infrastructure limitations associated with smaller scale operations (sawmill operations and fish processing plants in remote regions of Canada) and regional needs (industry development through product development, offsetting fuel transport costs etc.).

1.2 Research objectives and scope

The focus of this study is exploring the possibility of "greening" the R-UELO by blending with bio-oils. Physical, chemical, and thermal properties must be established to assess the possibility of blending R-UELO with oils derived from biomass for use as heating fuel. There are several studies where various bio-oils are blended with petroleum-based fuels [5]. However, the bulk of these studies have focused on conversion of bio-oils to biodiesel and then blending them with petroleum-based diesel [6]. There is limited or

no work on the compatibility and application of UELO or R-UELO with either pyrolysis derived woody biomass or fish oil extracted from processing waste. The overall objective of this work is to investigate the application of R-UELO and bio-oil blends as fuel.

The specific objectives include:

1. Perform a literature review on UELO recycling for use as lubricating base oil or heating fuel, combustion properties of fish oil (produced from by-product of fishmeal processing plant), and combustion properties of pyrolysis oil from pyrolysis of woody biomass.
2. Characterize physical, chemical, and thermal properties of neat R-UELO, fish oil, and pyrolysis oil and blends of R-UELO/fish oil and R-UELO/pyrolysis oil to determine their suitability as fuel and to screen a subset for use in combustion experiments.
3. Determine combustion and emission properties of select R-UELO and bio-oil blends with custom-built pilot-scale multi-fuel furnace.

1.3 Contribution of the thesis

Many regions like Newfoundland and Labrador do not have access to re-refineries. However, these regions often have the capability to generate bio-fuels such as fish oil and pyrolsyis oil. This research shows the advantages of combusting reclaimed UELO with bio-fuels such as fish oil and pyrolysis oil. This study contributes to generators of UELO

in proximity to fish processing plants because reclaimed UELO and fish oil blends show promising combustion and emission characteristics.

1.4 Thesis organization

Part 1 of this thesis is a literature review of topics pertinent to the scope of the study. Chapter 2 provides a comprehensive review of UELO composition, properties, and recycling methods, including alternative re-refining methods such as solvent extraction, pyrolysis, and ultrafiltration. Chapter 3 reviews the literature on fish oil production from fish waste and gives an overview of fish oil composition and properties. Chapter 4 reviews the literature on pyrolysis oil production from woody biomass and describes pyrolysis oil composition and properties. Chapter 5 outlines literature regarding the use of UELO, fish oil, and pyrolysis oil as fuel and addresses fuel important fuel properties, and combustion and emission characteristics.

Part 2 of this thesis describes the experimental methodology and results, discusses them with reference to literature, and presents conclusions and recommendations. Chapter 6 describes the methodology used for production of R-UELO from UELO, fish oil from fish waste, and pyrolysis oil from woody biomass, blending of R-UELO with fish oil and pyrolysis oil, determination of physical, chemical, and thermal properties of the fuel blends, and combustion of the fuel blends in the pilot-scale multi-fuel furnace. Chapter 7 illustrates and provides a discussion of the experimental results. Finally, chapter 8 summarizes overall conclusions and recommends future work on the subject.

PART 1 – LITERATURE REVIEW

2 USED ENGINE LUBRICATING OIL (UELO)

2.1 Background of used oil

Poorly managed used oil can cause considerable environmental damage whereas properly managed used oil is a valuable resource that is used as a feedstock for lubricating base oils or other products such as fuels [7]. Used oil that is leaked, spilled, or improperly disposed into landfills and waterways may enter storm water runoff and adversely affect the environmental health of our water bodies [8]. Used oil municipal water treatment systems unnecessarily tax the treatment processes and can block pipes and flow lines. Since virgin lubricating oil accumulates metal particles from engine wear and contaminants that might damage the crankcase, used lubricating oil contains toxic quantities of heavy metals such as cadmium, chromium, arsenic, and zinc [9]. Furthermore, polycyclic aromatic hydrocarbons (PAHs) accumulate in used oil with increasing distance driven and are considered carcinogenic [8].

Pawlak et al. reviewed and compare used oil management programs in the USA, the European Union (EU), and Australia. Of the 4.5 billion kg of lubricating oil consumed in the USA, approximately 2.6 billion kg of the used oil is collected by used oil management programs and 660 million kg may be lost to the environment (i.e. disposed of outside of regulations). The 1.2 billion kg not accounted for is related to losses during

consumption (such as leakages from crankcase seals and gaskets) and combustion during its use [10, 1]. As seen in Figure 2-1, the numbers are similar in the EU and Australia. Estimates for China's yearly lubricating oil consumption in 2011 were in the range of 7.1 billion kg [11]. Of the 274 million kg of used oil per year in Pakistan, 60% is burned in sugar mills, cement factories, furnaces and low pressure boilers, 25% recycled in sub-standard re-refining and grease making, 10% disposed in sewers, and 5% disposed in landfills [9]. In 1990, the volume of crankcase oils sold in the automotive sector in Canada was estimated to be 372 million kg and in 1993, of an estimated 206.1 million kg of recoverable used oil, 50.6% is re-refined, 33.6% is used as fuel, 7.2% is disposed in landfills, 2.9% is used as dust suppression, 2.8% is disposed on land, 1.75% is disposed in sewers, and 1.08% is unknown [12]. As of 2015, the global consumption of lubricant oil was 35.6 billion kg [13].

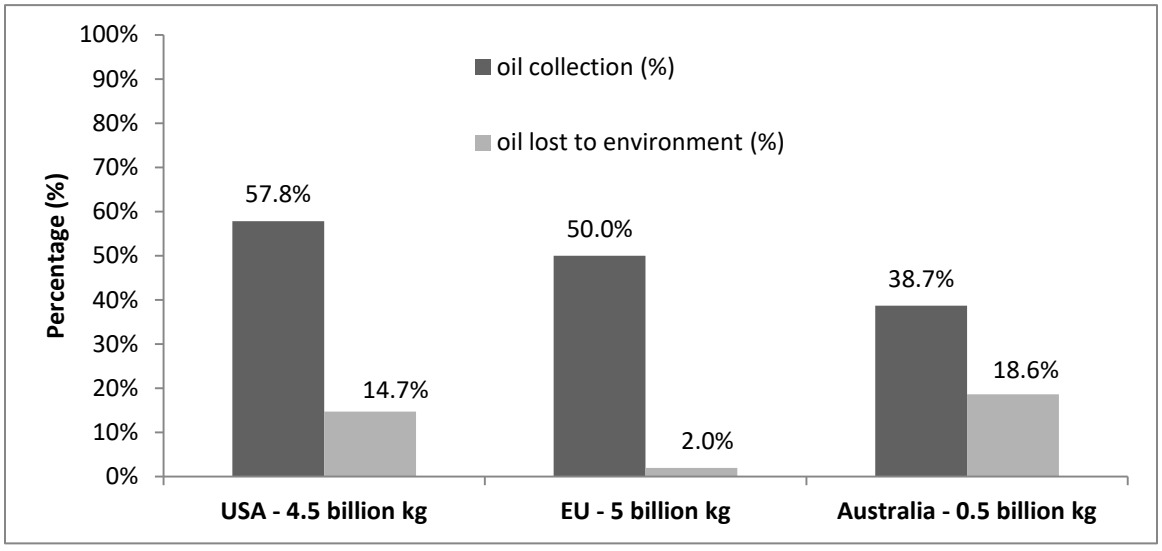

Figure 2-1: Comparison of used oil collection and lost to environment [1]

Due to continuing modernization of developing countries, consumption of lubricating oils is increasing and many developing countries do not properly manage their used oil [14]. Nwachukwo et al. outlined uses of used oil in Nigeria, a developing country without access to a re-refinery, as fuel for foundries, brick and lime kilns, bakeries, asphalt production plants, and diesel engines. Used oil is also added to low quality grease made from palm kernel oil and is even used by individuals as a timber-protecting agent, a protective medicine on livestock, a dust controller on floors, and a raw fuel in minor burning for heat or illumination [15]. In order to reduce the health and environmental impact of used oils, the development of proper management and sustainable recycling process is important [16].

The proper management of used oils is based on collecting used oils from recognized points of generation (factories, vehicle workshops, etc.) and residential or do-it-yourself sources and ensuring the used oil is recycled [17]. There are two steps in the collection of used oils. The first step is initial aggregation, collection, and storage either at the point of generation (industrial factories or vehicle workshops) or at public points of collection where individuals deposit their used oils. The second step is removal and transportation from collection locations. While most European countries have different laws and regulations for the collection of used oils, all maintain the basic principle that generators of used oil are responsible for safe collection, on-site storage, and eventual removal of used oils [16].

There are two basic approaches to reusing used oil, as a fuel in combustion or in a re-refining process where base oil (mineral or synthetic) is recovered. Figure 2-2

summarizes the percentage of burned versus re-refined used oil in USA, EU, and Australia.

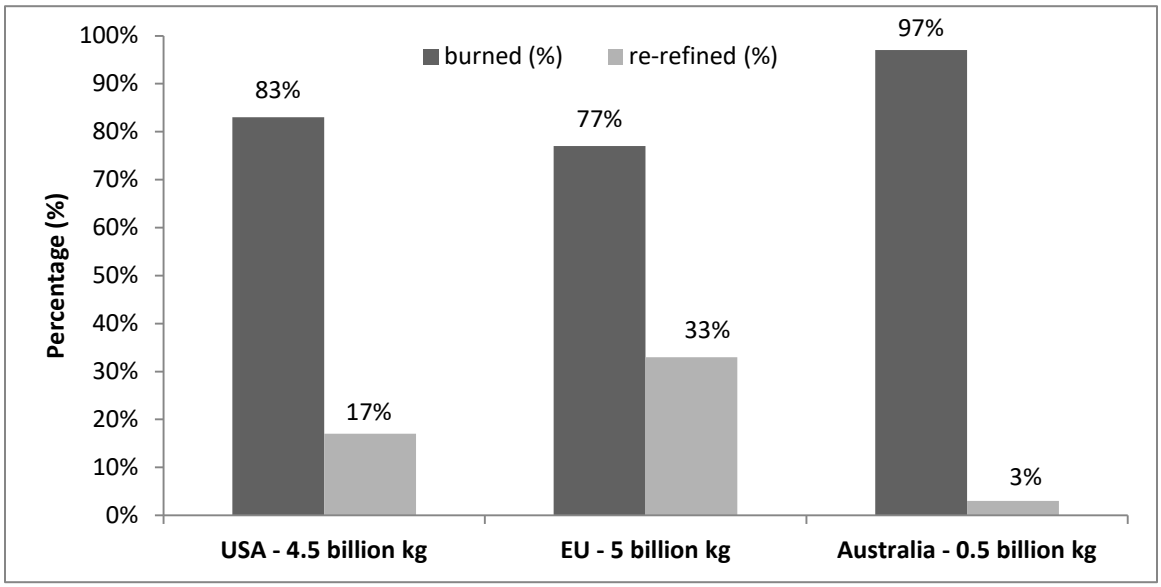

Figure 2-2: Comparison of burned and re-refined used oil in selected regions [1]

In the USA, the EU, and Australia in the early 2000s, over 80% of all recycled used oil was burned and less than 25% was re-refined [1]. However, choosing the best recycling option depends on the contamination of used oil. Based on contamination level and viscosity index, the European Re-refining Industry Association indicates only 60 to 65% of used oils are suitable for re-refining. The value decreases to 50% when taking into account difficulties in the re-refining process from dispersants added to lubricating oils, difficulties in the re-refining process from used synthetic lubricating oils, discarded biodegradable lubricating oils, and difficulties in the re-refining process from biodegradable lubricating oils [18]. Liu et al. studied re-refining, reclamation, and refortification (replenishing depleted additives) of seven types of mineral lubricating oils

and showed that while refortification was the most economic option, it was impossible to refortify lubricating oils containing excessive amounts of water, additive degradation and oxidation particles, or other oils [11].

Lubricants are divided into seven categories according to consumption (engine oils, gear and transmission oils, greases, metalworking oils, highly refined oils, other oils, and processing oils) and used oils are divided into three categories (black oils, light oils, and lost oils). Table 2-1 shows virgin lubricating oil categories and their respective used oil streams. Black engine oils or used engine lubricating oils (UELOs) represent more than 65% of used oils and are a desired feedstock for recycling facilities due to their homogeneity. Black industrial oils represent less than 10% and generally contain more additives (for high pressures and temperatures, etc.) and contaminants. Light industrial oils represent 25% and are often refortified or laundered for another purpose onsite (lower grade lubricating oil or heating fuel) [17].

Table 2-1: Categorization of European lubricating oil and used oil [17]

Category	Application	Type
Engine oils	engine oils for passenger cars; engine oils for commercial vehicles; multipurpose diesel oils; two-stroke engine oils; other engine oils	Black oil
Gear & transmission oils	automatic transmission fluids; automotive gear oils; industrial gear oils; hydraulic transmission oils; shock absorber oils	Black oil
Greases	automotive greases; industrial greases	Black oil
Metalworking	quenching oils; neat oils for metalworking; soluble oils for metalworking; rust prevention products	Lost oil
Highly refined oil	turbine oils; electrical oils	Light oil
Other oils	compressor oils; general machine lubricants; other oils for non-lubricating use	Black oil
Processing oils	process oils; technical white oils; medical white oils	Light oil

According to the Environmental Protection Agency (EPA), “used oil” and “waste oil” are not interchangeable terms as waste oil includes more than used oil. For example, bottoms from oil storage tanks are waste oil but not used oil because the material has never been in application. [19]. Definitions of used oil and waste oil vary across literature. This review examines current recycling methods and technologies for used engine lubricating oil (UELO), also called waste engine lubricating oil, black, used, or waste engine oil, used or waste motor oil, used or waste crankcase oil, used or waste automotive lubricating oil, and spent engine oil. While most reviews focus on medium to large scale recycling (2 to 250 million kg/year) [14, 16, 18, 10, 20, 21, 1], few consider the limited small scale recycling options of less than two million kg/year [10, 22, 9].

2.2 Composition and properties of virgin engine lubricating oil

Virgin engine lubricating oil is composed of 75 to 85 wt% hydrocarbons (referred to as base stock or base oil) and 15-25% performance enhancing additives (including zinc, magnesium, molybdenum, phosphorus, sulfur, and bromine) [8]. Conventional petroleum base oil (base oils derived from crude oil) make-up 90% of world-wide base oil production while synthetic base oils represent 10% [10]. Conventional crude oil refining produces base oil with hydrocarbon chain lengths of 20 to 40 carbon molecules while synthetic base oils such as poly-α-olefins (PAO) have much less variation in molecular structure and do not contain the impurities or waxes found in conventional mineral oil [8]. Although many vehicles recommend synthetic lubricating oils, cost/benefit analysis still indicates that petroleum base oils have the advantage. [23].

Additives used in crankcase oil include anti-oxidants, detergents, dispersants, anti-wear additives, additives improving viscosity index (VI), additives lowering pour point, anti-rust and anti-corrosion additives, and anti-foam additives [10]. The aging of lubricants occurs via oxidation of the lubricant molecules due to oxygen and/or thermal decomposition or cracking at high temperatures. The oxygen reaction is the more dominant process, and results in hydrogen abstraction of the hydrocarbon, and then the formation of an alkyl radical. The alkyl radical can react again with oxygen to form an alkylperoxy radical. This peroxy radical attacks another hydrocarbon to form a hydroperoxide and an alkyl radical which can again react with oxygen as described above. The oxidation reaction continues in this form, increasing the number of reactive free radicals, while also recombining as two radicals combine to yield a non-reactive,

non-radical species. The products of oxidation are responsible for the typical viscosity increase of aged oil as well as the varnish-like deposits and sludge [24]. The rate formation of oxidized products in base oil increases by a factor of two for every 10°C increase in temperature [23]. *Anti-oxidants* function either as radical inhibitors that neutralize the free radicals produced by oxidation, or as hydroperoxide destroyers that reduce the amount of hydroperoxide – an important reactant for the oxidation reaction.

Acids produced during oxidation and combustion of fuel form deposits on the surface of the engine crankcase at high temperature. *Detergents* are calcium or magnesium salts with high alkalinity that neutralize these acids. Fine particles such as dust, water, soot, wear metals, and solid oxidation residues also build up and settle on surfaces of the engine crankcase. *Dispersants* are surfactants that bind and stabilize particles in the lubricating oil to keep them off the engine surfaces [23].

Moving adjacent metal surfaces are separated only by a thin film of lubricant. With too much pressure between the metals, the lubricant can be pushed away, and quick deterioration of the surfaces can occur. *Anti-wear additives* form a solid film of protection by being adsorbed onto the interior surfaces of the engine crankcase. These additives include polar organic compounds such as alcohols, fatty esters, fatty amines, or acids, as well as organic compounds with sulfur, phosphorus, chlorine, nitrogen, oxygen, lead, or zinc molecules [23].

Engine lubricating oils are designed to have good cold flow properties and be sufficiently viscous at hot temperatures. The temperatures encountered range can range from as low as -40°C to sump temperatures of 100°C, to peak values of over 300°C [25]. The measure

of the change in viscosity at different temperatures or the viscosity index (VI) is dependent on climate and engine conditions. The higher the VI, the less viscosity changes with temperature. A low VI can be attributed to aromatic and volatile compounds. Additives that improve VI are very important to new lubricating oil, however, an engine lubricating oil with a high amount of VI improver additives will tend to degrade more rapidly. Additives that improve VI include alkyl-polymetacrylates and polymers made from olefins or hydrogenated diene/styrene [23, 26].

At low temperatures, paraffins in the base oil crystallize and produce a wax that obstructs the flowability of the lubricant. The highest temperature at which these waxes form is referred to as the pour point. *Additives that lower pour point* are similar to those that improve the VI and include polymetacrylates.

Corrosion of metal surfaces in the engine crankcase occurs in acidic conditions created by sulfur compounds in the base oil and acids produced from the oxidation of hydrocarbons. In order to mitigate corrosion, detergent additives neutralize acids and dispersant additives keep water in suspension. However, a*nti-rust and anti-corrosion additives* are also used. These additives are surface active materials with a high affinity for metal surfaces to prevent water and acids from contacting the metal surfaces. Typical anti-rust additives include sulfonates, phenols, and succinic acids [23].

Foaming of lubricants occurs due to detergents and dispersing additives. Foam is gas bubbles separated from each other by liquid or solid sheets called lamellae. It causes product loss when it overflows and inefficient dirt removal [27]. *Anti-foam additives*,

such as silicone and alkyl-polymetacrylate, are soluble in oil and drawn to the liquid/air interface where the weak surface tension inhibits the formation of bubbles [23].

During the use of any lubricating oil, the oil will age, deteriorate, lose lubricating efficiency, and collect foreign matter such as metal powder, fillings, other oils, and additives. As the oil becomes oxidized, its color becomes darker and the acidic conditions generate precipitate, oil sludge, varnish, and hard varnish [18].

2.3 Composition and properties of UELO

UELO contains similar hydrocarbons as virgin engine lubricating oil, such as aliphatic and aromatic hydrocarbons. However, UELO changes compositionally in the presence of incomplete combustion products, chemical additives, metals from engine wear, coolant contamination, and water [10]. UELO properties are determined by factors such as type of engine oil (conventional, semi-synthetic, synthetic, etc.), additive package used, kilometers traveled, type of fuel used (gasoline, diesel, etc.), age and state of engine, and storage and handling of UELO [23]. UELO contains the same base oil of virgin engine lubricating oil, the remaining fraction in UELO is a complex mixture of metals (barium, magnesium, boron, zinc, iron, chromium, aluminum, copper, tin, lead, vanadium, molybdenum, silicon, sodium, nickel, chlorine, and cadmium); water; gasoline; sulfur; antifreeze (glycol); breakdown products of various hydrocarbons (sludge and soot) [10].

Water is usually present in less than 1 wt% but can be as high as 10 wt%. Water content can be much higher than normal values because moisture and rain can enter through poor seals. Longer drive times and higher temperatures allow water to evaporate from engine oil while short trips and cold running result in more water contamination. UELO also forms stable water-oil emulsions where the oil fraction contains less than 1.0 wt% water and the water fraction contains more than 60 wt% water [10]. Many contaminants originate from the break-down of additives, friction wear of engine parts, unburned fuel, and combustion products. Table 2-2 summarizes concentrations of elements, sources of elements, and descriptions of origin.

Table 2-2: Origin of main contaminants in UELO [10]

Element	Concentra-tion (ppm)	Sources of elements	Description of origin
Aluminum	5-30	Stearate; hydroxystearate	Grease; piston wear; bearing wear
Calcium	2,000-3,000	Sulfonate; phenate; salicylate; calcium soap	Detergents; anti-oxidants; corrosion inhibitors; grease; atmospheric dust; cooling circuit water
Chlorine	300-600	Chlorinated paraffin; PCB	Anti-wear additives; hydraulic fluids; insulators; thermal fluid; pressure additives
Iron	50-100	Metal iron	Steel and cast iron corrosion
Boron	75-100	Borax; borates; boric acid	Anti-wear additives; pressure additives; dispersants; anti-oxidants; friction reducer; anti-corrosion additives
Copper	25-40	Dithiophosphate; naphthenate	Anti-oxidants; anti-wear additives; cuprous metals wear/corrosion
Magnesium	100-300	Sulfonate; phenate; salicylate	Detergents; light alloy wear/corrosion
Nickel	3-5	Metal nickel	Steel and cast iron wear/corrosion
Nitrogen	700-900	Succinimide; amines	Dispersants; anti-oxidants; polyureaadditives; grease
Sodium	50-100	Sulfonate; stearate; NaCl	antirust additives; grease soap
Phosphorus	800-1,200	Phosphate; Phosphonate; phosphate; dithiophosphate	Anti-wear additives; anti-oxidants; anti-corrosion additives; non-flammable hydraulic fluids
Lead	50	Dithiophosphate; naphthenate	Extreme pressure additives; grease soap; bearing wear
Sulfur	0.4-0.9 (%)	Phenate; sulfur; sulfonate; dithiophosphate; thiophosphonate; dithiocarbomate; polysulfur	Detergents; anti-oxidants; anti-wear additives; pressure additives; wear/corrosion
Silicon	30-120	Silicone	Base oil; antifoam additives; atmospheric dust; silicon steel wear/corrosion
Zinc	1,000-1,200	Dithiophosphate; dithiocarbamate	Anti-oxidants; anti-wear additives; anti-corrosion additives
Molybdenum	5-20	Molybdenum; sulfur; dithiocarbamate; phosphate	Anti-wear additives; pressure additives

Aromatics hydrocarbons are considered to be the most acutely toxic component of petroleum products [28, 29]. Light, mono-aromatics (one ring) include benzene, toluene, ethylbenzene, and xylenes. Aromatics with two or more rings are referred to as poly-cyclic aromatic hydrocarbons (PAHs). Table 2-3 below summarizes concentrations of PAHs in one sample of UELO from a 1993 study. However, there are no standard concentrations because PAH concentrations increase with increasing engine mileage. For example, pyrene has been found in concentrations ranging from 10.7 to 743 ppm [30]. There are also more modern techniques to examine aromatic hydrocarbon contamination in used oil [31].

Table 2-3: Concentration of PAHs in a UELO sample from a 1993 study [30]

Compound	Concentration (ppm)	Compound	Concentration (ppm)
Low-molecular-weight PAHs		**High-molecular-weight PAHs**	
Naphthalene	52	Fluoranthene	55
Acenaphthylene	1.5	Pyrene	120
Acenaphthene	3.7	Benz(a)anthracene	38
Fluorene	67	Chrysene	45
Phenanthrene	200	Benzofluoranthenes	46
Anthracene	22	Benzo(e)pyrene	32
Alkylated PAHs		Benzo(a)pyrene	15
C-1 naphthalenes	31	Perylene	1.1
C-2 naphthalenes	60	Indo(1,2,3-cd)pyrene	14
C-3 naphthalenes	80	Dibenz(ah)anthracene	1.5
C-4 naphthalenes	52	Benzo(ghi)perylene	72
C-1 phenanthrene	300	**High-molecular-weight PAHs**	
C-2 phenanthrene	300	Dibenzothiophene	1.9
C-3 phenanthrene	140		
C-4 phenanthrene	35		

Table 2-4 indicates physical properties of UELO from various samples. The density of UELO is higher than virgin engine lubricating oil and base engine lubricating oil (880 kg/m^3) because of the presence of oxidation products, metals, and contamination in UELO. Solids in UELO increase the specific gravity by approximately 0.007 every 1 wt% of solids [26, 23]. While the viscosity of UELO is less than the virgin engine lubricating oil, increases in viscosity indicate oxidation and polymerized products suspended or dissolved in the oil and decreases indicate contamination by lighter fuels such as gasoline [23, 26].

UELO contaminated with gasoline impacts properties such as flash point. For example, with 3.5% gasoline, the flash point will potentially reduce to below 55 °C. Virgin engine lubricating oil has a higher flash point because it contains additives to increase flash point and UELO has a lower flash point due to oxidation contamination and fuel combustion products [26, 23].

Table 2-4: Physical properties of UELO from various samples [10]

Property	UELO from service station in 2001	UELO from ESSO 15W40 in 2001	UELO from semi-synthetic lubricating oil in 2005
Density (kg/m^3)	904	889	878
Viscosity at 40 °C (cSt)	123.7	99.44	84.21
Viscosity at 100 °C (cSt)	17.16	13.44	13.04
Water content (wt. %)	0.5	0.14	0.37
Ash content (wt. %)	1.24	1.02	-
Flash point (°C)	180	208	214
Pour point (°C)	-39	-36	-

2.4 UELO recycling

UELO with little to no reprocessing is either burned alone or blended with other fuel oils in small-scale space heaters, or UELO is re-processed or reclaimed into higher quality heating fuels [32]. Reclaiming separates less desirable bottoms fraction containing metals, ash, sediments, and additives by physical separation, dehydration/defueling, and/or vacuum distillation [16, 17]. However, recycling used oil into base oil is a preferred recycling option because it conserves crude oil resources, minimizes waste, and reduces damage to the environment. As well, recycling into base oil conserves more energy than recycling into fuel because the energy required to produce re-refined base oil is one-third of the energy required to produce virgin lubricating oil from crude oil [16].

Recycling of used lubricating oils into base oil is subdivided into laundering of lightly contaminated oils and re-refining of heavily contaminated oils. Laundering is applied to hydraulic and cutting industrial oils and produces a small amount of by-product. Re-refining is applied to UELO and similar black oils and produces more waste by-products [15, 16]. Selection of a UELO recycling process depends on technology limitations (such as operating conditions, feedstock, product quality, and process development stage), economics (such as water costs, energy costs, equipment capital, and operational costs), and environmental protection requirements (such as PCB removal, acidic sludge generated, residual oil sludge produced, and hazardous chemicals used) [14].

While conventional crude oil refineries deal with high tonnage (100 to 300 million kg/year), the UELO re-refining industry is characterized by 20 to 80 million kg/year due

to cost and logistics of UELO collection and transportation [10]. UELO re-refining process technologies generally follow the same four steps: dewatering/defueling, de-asphalting, fractionation, and finishing. They usually differ with respect to the de-asphalting and finishing methods [14, 18]. Dewatering/defueling involves filtration, settling, centrifugation, and dehydration to separate water, light fuel, and sediment based on boiling point, specific gravity, and solubility [14]. Filtration is accomplished by coarse filters (150 to 250 microns). Settling separates contaminants such as water and sediments. However, dissolved and emulsified water and particles chemically bound to the oil are not removed. Centrifugation also separates water and sediments. Dehydration uses low temperature distillation (160 to 180 °C) to remove antifreeze, water, and other solvent but does not remove oxidation products or carbonaceous residues [10]. De-asphalting is accomplished by solvent addition with a solvent such as sulfuric acid, thin-film evaporation (TFE) separation, or thermal de-asphalting (TDA). Fractionation involves separation based on the boiling points of different components and the goal is generally to select or eliminate a certain material. Finishing involves either clay finishing or hydro-treatment to remove foreign components such as chlorine, nitrogen, oxygen, and sulfur.

There are five main UELO de-asphalting technologies commonly used in the industry: acid/clay, vacuum distillation, solvent extraction, TFE, and TDA. Table 2-5 compares technology and annual tonnage for commercialized re-refining processes in standard order of dehydration/defueling, de-asphalting, fractionation, and finishing unless indicated with letters.

Table 2-5: Comparison of existing commercialized re-recycling processes [10, 17]

Process	Dehydration defueling	De-asphalting	Fractionation	Finishing	Tonnage Feed (million kg/year)	Base oil yield (%)
Meinken (acid/clay)	Atmospheric Distillation	Sulfuric Acid Treatment	-	Clay treatment	Small (2 to 10)	63%
Ecohuile	Atmospheric distillation	Vacuum distillation		Clay treatment	Medium (25 to 50)	50 %
Vaxon	Vacuum Distillation (2 stages)	Vacuum distillation (3rd stage)		Chemical treatment	Medium (25 to 50)	65 - 70%
Mohawk/ Evergreen Oil	Atmospheric distillation	TFE	Vacuum distillation	Hydro-finishing	Medium (25 to 50)	72%
Sotulub	Atmospheric distillation	TFE	Vacuum distillation	Clay treatment or hydro-finishing	Medium (25 to 50)	
Recyclon-Degussa	Atmospheric distillation	TFE	Vacuum distillation	Clay treatment or hydro-finishing	Medium (25 to 50)	
KTI	Atmospheric distillation	TFE	Vacuum distillation	Clay treatment or hydro-finishing	Large (50+)	
Snamprogetti	Atmospheric distillation	Propane extraction	Vacuum distillation	Hydro-finishing	Medium (25 to 50)	74%
Interline	(b) Atmospheric distillation	(a) Propane extraction	(c) Vacuum distillation	Clay treatment or hydro-finishing	Medium (25 to 50)	79%
Bechtel	Atmospheric distillation	NM2P extraction	Vacuum distillation	-	Extra Large (200+)	
Revivoil (TDA)	Atmospheric distillation	TDA		Clay treatment or hydro-finishing	Large (50+)	74 - 77%

The Meinken process uses the standard sulfuric acid and clay treatment and the Ecohuile process is based on vacuum distillation. However, the Meinken and Ecohuile processes were developed in the 1960s and newer processes dominate the market today. The Vaxon process includes many vacuum distillation columns in series with chemical treatment. The Mohawk/Evergreen Oil process, Sotulub process, Recyclon-Degussa process, and Kinetics Technology International (KTI) process all use the TFE technology. The Snamprogetti process, the Bechtel process, and the Interline process all use solvent extraction and while Snamprogetti and Interline use propane as the solvent, Bechtel uses n-methyl-2-pyrrolidone (NM2P) as the solvent. The Revivoil process uses thermal de-asphalting (TDA) [17, 10].

2.4.1 Acid/clay process

The acid/clay process using sulfuric acid has been used for many decades to recycle UELO due to the low start-up cost and ability to handle low feedstock (5 to 10 million kg/yr). Concentrated sulfuric acid (92%) is mixed with UELO at 30-50°C for 15-30 minutes. Suspended particles and polar compounds such as oxidized and acidic products, residual additives, and associated byproducts will form sludge that can be separated using porcelain clay or aluminum silicate clay. The oil is then filtered to yield base lubricating oil [10]. The quantity of sulfuric acid added depends on upstream treatments: 12 to 16 wt% sulfuric acid for dehydrated UELO, 6 to 8 wt% sulfuric acid for dehydrated and thermally treated UELO, 3 to 5 wt% sulfuric acid for dehydrated, and propane extracted or ultrafiltered UELO, 2 to 3 wt% sulfuric acid for dehydrated, thermally treated, and

propane extracted or ultrafiltered UELO. Thermal treatment (250 to 400 °C) partially destroys dispersing additives so that acid/clay treatment is more effective. When added properly to the acid/clay process, thermal treatment can reduce sulfuric acid consumption by 50%. Figure 2-3 is a flow chart of the process.

The acid/clay process is only allowed in a few developing countries and is being phased out globally due to concerns of the sulfurous sludge byproduct. Although the malodorous sludge is combustible, high sulfur concentration, oxide emissions, and formation of metal sulfates prevent its direct combustion. As well, the acid/clay process is unable to treat modern multi-grade and synthetic lubricating oils and does not remove enough asphaltic impurities. [33, 34, 35, 10].

However, researchers are studying novel methods to improve the process. Newer methods can decrease the volume of acid sludge produced, acid sludge can be incinerated at high temperatures, environmental and health hazards of acidic sludge can be decreased by neutralization, and novel methods are reusing acidic sludge as fertilizers, explosives, paint, ink, chemical fibers, and industrial detergent [36, 14]. Another option is using glacial acetic acid instead of sulfuric acid which produces comparable base oil with less environmental impact. While sulfuric acid is strong enough to modify the molecular structure of base oil, glacial acetic acid showed almost no reaction [26].

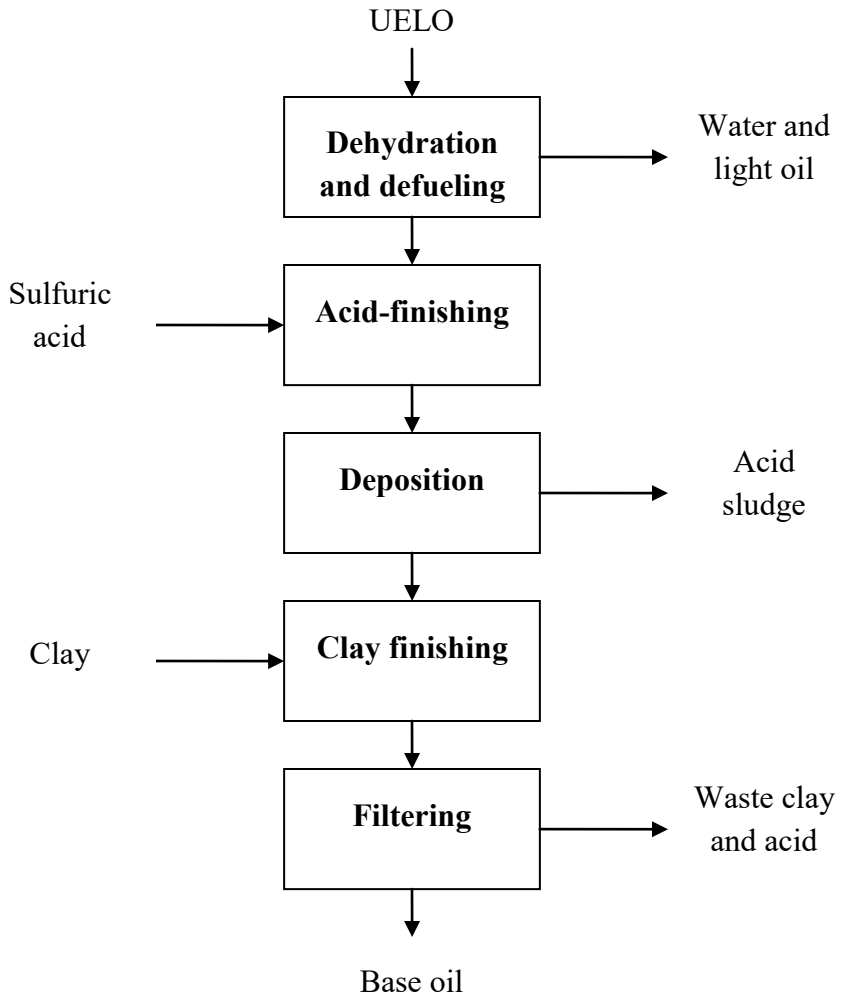

Figure 2-3: Schematic diagram of the acid/clay process

2.4.2 Vacuum distillation process

Vacuum distillation is used for UELO so that heavier molecules can be distilled at temperatures low enough to prevent cracking. Preventing cracking requires column temperatures to not exceed 400 °C if the column residence time is only a few minutes, while a temperature of 250 to 280 °C is the maximum if the residence time is 30 to 60 minutes [10]. Vacuum distillation produces a light fraction (water, gasoline, and light

additive byproducts), a diesel oil fraction, and a residual fraction of about 6 wt%. The process usually includes a first stage dehydration to remove water, light hydrocarbons, and other light constituents [14, 18]. Figure 2-4 is a schematic diagram of the distillation process.

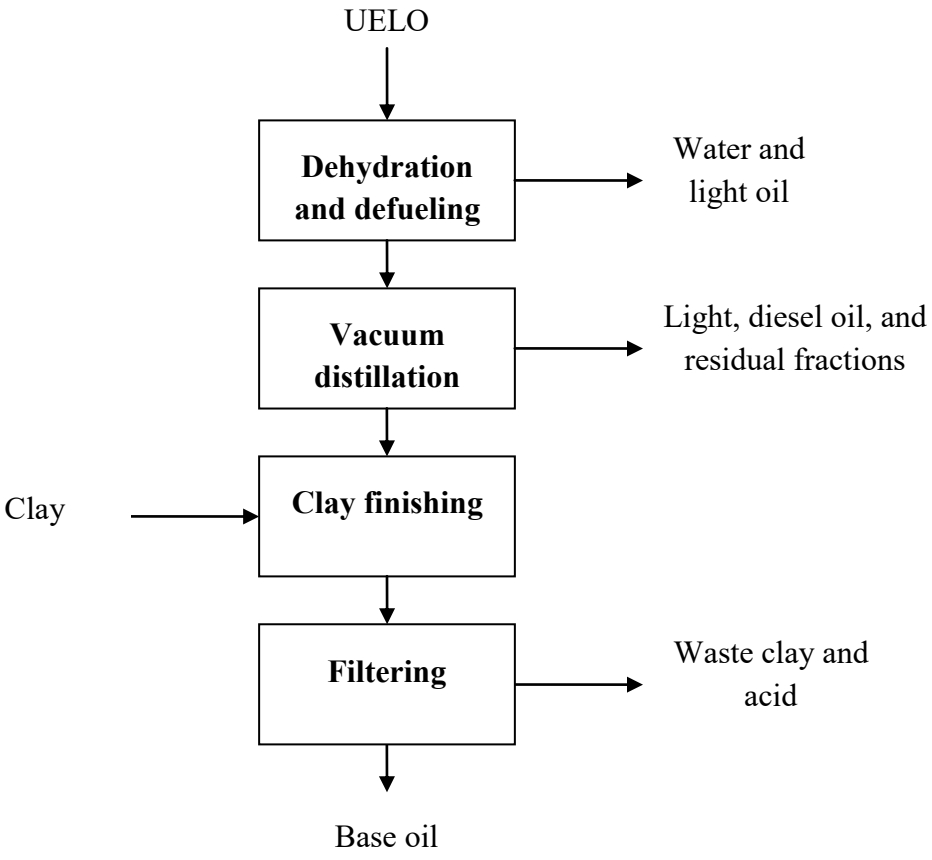

Figure 2-4: Schematic diagram of the distillation process

2.4.3 Solvent de-asphalting or solvent extraction process

Solvent extraction separates suspended compounds such as asphalt, metals, and resin in UELO by contact with a solvent. Centrifugation recovers a base oil raffinate of saturated

hydrocarbons and an extract of undesired aromatic components from additives and carbonaceous impurities. The average yield of base oil from the process is 0.7 kg per kg of UELO [21]. Extraction operating condition (temperature and pressure) and solvent ratio are important factors affecting yield. Optimal operating conditions are generally close to the critical point of the solvent (for example 42 bar and 95 °C for propane), but are always in the liquid phase [10]. Although propane is the most common solvent, a hydro-finishing step is still needed to remove impurities [37].

Elbashir et al. compared the extraction performance of the solvents 2-propanol, 1-butanol, and methyl-ethyl-ketone (MEK) at different solvent-to-oil ratios and temperatures. MEK, followed by 2-propanol and 1-butanol, achieved the highest yields and as temperature increased from 20 to 50 °C, the yield increased [38].

Rincon et al. studied the effect of pressure (30 to 60 kg/cm^2) and temperature (20 to 140 °C) using liquid and supercritical propane as a solvent. While lower pressures were more effective at removing oxidation products, pressure changes did not have an effect on removing metallic compounds. Removal of metallic and oxidation compounds increased as temperature increased as long as the propane remained a liquid. Optimum conditions were 30 kg/cm^2 and 90 °C [39].

Rincon et al. compared yield and quality using three alcohol solvents (2-propanol, 2-butanol, and 2-pentanol) and two ketone solvents (MEK, and methyl-n-propyl-ketone) at solvent-to-oil ratios of 2:1, 5:1, 7:1, 10:1, and 15:1 and for 30 minutes at atmospheric pressure and 25 °C. In terms of base oil yield, solvent-to-oil ratios could be increased up to a point at which the yield stabilized and that the extraction yields increased with

solvent molecular weight. However, the ratios at which stabilization occurred were smaller with ketones than for alcohols. The stabilization of ketones occurred at a lower ratio due to smaller viscosities and solubility parameters. All the solvents removed more impurities with increasing solvent-to-oil ratios. While alcohols and ketones of equal carbon numbers removed similar amounts of metallic and oxidation compounds, alcohols were slightly more efficient than ketones in removing polymeric additives [40].

Hamad et al. compared liquefied petroleum gas (LPG) condensate and stabilized petroleum (SP) condensate at solvent-to-oil ratios of 1:1 to5:1 at standard pressure and temperature. They found that a solvent-to-oil ratio of 4:1 was optimal and that SP condensate resulted in a higher removal ratio than LPG condensate. With a yield of 79%, the extraction process using the SP condensate showed characteristics that were competitive with existing UELO recycling processes [28].

Rincon et al. studied the effect of pressure (40 to 145 kg/cm^2) and temperature (25 to 95 °C) on the use of liquid and supercritical ethane as a solvent. Although pressure did not have an effect on the removal of metallic compounds, yield increased with pressure and removal of oxidation products decreased with pressure. Similarly to propane, as long as ethane remained a liquid, the removal of metallic and oxidation compounds increased with temperature. Optimum operating conditions of 100 kg/cm^2 and 40 °C produced a base oil yield of 72% [37].

Al-Zahrani and Putra studied solvent extraction of UELO at different solvent-to-oil ratios (0.8:1 to 5:1) and different temperatures (23, 30, 40, and 50 °C) for 2-propanol, 1-butanol, MEK, trichloro-trifluoro-ethane (CFC-113), and tri-chloro-fluoro-methane (R-

11). While higher temperatures resulted in higher base oil yield and lower oil losses, it was found R-11 had the lowest percent oil losses at a solvent-to-oil ratio of between 1.22:1 to 1.4:1, followed by CFC-113, MEK, 1-butanol, and 2-propanol [41].

Filho et al. compared the solvent extraction of UELO at standard temperature and pressure of 1-butanol, tert-butanol, 2-propanol, and ethanol at solvent-to oil ratios of up to 60:1. It was concluded that 1-butanol recovered base lubricating oil most efficiently, with a yield of 86% and an oil-to-solvent ratio of 1:3 [42].

Mohammed et al. looked at the performance of six extracting solvents (n-hexane, 1-butanol, petroleum ether, 1-hexanol, carbon tetra chloride, and acetone) with solvent-to-oil ratios of 1:1 to 4:1, atmospheric pressure and temperature, as well as the effect of potassium hydroxide (KOH) to enhance flocculation. The results showed that 1-butanol removed the most sludge, followed by n-hexane, petroleum ether, 1-hexanol, carbon tetrachloride, and then acetone. They also found that the solvent-to-oil ratio of 3:1 produced the highest percent sludge removal and that the addition of KOH significantly improves the sludge removal and decreases oil loss [43].

Shown in Figure 2-5, solvent de-asphalting includes removal of volatiles, water, and light hydrocarbons by dehydration, solvent extraction of the dehydrated oil, and a finishing that includes vacuum distillation followed by clay treatment or hydro-finishing to remove color and odor [20].

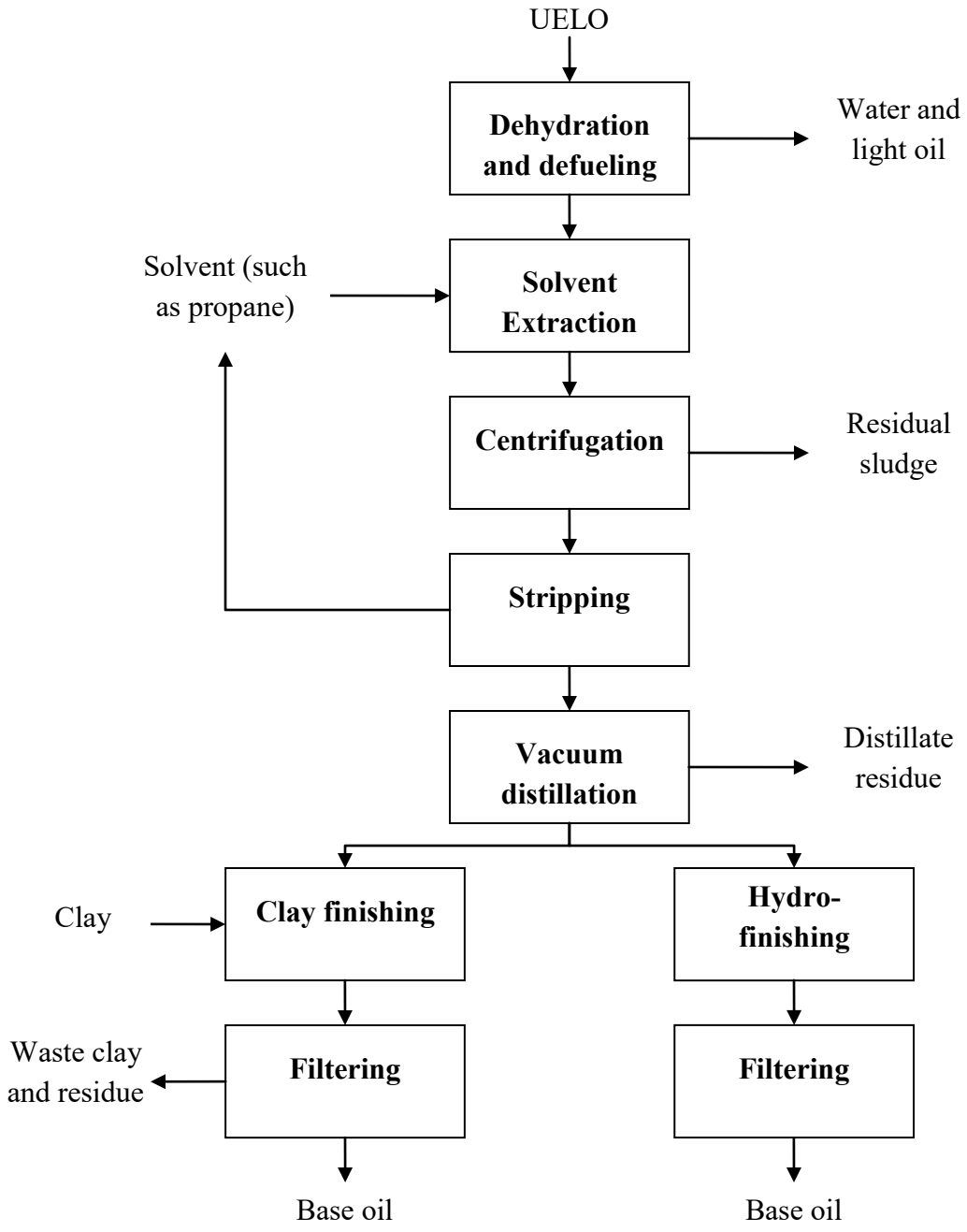

Figure 2-5: Schematic diagram of the solvent de-asphalting process

2.4.4 Thin film evaporation process

Thin film evaporation (TFE) is a vacuum distillation technique that consists of a cylindrical column warmed by thermal fluid in double walls. UELO flows downward along a series of sweeping blades in the internal wall that control falling oil film thickness. TFE allows precise control of residence time for a given oil flow rate and temperature transfer. UELO is distilled under vacuum at high temperature (over 400 °C) and short residence time to separate fractions while avoiding degradation and cracking [10]. UELO undergoes dehydration and defueling followed by TFE paired with either hydro-finishing, clay finishing, or solvent finishing to remove organic components such as nitrogen, oxygen, and sulfur [18, 14]. Figure 2-6 summarizes the process [18, 14].

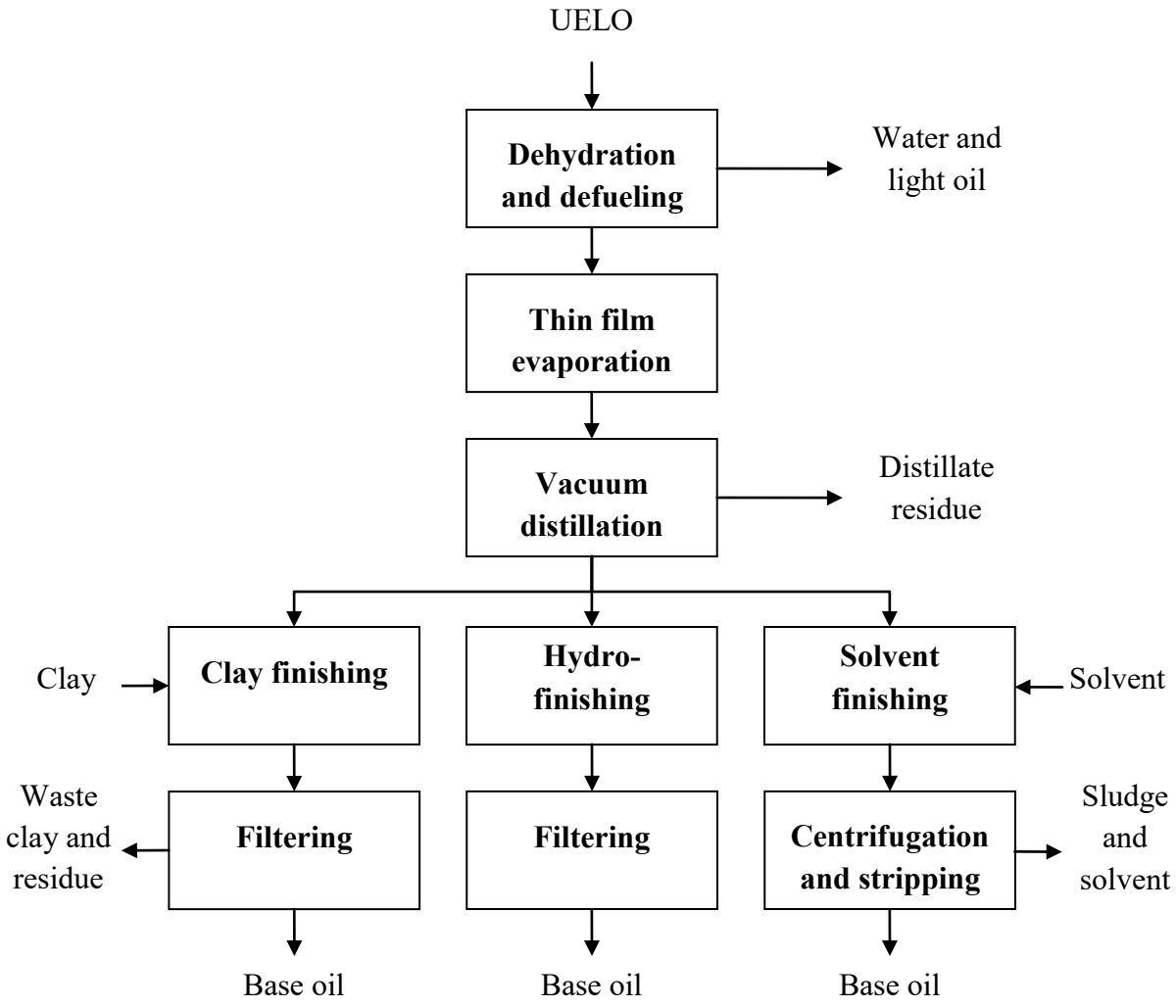

Figure 2-6: Schematic diagram of the TFE process

2.4.5 Thermal de-asphalting process

Thermal de-asphalting (TDA) process starts with dehydration/defueling followed by distillation at a vacuum pressure of 2 KPa and 360 °C in a high-efficiency packed column with a high liquid recycle flow to avoid internal fouling [10]. Ash remains at the bottom

and UELO is separated into light oil, base oil, and heavy oil. TDA finishes with hydro-finishing or clay finishing [14, 18].

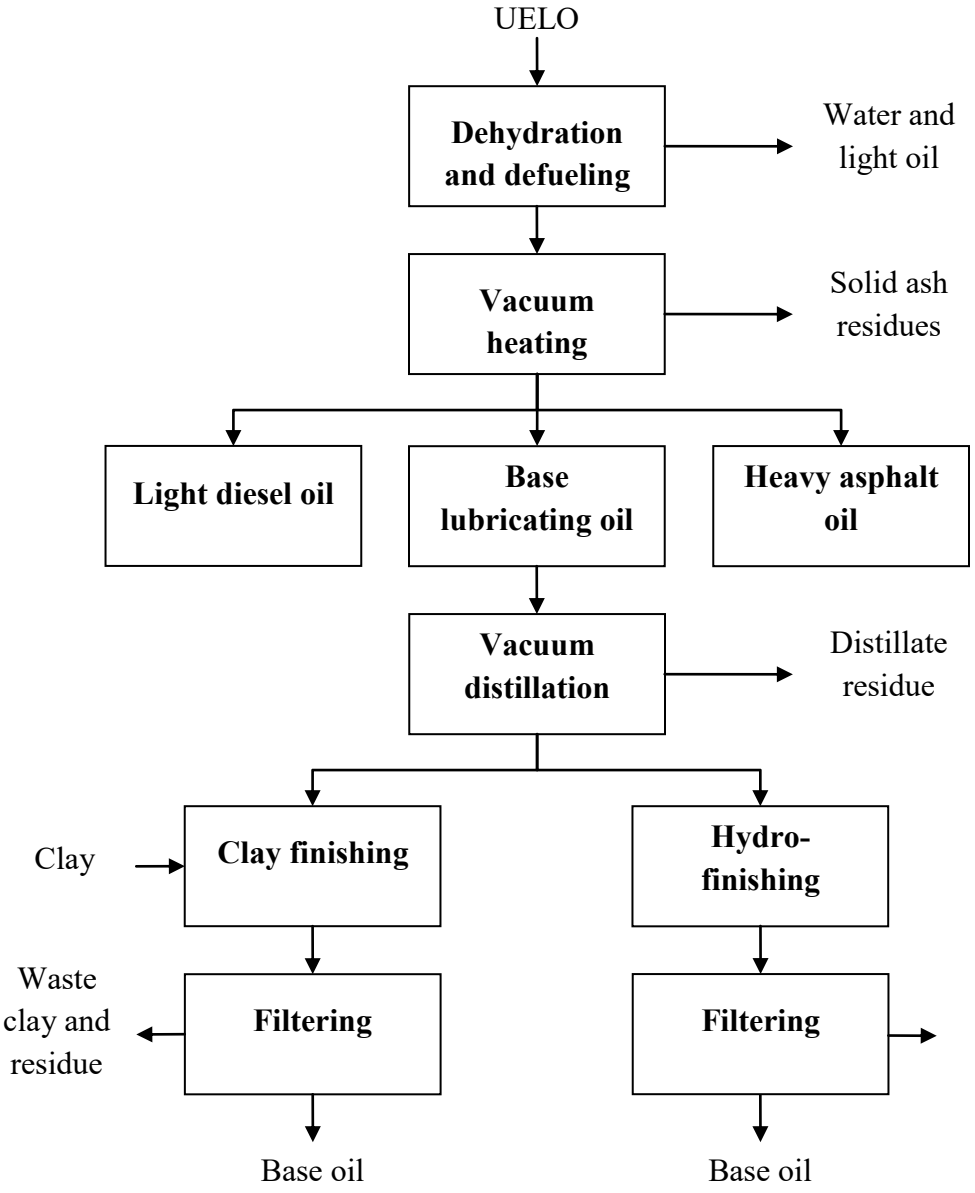

Figure 2-7: Schematic diagram of the TDA process

2.4.6 Modern UELO recycling technologies

UELO recycling has a short history and new recycling technologies are currently studied. Ultrafiltration (UF) and pyrolysis are viable options for recycling UELO however neither technology has been proven in large scale. UF is achieved by a tangential liquid flow that creates differential pressure across a membrane. The membrane contains small pores (10 to 1000 angstroms) and requires periodic back washes and chemical washes to prevent plugging. Membranes are assembled in modules that minimize pressure drops and achieve high surface to volume ratios [10]. In the 1970s and 80s, UF using organic membranes could only withstand temperatures of 100 °C and the viscosity of UELO was reduced with addition of a solvent such as hexane which rendered the process uneconomical due to costly solvent recovery. Now, inorganic membranes can withstand temperatures up to 300 °C. However, different thermal expansions of the process materials (steel bearing structure and carbon membranes) can cause ruptures in the membrane [10]. Recently, adding 10 wt% supercritical CO_2 and increasing pressure to 15 MPa can reduce UELO viscosity and avoid solvents or high temperatures [44, 10].

Pyrolysis is the thermal decomposition of organic matter in the absence of oxygen or when significantly less oxygen is present than required for complete combustion. Pyrolysis is being developed to recycle UELO and other used oils because of the potential valorization of pyrolysis products (non-condensable gases, condensable liquids, and carbonaceous residue). Numerous studies since 1997 have looked at operating parameters and yields [45, 46, 47, 48, 49, 50, 51, 52, 53]. As recently as 2010, studies have shown that microwave pyrolysis (MP) improves cracking reactions produced higher

gaseous and liquid yields [54, 55, 56, 57]. MP is when a bed of particulate carbon is heated by microwaves to facilitate heat transfer.

2.4.7 Comparison of UELO recycling options

While UELO combustion is specifically discussed in section 5.3, many studies propose that direct burning of untreated UELO in unregulated small space-heaters or small industrial boilers and furnaces without pollution control is the environmentally worst option next to disposal and should be forbidden [58, 7, 16].

A 2003 study ranked UELO recycling options in descending order of environmental and economic benefits as re-refining in a lubricating oil refinery, re-refining in a dedicated facility, reprocessing into fuel, burning untreated, and disposal. UELO re-refining integrated into existing lubricating oil refineries minimizes costs for equipment, facilities, utilities, and pollution control compared to re-refining in a dedicated facility. Reprocessing into fuel and burning untreated in space heaters are sometimes ranked equally because while burning untreated avoids the energy consumption and environmental impacts of transporting and reprocessing, the uncontrolled emissions from space heaters may be more harmful that burning reprocessed UELO at an industrial site equipped with pollution control equipment. Disposal loses the energy value of the UELO and creates environmental problems [16].

Kanokkantapong et al. studied global warming potential, acidification potential, heavy metals emission, and eutrophication potential for six used lubricating oil management options. Two options were recycling into lubricating oil (acid/clay treatment and solvent

extraction process) and four options were recycling into fuel oil (small boiler, boiler vaporizing burner, boiler atomizing burning, and cement kiln). Although acid/clay treatment performed poorly in acidification potential, it performed well in global warming and eutrophication potentials. Of the burning options, the cement kiln showed the lowest environmental impact due to the high temperature and long residence time of combustion [21].

Hsu et al. compared UELO re-refining processes in terms of technologies used, economic efficiency, and environmental impact. Table 2-6 describes re-refining technologies and their economic and operational requirements and Table 2-7 compares the environmental concerns [18].

Table 2-6: Technologies, economics and operational requirements for various re-refining processes [18]

Re-refining process	Dehydration defueling	De-asphalting	Fractionation	Finishing	Energy demand	Yield	Product quality	Cost	Scale (million kg)
Acid/clay process	Vacuum distillation or centrifugation	Adding sulfuric acid and clay	-[a]	-[a]	Low	63%		Low	2 - 10
Distillation process	Vacuum distillation	Adding acid and clay to distillation	-[a]	-[a]	High	50%		Low	25
Solvent extraction + clay finishing	Vacuum distillation	Solvent extraction	Vacuum distillation	Clay finishing	High	65 - 70%	API GROUP I	High	25
Solvent extraction + hydro-finishing	Vacuum distillation	Solvent extraction	Vacuum distillation	Hydro-finishing	High	74%	API GROUP II	High	60
TFE + hydro-finishing	Vacuum distillation	TFE	Vacuum distillation	Hydro-finishing	High	72%	API GROUP II	High	50 - 80
TFE + clay finishing	Vacuum distillation	TFE	Vacuum distillation	Clay finishing	High	72%	API GROUP II	High	100
TFE + solvent finishing	Vacuum distillation	TFE	Vacuum distillation	Solvent finishing	High	72%	API GROUP II	High	100
TDA + clay finishing	Vacuum distillation	TDA	Vacuum distillation	Clay finishing	High	74 - 77%	API GROUP II	High	100 - 180
TDA + hydro-finishing	Vacuum distillation	TDA	Vacuum distillation	Hydro-finishing	High	74 - 77%	API GROUP II	High	100 - 180

[a] acid/clay and distillation processes do not have fractionation and finishing steps because they represent processes used in developing countries

Table 2-7: Environmental aspects of various re-refining processes [18]

Re-refining process	Water consumption	Operating temperature	Residual oil sludge	Harmful chemicals	Secondary pollution
Acid/clay process	Low	Low	High	Sulfuric acid	High
Distillation process	Low	High	High	Sulfuric acid	High
Solvent extraction + clay finishing	Low	High	High	Volatile organic solvent	High
Solvent extraction + hydro-finishing	Moderate	High	High	Volatile organic solvent	Low
TFE + hydro-finishing	Moderate	High	Low	None	Low
TFE + clay finishing	Moderate	High	Low	None	Low
TFE + solvent finishing	Moderate	High	Low	Volatile organic solvent	Low
TDA + clay finishing	High	High	Low	None	Low
TDA + hydro-finishing	High	High	Low	None	Low

Comparing the re-refining processes in Table 2-6 and Table 2-7 (acid/clay, distillation, solvent de-asphalting, TFE with hydro-finishing, clay finishing, and solvent finishing, solvent extraction with hydro-finishing, and TDA with clay finishing and hydro-finishing), operating costs and required temperature of the acid/clay process is comparatively lower than other processes. Water required for TDA process is higher than other processes. Environmentally speaking, the acid/clay process increases PAH in the base oil product by 4 to 17 times compared to base oil obtained from crude oil. Processes

with clay finishing do not decrease PAH levels and processes with hydro-finishing decrease PAH levels [14].

A 2001 European report compared economics of seven existing re-refining processes (acid/clay process, TFE + clay finishing, TFE + solvent finishing, TFE + hydro-finishing, TDA + clay finishing, TDA + hydro-finishing, and PDA + hydro-finishing) at three different capacities (small, medium, and large or 35, 50, and 80-100 million kg/year). The study found that while economic success of a re-refinery is highly dependent on the selling price of re-refined base oil and UELO feed cost, the breakeven point of UELO collection supply is between 60 and 80 million kg per year [17]. Durrani et al. studied UELO management options in Pakistan and proposed re-refining as the preferred method. However, feasibility depends on the economies of scale as millions of kilograms per year of UELO are needed for re-refining. Solvent extraction was recommended as the most suitable re-refining method because it generates sludge that can be used for print media such as ink [9].

The same 2001 European report compared eight UELO recycling life cycle analysis studies and found recycling processes that replaced petroleum fuels from being burned or base oil from being refined from crude oil had the largest effect on environmental impact. In fact, ranking environmental impacts of different methods for recycling UELO into fuel options was dependent on which petroleum fuel was being replaced. In effect, for almost all environmental impacts considered (consumption of fossil resources, contribution to climate change, contribution to acidifying potential, emission of VOC, waterborne emissions, and solid waste), burning in cement kilns (where used oil would replace fossil

fuels) is more preferred to burning in an asphalt plant (where used oil would replace gas oil). Also, depending on the impacts considered, re-refining may be preferred to burning in an asphalt plant and it is unclear whether burning in a cement kiln is more favorable to re-refining [17].

In fact, there is a considerable debate on whether UELO should be re-refined into base oil or reused as fuel [58]. A 2001 study on waste oil management in Lebanon analyzed re-refining into lubricating oil, re-processing into fuel oil that is low in water and sediment content, and controlled destruction in the form of high-temperature incineration in cement kilns [29]. It was proposed 70% of waste oil be re-refined and the remaining burned in cement kilns to minimize potential atmospheric emissions associated with highly contaminated waste oil [29].

3 FISH OIL FROM PROCESSING PLANT WASTE

3.1 Background of fish oil

Approximately 50% of landed fish can end up as "waste" depending on the species, product, and processing techniques [6]. For instance, the 130 billion kg of fish caught in 2006 resulted in 64 billion kg of fish waste according to the Food and Agriculture Organization (FAO) [59]. Fish waste is composed mainly of lipids, proteins, metals, carbohydrates, and moisture, and its composition depends on harvesting region, season, species, and processing. Lipids are the major component of fish oil and recovery of oil from fish waste varies with species and fish part [6]. Table 3-1 below shows compositions of various fish wastes.

Table 3-1: Average composition of fish waste [6]

Type of fish	Fish part	Protein (wt. %)	Moisture (wt. %)	Ash (wt. %)	Lipid/oil (wt. %)
Pink salmon	Liver (6 – 16% of fish)	18.6	76.6	1.5	3.3
Walleye pollock	Liver (9 – 32% of fish)	7.77	41.0	0.89	50.3
Pacific halibut	Liver	13.4	73.3	1.3	12.0
Cod	Viscera	22.1	-	1.8	74.4
Salmon	Viscera	-	59.4	-	24.1
Catfish	Whole viscera (33.6% of fish)	14.7	50.1	-	33.6
	Digestive tract	13.4	79.5	-	5.8
	Liver	11.4	74.9	-	8.8
	Gallbladder	2.6	88.9	-	0.3
	Visceral Storage (10% of fish)	1.3	8.0	-	90.7
	Fillet	14.4	74.4	-	9.0
	Nugget	13.5	71.2	-	14.7

Recovery of fish waste occurs at some fish processing plants however this is not the case for plants in many remote communities. For example, the fish processing industry in Atlantic Canada produces 418,000 t/y of fish waste and in Newfoundland and Labrador (NL), 35,000 t/y of fish waste from capelin, herring, mackerel, seal, and farmed salmanoids is generated in the form of viscera, bones, liver, belly trimmings, kidney, skin, and blood. With the exception of seal processing plants and fish meal plants (two sites) the fish waste is mixed with wastewater and discharged into the ocean [60].

Fishmeal plants are of particular interest because a major by-product is fish oil that can be used for a variety of purposes depending on quality: for metal processing and leather treatment, and for production of margarine, peanut butter, ink, soap, rubber, lubricants, paints, varnishes, fire retardants, fungicidal derivatives, rust inhibitors, candles, water repellents, and plasticizers. In 2002, 56% of fish oil was used as aqua feed, 30% as edible oil, 12% for industrial purposes, and 2% in the pharmaceutical industry [6].

In Alaska for example, approximately 28 million kg of fish oil are produced annually. Fish oil is used onsite as an alternative fuel for industrial boilers or diesel engines and also transported offsite for use in animal feed, aquaculture, human dietary supplement, and for the manufacture of pharmaceuticals and cosmetics. Given the remoteness of most fish processing plants, fish oil is most commonly burned as fuel onsite or locally because storage and transportation are made difficult by degradation of the oil [61].

3.2 Composition and properties of fish oil

Fats and oils derived from biomass such as plants, animals, or microbes, are known as lipids. Classes of lipids include triaclyglycerol (TAG), straight chain hydrocarbons (HC), steryl esters (SE), ethyl esters (EE), methyl esters (ME), ethyl ketones (EK), methyl ketones (MK), glycerol ethers (GE), free fatty acids (FFA), alcohols (ALC), sterols (ST), diacylglycerols (DAG), acetone mobile polar lipids (AMPL), and phospholipids (PL) [3]. Table 3-2 shows the concentration of water and lipid classes in unrefined salmon fish oil from the fishmeal process from a previous study.

Table 3-2: Water and lipid composition of unrefined salmon fish oil [3]

Component	Concentration (wt. %)
Water	1.0 ± 0.1
Total Lipids	87.2 ± 4.4
HC	1.8 ± 0.3
EK	0.0 ± 0.0
TAG	53.3 ± 10.1
FFA	3.2 ± 0.7
ST	17.4 ± 2.9
DAG	0.0 ± 0.0
AMPL	6.5 ± 0.2
PL	4.8 ± 3.0

TAG is comprised of three fatty acids with a glycerol molecule and a high TAG content in bio-oil is an indication of quality. On the other hand, high FFA levels (>5%) limit the bio-oil's use as a fuel due to high acidity. Bio-oils can have up to a 20% FFA content from the decomposition of TAG and other complex lipid classes due to steam, salts,

chemicals, and processing heat. Approximately 95 wt. % of a TAG molecule is fatty acid content and the types of fatty acids can vary depending on the carbon chain length and the level of saturation and unsaturation of the carbon bonds. Three types of fatty acids include saturated (SFA), monounsaturated, and polyunsaturated (PUFA) fatty acids [6]

Fish oil contains TAGs in the range of 65 – 99 wt. % depending on the extraction method with fatty acids of carbon lengths varying between 14 and 22 and with multiple double bonds present. As often advertised in human supplements, fish oil contains a high amount of PUFAs in the form of n-3 or ω-3 fatty acids [6].

Thermal properties of fish oil are important for determining storage conditions, end use, and stability. Differential scanning calorimetry (DSC) analysis is used to measure melting point, enthalpy of melting, and specific heat capacity of a sample. Table 3-3 below shows the thermal properties of unrefined pollock oil, red salmon oil, and pink salmon oil. The melting point decreases with each purification step with deodorized oil showing the highest melting point reduction. However, enthalpy of melting range was not affected [6].

Table 3-3: Thermal properties of unrefined fish oils [6]

Type of fish	Melting range (°C)	Enthalpy of melting (kJ/kg)	Specific heat capacity (kJ/kg °C) at 20 °C
Unrefined pollock oil	-69.5 – 14.2	36.9	1.5 – 3.2
Unrefined red salmon oil	-69.6 – -0.36	40	0.8 – 1.6
Unrefined pink salmon oil	-64.7 – 20.8	39	1.3 – 2.3
Crude catfish oil	-46.2 – 21.2	74.1	1.69
Degummed catfish oil	-45.9 – 11.5	74.7	1.96
Neutralized catfish oil	-44.3 – 11.4	75.1	1.97
Bleached catfish oil	-47.1 – 9.9	79.3	1.91
Deodorized catfish oil	-52.3 – 8.0	84.3	1.83

Thermo-gravimetric analysis (TGA) measures the loss of mass due to decomposition as a steady temperature ramp is applied to a sample up to 800 °C and is an indirect measure of volatiles, ash, and distribution of components based on boiling point. The mass loss in fish oil is due to decomposition and interaction between molecules such as phospholipids, complex metals, minerals, FFAs, peroxides, and other oxidation products [6]. High initial temperature of decomposition indicates stability and the mass remaining at 800 °C indicates ash content. Adeoti et al. observed the onset weight loss temperature of fish oil and salmon oil as 187 °C and 229 °C respectively [4]. Analyses of unrefined pollock oil, waste fish oil, and unrefined salmon oil show large mass losses (up to 95 wt. %) between 200 and 450 °C. and unrefined pollock oil shows complete decomposition at 535 °C [4]. Thermal decomposition was higher in refined fish oil than in crude fish oil because with less impurity, there is more heat available for the evaporation of volatiles and decomposition of components [62, 4].

Rheological properties such as viscosity, cloud point, and pour point are parameters that determine transportation and handling requirements. Viscosity is an important indicator of flow characteristics that increases with decreasing temperature for fish oil and is measured using a rheometer [6]. Table 3-4 below shows viscosity measurements for various fish oils.

Table 3-4: Viscosity measurements of various fish oils [4, 62]

Type of fish oil	Temperature (°C)	Viscosity (Pa s)
Waste fish oil	20	0.144
	30	0.065
	40	0.017
	50	0.013
	60	0.009
Unrefined salmon oil	20	0.058
	30	0.038
	40	0.025
	50	0.017
	60	0.013
Cod oil	20	0.051
	30	0.035
	40	0.022
	50	0.017
	60	0.013
Unrefined pollock oil	20	0.04

FFA and peroxide content in fish oils are direct indications of oxidation stability and are measured by titration, Fourier Transform Infrared Spectroscopy (FTIR) and Near-Infrared Spectroscopy (NIR). Spectrophotometry has also been used to measure secondary oxidation products such as ansidine [6]. Main factors that affect oxidation are storage temperature, time, and atmosphere. Oxidation increases with storage time and temperature and nitrogen environments inhibit oxidation. Sathivel et al. showed that peroxides increased after 10 weeks of storage at 24 °C [62]. Skara et al. showed that storage at 4 °C and in the presence of nitrogen resulted in lower changes in primary and secondary oxidation products when compared to higher temperatures and oxygen environments [63]. However, there are sometimes antioxidants within the fish waste such as caretonoid, astaxanthin pigments, peptides, and certain fatty acids inhibit the formation

of oxidation product. For instance, salmon oils in air at 23 °C did not show high levels of oxidation after 60 days [63, 6].

Other physical properties such as color, water content, and specific gravity are useful characterizations of fish oil. The color and water content of fish oil both depend heavily on the type of fish and the level of refining of the oil. Density values for oils made from pollock, red salmon, pick salmon, and herring are 0.902 g/mL, 0.900 g/mL, 0.810 g/mL, and 0.911 g/mL respectively [6].

3.3 Recovering fish oil from fish waste

Fish oil can be recovered from fish waste using physical, chemical, and biological extraction. While the properties of fish oil largely depend on the species of fish used as feedstock, fish oil properties are also dependent on type, maturation, age, sex, geographical habitat, and season. Fish processing method, fishing technique and length of time and method of storage are factors that influence fish oil properties [64, 6]. The most common extraction process of fish oil is as a by-product from fishmeal production as shown in the process flow diagram in Figure 3-1.

Fish waste is homogenized and "cooked" to free the oil, solids are removed by pressing. The press cake is processed into fishmeal by drying and grinding while the press liquor (oil, water, and fine solids) is further processed into fish oil by separation, water washing, and finally polishing [64, 2, 6].

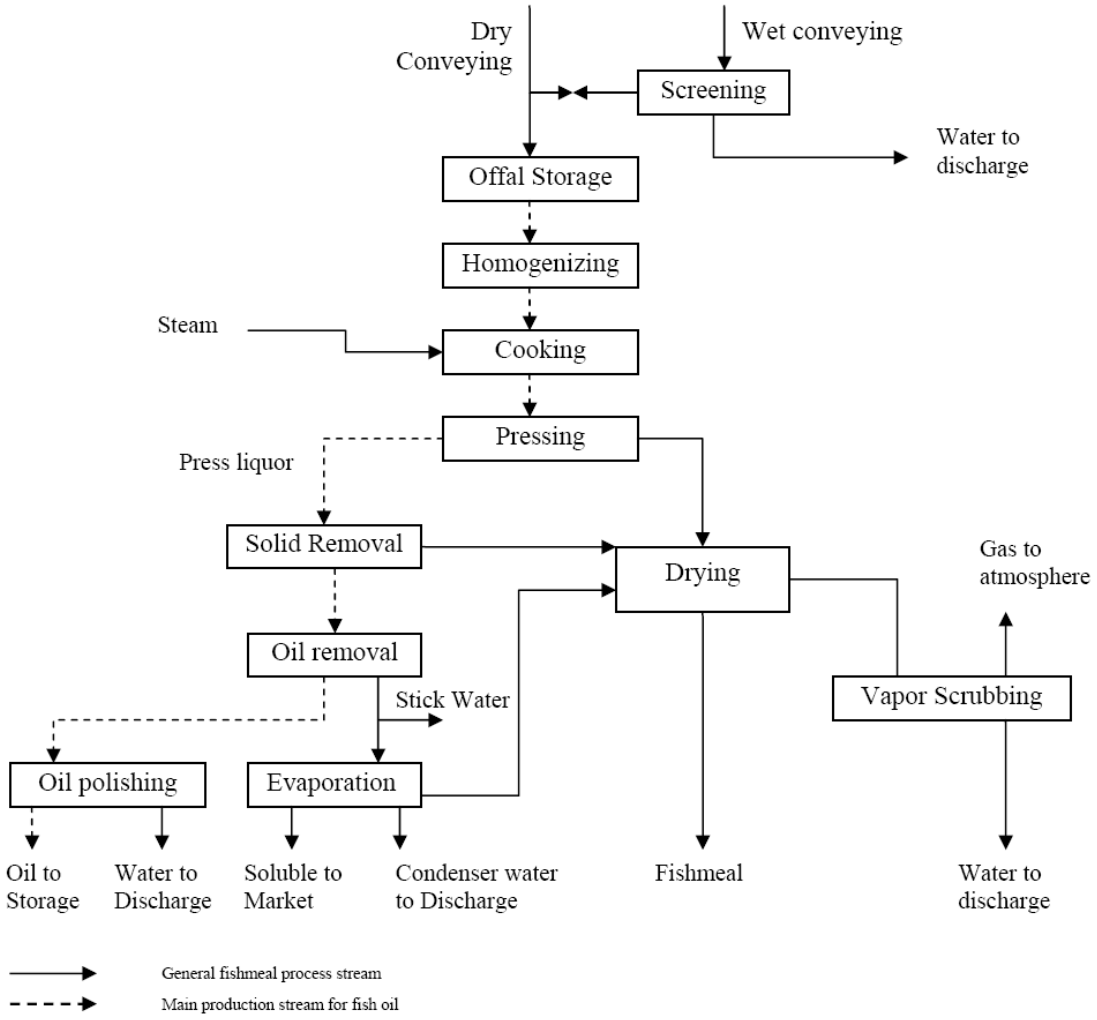

Figure 3-1: Extraction of fish oil within the fishmeal production process [6]

The fish waste is homogenized using hashers, mincers, grinders, or blenders. Then, in process known as "cooking", fish waste is heated to rupture the lipid cells and in turn release the contained oil. Cooking also frees the physio-chemically bound water by coagulating the proteins. Traditional cooking processes include temperatures of 95 – 100 °C for 15 – 20 minutes. Lipid cells begin cracking at temperatures less than 50 °C and physico-chemically bound water molecules release between temperatures of 65 – 120 °C.

Over-heating can result in large suspended solids being formed that inhibit pressability [6]. The waste is passed through a screw press or put in batches to squeeze the liquid out of the heated slurry as press liquor. 70 wt. % of the material ends up as press liquor and the rest becomes press cake. Press liquor contains oil, water, sludge, and suspended and dissolved solids. A decantor or centrifuge can also be used to replace the press. While advantages of centrifugation include better process controls, a faster and simpler process, and the ability to process fluid-like slurry, disadvantages are higher moister content in the fishmeal products and difficult subsequent oil separation due to formation of emulsions and fine particles in the liquid [6]. The separation of oil from press liquor is accomplished using gravity separation in settling tanks, using centrifugation separation in centrifuges, decanters, or desludgers, or, in small plants, vibrating strainers. Finally, the oil is polished by hot water mixing and subsequent centrifugation to extract impurities and facilitate oil stability during storage [65].

Chemical extraction of fish oil from fish waste is typically accomplished via solvent extraction or acid digestion. Traditional solvent extraction uses organic solvents (such as hexane, benzene, cyclohexane, acetone, and chloroform) to disrupt interaction forces between lipids and the tissue matrix. Supercritical fluid extraction where supercritical CO_2 is used as the solvent is also used. Acid digestion uses concentrated HCl and tertary butylhydroquinone (TBHQ) as an anti-oxidant for extraction fatty acids [6].

The biological extraction of fish oil from fish waste is carried out by enzymatic hydrolysis or fermentation. Enzymatic hydrolysis either uses digestive enzymes in the fish viscera such as lipases for autolysis or uses external enzymes such as commercial

protease for hydrolysis. Autolysis is time consuming and results in a lower quality product due to deterioration. Advantages of hydrolysis are that it is a faster process with milder conditions that is easier to control. The disadvantage of hydrolysis is that while a high FFA content is not ideal for bio-fuel, hydrolysis occurs more favorably in fish waste high in FFA. The fermentation of fish waste is accomplished by the addition of bacteria in the presence of carbohydrates or organic acids. The process produces silage and oil, and the resulting oil is separated by centrifugation [64, 6].

4 PYROLYSIS OIL FROM WOODY BIOMASS

4.1 Background of pyrolysis oil

Pyrolysis is one of the oldest methods of biomass conversion and was introduced in ancient Egypt for the production of tar used in caulking and embalming. Pyrolysis is a thermo-chemical decomposition process in which organic material (biomass) is converted to a carbon-rich solid (bio-char), a liquid high in organic molecules (pyrolysis oil), and a non-condensable gas (bio-gas) [66].

The process produces bio-gas in the form of non-condensable gases such as CO_2, CO, CH_4, and H_2. The condensable gases produced during pyrolysis are converted to pyrolysis oil via a condenser system. Pyrolysis oil is an organic multi-component mixture also referred to as bio-oil, pyrolysis liquid, prolytic oil, liquid wood, and liquid smoke [67]. It is composed of organic acids, esters, alcohols, ketones, aldehydes, phenols, alkenes, nitrogen compounds, furans, guaiacols, syringols, sugars, miscellaneous oxygenates, and inorganic metals. Bio-char is predominantly elemental carbon and hydrogen and any inorganic compounds [68]. The ratio and composition of the products bio-gas, bio-char, and bio-oil are a function of the feedstock, operating temperature and pressure, condensing system, and type of pyrolysis.

Pyrolysis oil is a suitable as a fuel in heating or electrical generation and is increasingly attractive as a fuel due to the rising price of petroleum fuels, the environmental advantages of the process, and the potential of rural economic development. As a fuel,

pyrolysis oil produces less greenhouse gas emissions, especially CO_2, and eliminates sulfur emissions [5]. As well, locally sourced biomass can be used to produce pyrolysis oil, which is attractive for northern countries with large surface areas, abundant wood resources, and cold climates such as Canada and Russia, or Scandinavian countries [68, 64]. However, limitations of the pyrolysis process are the low quality of pyrolysis oil (high acidity, low thermal stability, low heating value, high viscosity, deposit build-up, and poor ignition properties), high production costs, and addition of energy conversion systems [64].

The use of pyrolysis oil will become more viable when more regulations are introduced to combat climate change. Technical advances of the pyrolysis process will be a product of policies direct toward environmental change. For example, the introduction of ASTM standard D7544, “Standard Specification for Pyrolysis Liquid Biofuel”, has been an important step in the introduction of pyrolysis oil as a standard fuel for transportation, heating, and electrical generation [64].

4.2 Composition and properties of pyrolysis oil

Pyrolysis oil is a mixture of more than 300 different chemicals [69]. While characterization is accomplished in most labs by GM-MS or GC-FID, there are many drawbacks such as insufficient chromatographic resolution, peak co-elution, unknown mass spectra for certain compounds, lack of analytical calibration standards, and inability to characterize non-volatiles (sugars and lignin oligomers). Other analytical techniques include comprehensive two-dimensional gas chromatography (GC-GC), liquid chromatography (LC), high-resolution mass spectrometry (HRMS), nuclear magnetic resonance (NMR), and Fourier transform infrared spectroscopy (FTIR) [70].

Wood and forestry residue feedstock vary with tree species and consist of cellulose (40 – 47 wt. %), hemicelluloses (25 – 35 wt. %), lignin (16 – 31 wt. %), organic extractives, and inorganic minerals. Wood and forestry residues come from harvest residues (tops, branches, and leaves from forestry operations), small and low value standing trees, and sawmill residues (chips, slabs, sawdust, shavings, and bark). While harvest residues are generally left to decompose in the forest, sawmill residues are collected and used for energy generation, pulp, particleboard production, pellet production, compost, garden and playground bedding, and livestock bedding. In Newfoundland and Labrador in 2009, the production of 75 million board feet resulted in 24,414 bone dry tones (BDT) of harvest residues left in the forest, 7,568 tones (with 20 – 40 wt. % moisture content) of sawmill residues, and 29,000 BDT of pulp and paper residues. In total, 250,000 tones of residues are generated per year by sawmill and forestry operations [70].

During pyrolysis, cellulose decomposes into 27 compounds with the main products being levoglucosan, hydroxyacetaldehyde, furfural, formic acid, acetic acid, and aldehydes. Hemicellulose decomposes into water, methanol, formic acid, propionic acid, hydroxyl-1-propane, hydroxyl-1-butanone, 2-methylfuran, 2-furfuraldehyde, dianhydroxylopyranose, and anhydroxylopyranose. Lignin in softwood mainly decomposes into guaiacol and lignin in hardwood mainly decomposes into guaiacol and pyrogallol dimethyl ether. Pyrolysis oil from hardwood also contains phenols/syringols which are natural antioxidants that improve storage stability [71]. Table 4-1 below indicates the major families of compounds found in pyrolysis oil [70].

Table 4-1: Chemical composition of pyrolysis oil [68, 70]

Compound	Concentration Range
Water	20 – 30 wt. %
Aldehydes	10 – 20 wt. %
Carboxylic acids	10 – 15 wt. %
Furfurals	1 – 4 wt. %
Alcohols	2 – 5 wt. %
Ketones	1 – 5 wt. %
Pyrolytic lignin	15 -30 wt. %

The chemical and physical properties of fast pyrolysis oil are given in the ASTM standard D7544 and are shown in Table 4-2 below. Grade G bio-oil is intended for use in industrial burners and grade D bio-oil is intended for use in commercial/industrial burners requiring lower ash content and solids. Grade D bio-oil is suitable in residential heaters, engines, and marine equipment modified to handle bio-oils.

Table 4-2: Requirements for Grade G and D pyrolysis oil from ASTM D7544

Property	Unit	Test method	Grade G	Grade D
Gross heat of combustion (minimum)	MJ/kg	D240	15	15
Water content (maximum)	wt. %	D203	30	30
Pyrolysis solids content (maximum)	wt. %	D7579	2.5	0.25
Kinematic viscosity at 40 °C (maximum)	mm^2/s	D445 [a]	125	125
Density at 20 °C	kg/dm^3	D4052	1.1 – 1.3	1.1 – 1.3
Sulfur content (maximum)	wt. %	D4294	0.05	0.05
Ash content (maximum)	wt. %	D482	0.25	0.15
pH level	-	E70	report	report
Flash point (minimum)	°C	D93-B	45	45
Pour point (maximum)	°C	D97	-9	-9

[a] without filtering

Water content is dependent on the feedstock moisture content, processing conditions, and secondary reactions that occur during pyrolysis [72]. Pyrolysis oil is combustible however it is not flammable because significant energy is needed for ignition due to the high water content. When pyrolysis oil is used as a fuel, high water content reduces gross heat of combustion, increases ignition delay, and reduces combustion rate. Although, high water content also improves flow characteristics by reducing viscosity, improves flame characteristics by creating a uniform temperature profile, and reduces the amount of NO_x emissions due to a lower combustion temperature [70].

The kinematic viscosity of pyrolysis oil at 40 °C ranges from 15 – 35 cSt and as a result pyrolysis oil has good flow properties if pre-heated. However, viscosity increases with age. Pyrolysis oil is acidic (pH of 2 – 3) due to the presence acetic and formic acids [69, 73]. Drawbacks of pyrolysis oil are summarized in Brown's "Thermochemical Process of

Biomass" and include low pH, degradation with age, high alkali metal content, char in the oil, dark staining color, contamination of feedstock with soil, chlorine, nitrogen, or sulfur, poor distillability, high viscosity, non-homogeneous, low hydrogen:carbon ratio, material incompatibilities, poor miscibility with hydrocarbons, high oxygen content causing reactivity and instability, strong odor, high solid content, high temperature sensitivity, high toxicity, and high water content [74].

4.3 Pyrolysis of woody biomass

As shown in Figure 4-1, pyrolysis is the addition of heat to biomass in the absence of oxygen and sometimes in the presence of a catalyst. Different types of pyrolysis include slow and fast pyrolysis, flash pyrolysis, microwave pyrolysis, and catalytic pyrolysis, with slow and fast pyrolysis being the most common [2, 64].

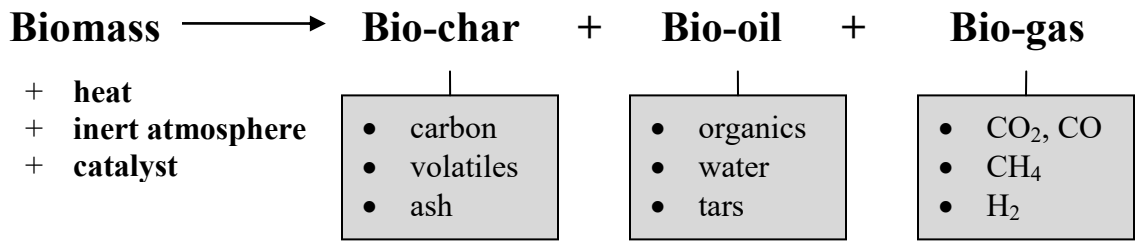

Figure 4-1: Simple flow chart of pyrolysis process [66]

Table 4-3 below explains the differences in process parameters and the yields between slow and fast pyrolysis. Process parameters for slow pyrolysis are relatively low temperatures of 200 to 350 °C, long residence times of 2 to 30 minutes, large feedstock particle sizes, and heating times that are longer than reaction times. Process parameters for fast pyrolysis are high process temperatures of 450 to 550 °C, short residence times of 1 to 60 seconds, small feedstock particles sizes, and heating times that are much shorter than reaction times [68, 64].

Table 4-3: Process parameters and yields of slow and fast pyrolysis [68]

Property	Slow pyrolysis	Fast pyrolysis
Temperature range	200 – 400 °C	450 – 550 °C
Feedstock particle size measurement	centimeters	millimeters
Residence time range	2 – 30 minutes	1 – 60 seconds
Heating time versus reaction time	$t_{heating} >> t_{reaction}$	$t_{heating} << t_{reaction}$
Bio-char yield	25 – 35 wt. %	10 – 25 wt. %
Bio-oil yield	20 – 50 wt. %	50 – 70 wt. %
Bio-gas yield	20 – 50 wt. %	10 – 30 wt. %

Conventional or slow pyrolysis can be divided into traditional processes and modern processes. The traditional process use pits, mounds, or kilns that are heated directly by the combustion of the biomass which is usually wood. The process can be operated in batch or in continuous modes to produce charcoal, and organic liquid products before the widespread availability of petrochemicals such as acetic acid and methanol. The bio-liquid and bio-gas escape directly into the environment or are recirculated to provide heat internally or externally [66]. Modern slow pyrolysis technologies include drum kilns, rotary kilns, and screw pyrolysers, and are generally based on a horizontal tubular kiln that feeds the biomass through at a controlled rate. Slow pyrolysis is of interest for bio-char production because of the high yields of bio-solids [75].

The development of fast pyrolysis as a way of increasing the yield of bio-fuels from woody biomass progressed rapidly following the petroleum crisis of the 1970's [76]. The short residence times are designed to reduce the secondary reactions and produce a high yield of bio-oil. Several well-established commercial processes are used today such as Ensyn Corporation's Rapid Thermal Process or Dynamotive's Biotherm process [66, 69].

Figure 4-2 below is a flowchart of the fast pyrolysis process. First, the biomass is dried to less than 10 wt. % water and ground to 2 mm for fluidized bed reactors. Then, the treated feed is cracked in the pyrolysis reactor, the solids are separated using a cyclone, and the condensable liquids are separated from the non-condensable gases using a condenser [77, 70].

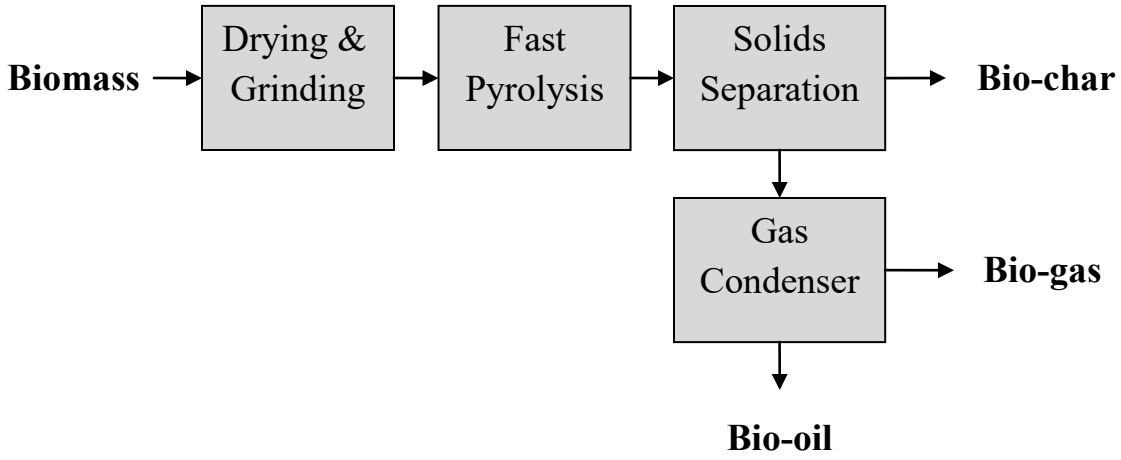

Figure 4-2: Fast pyrolysis of biomass into bio-char, bio-gas, and bio-oil [77]

There are six main factors that influence the composition and properties of pyrolysis oil: type of biomass or feedstock, feedstock ash content, feedstock particle size, pyrolysis temperature, reactor type, and condensation system [72]. The optimal pyrolysis temperature for fast pyrolysis is between 450 and 550 °C as secondary cracking reactions occur at 550 °C and reduce the oil yield by increasing the water content. The optimum feedstock particle diameters are between 0.1 and 1 mm [70]. Pyrolysis reactors include fluidized bed, plasma pyrolysis, free-fall, fixed bed, rotating cone, microwave, and auger reactor. The advantage of the auger reactor over other reactor types is that no cost

intensive inert fluidizing gas is needed [78]. A heat carrier of either steel shot or sand is used to heat the feedstock [75]. The particles are well-mixed due to the screw rotation of the auger reactor. A more detailed review on pyrolysis reactors can be found in [68, 79, 80]. The condensation system determines the vapors that become condensed. Fractional condensation systems can optimize oil homogeneity even when the vapor product has high moisture content [70].

5 UELO, FISH OIL, AND PYROLYSIS OIL AS FUEL

5.1 Fuel properties

Certain properties are important for all fuels and certain properties are only important for bio-fuels. The ASTM standard D396, “Standard Specification for Fuel Oils” covers many different grades of hydrocarbon based oils with less than 5% biodiesel. The ASTM standard D6448, “Standard Specification for Industrial Burner Fuels from Used Lubricating Oils”, covers the requirements for four grades of reprocessed fuel oils (RFOs) from RFO4 to RFO6 made in whole or in part with hydrocarbon-based used or reprocessed lubricating oil. The ASTM standard D6823, “Standard Specification for Commercial Boiler Fuels with Used Lubricating Oils”, describes requirements for four grades of recycled fuel oil for commercial boilers (RFC) from RFC4 to RFC6 made of at least 25% used lubricating oil. The ASTM standard D7544, “Standard Specification for Pyrolysis Liquid Biofuel”, specifies requirements for a pyrolysis liquid biofuel produced from biomass intended for use in industrial burners equipped to handle them. There are ASTM standards for biodiesel made from vegetable oils and animal fats, and although fish oil falls under these standards, there are no specific ASTM specifications for fish oil extracted using the fishmeal process. Table 5-1 below shows the required properties of various fuel types in each ASTM specification. Although RFO4 and RFC4 are meant to be comparable to No. 4 heavy fuel and RFO6 and RFC6 are meant to be comparable to No. 6 heavy fuel oil, they are not interchangeable fuels. Also, as specified in ASTM

specifications, certain properties of UELO-based fuels and pyrolysis liquid biofuels are negotiated between buyer and seller.

Table 5-1: Comparison of required properties for various fuel types

Property	D396 Petroleum Fuel Oils		D6448 UELO in Industrial Burners		D6823 UELO in Commercial Burners		D7544 Pyrolysis Biofuel
Grade of fuel	No. 4	No. 6	RFO4	RFO6	RFC4	RFC6	NA
Viscosity at 40 °C (cSt max)	5.5	-	-	-	-	-	125
Viscosity at 100 °C (cSt max)	-	50	5	50	5	50	-
Density (kg/m3 max)	867	-	report	-	report	report	1300
Flash point (°C min)	38	60	38	60	38	60	45
Pour point (°C max)	-6	-	-6	-	-6	-	-9
Water & sediment (vol. % max)	0.50	2.00	2.00	3.00	1.00	2.00	-
Water (wt. % max)	-	-	-	-	-	-	30
Solids (wt. % max)	-	-	-	-	-	-	2.5
Acid no. (mg KOH/mg max)	-	-	-	-	0.15	0.30	-
pH (min)	-	-	4	4	-	-	report
Ash (wt. % max)	0.05	-	0.7	report	0.2	report	0.25
Sulfur (wt. % max)	-	-	report	report	report	report	0.05
Heating value (MJ/kg min)	-	-	40.0	43.0	40.0	43.0	15
Arsenic (ppm max)	-	-	-	-	5	5	-
Cadmium (ppm max)	-	-	-	-	2	2	-
Chromium (ppm max)	-	-	-	-	10	10	-
Lead (ppm max)	-	-	-	-	100	100	-
Total halogens (ppm max)	-	-	-	-	1000	1000	-
PCBs (ppm max)	-	-	-	-	50	50	-

5.1.1 Density

Specific gravity or relative density is the ratio of the density of a fluid to the density of water [26]. The density in general increases with the number of carbon atoms and the

degree of saturation. The density of an engine fuel determines the injection compression ratio in engine cylinders and increases in density increase the droplet diameter which in turn affects injection timing and spray pattern. The density of a burner fuel impacts heating value, atomization, and emissions. As density increases, heating value increases, atomization becomes more difficult, and particulate matter and NO_x emissions increase [6]. The density of UELO increases with increasing solid content. One percent of weight of solids in the sample can raise the specific gravity by 0.007 [10].

5.1.2 Viscosity

Viscosity is a function of temperature and pressure, related to fuel performance in engines, boilers, and furnaces. In general, there is an inverse relationship between viscosity and temperature, in effect when the temperature decreases the viscosity increases and *vice versa*. As viscosity increases, the flowability of a fuel through lines, nozzles, and orifices becomes more difficult. A fuel with a high viscosity causes increases in pump pressure, reduction in fuel atomization, and incomplete or early combustion.

5.1.3 Water and sediment content

Water and sediment in a fuel oil cause fouling of the equipments involved in combustion. Sediment may accumulate in storage tanks, on filter screens, or in burner parts resulting in flow obstruction. High water content reduces the overall viscosity and the heat of combustion. Moreover, it reduces the flame temperature, thereby, contributing to lower

nitrogen dioxide emissions during combustion. In the case of pyrolysis oil, phase separation occurs if water content is too high (ASTM D7544 – 12). Water content also increases corrosion of tanks, pumps, or combustion equipment and may cause emulsions in heavier fuels such as pyrolysis oil and UELO. As well, presence of water can cause spattering during atomization and lead to erosion or explosive damage of burner nozzles.

5.1.4 Cold temperature performance

Cold temperature performance is indicated primarily by pour point and cloud point, however other cold flow properties include cold filter plugging point and freezing point. Pour point is the lowest temperature at which a fuel oil is still capable of flowing under low forces and cloud point is the temperature at which wax visually accumulates in the liquid. Fuels with high pour point require heated storage and adequate piping facilities. Fuels stored at or below their cloud point may cause problems during operation because of plugging. Animal-based bio-oils have higher pour and cloud points than vegetable oils due to higher SFA content [6, 64]

5.1.5 Sulfur content

The knowledge of sulfur content is important to evaluate the sulfur oxide emissions resulting from the combustion. SO_x emissions are directly dependent on the sulfur content and can be estimated by elemental sulfur content [7] .

5.1.6 Heating value

Heat of combustion, calorific value, or heating value is the amount of heat released during the combustion of a fuel. Higher heating value (HHV) or gross calorific value (GCV) is the energy determined by bringing all the products of combustion back to the original pre-combustion temperature. Lower heating value (LHV), net calorific value (NCV), or lower calorific value (LCV) is determined by subtracting the heat of vaporization of the water from the higher heating value. LHV calculations assume water is in a vapor state at the end of combustion, whereas HHV calculations assume water is in a liquid state after combustion.

5.1.7 Thermal degradation and ash content

Thermo-gravimetric analysis (TGA) is a method to investigate thermal degradation of a fuel and to determine ash content. Fuel is heated slowly from room temperature to 800 °C first in the presence of nitrogen and then switching to oxygen at 500 °C to burn off remaining carbon. TGA analyzes thermal stability by determining weight changes as a function of temperature.

Unrefined salmon oil shows resistance to thermal decomposition between 200°C and 350°C. Unrefined or unprocessed salmon and pollock oil contain phospholipids, metals, minerals, free fatty acids, and peroxides that absorb heat and slow decomposition [62]. Refined fish oils lose more weight loss in thermal decomposition because there is less impurities to absorb heat [3]. The temperature range from 350 to 450 °C shows a rapid thermal degradation in unrefined salmon oil (approximately 90 wt. %) [4].

5.1.8 Flash point

Flash point of a fuel indicates the presence of volatiles or flammable substances and reflects the maximum storage and handling temperature without fire hazard. UELO, pyrolysis oil, and fish oil generally have higher flash points than diesel oil. Animal-based bio-oils have higher flash points than vegetable-based bio-oils because of their higher SFA content. Fuels with high flash points show delayed ignition, difficulties with start-up, and commonly require preheating [6].

5.2 Combustion and emission characteristics

Fuel oil burners either vaporize, atomize, or spin-off oil in the presence of a spark to create a flame. Atomizing or gun-type burners use pressure to force the oil through a nozzle to form microscopic particles or droplets. Small droplets ignite quickly to establish a flam and larger droplets take longer to burn and spread the flame throughout the combustion chamber. Vaporizing or pot-type burners heat the fuel until it vaporizes, which is then naturally drafted or mechanical drafted towards an ignition spark. Rotary-type burners use a spinning disc that throws the fuel in a fine spray using centrifugal force. Atomizing burners are most common because they can take high viscosity fuels and the simple nozzle is affordable to purchase or replace.

In the presence of air, complete combustion of a pure simple hydrocarbon fuel can be expressed in Equation 5.1 where nitrogen is inert and CO_2 and H_2O are formed.

$$\boldsymbol{fuel + O_2 + N_2 + heat \rightarrow CO_2 + H_2O + N_2 + heat} \quad \textbf{Equation 5.1}$$

In reality, fuel composition and combustion reactions are extremely complex and complete combustion rarely occurs. Products of combustion frequently include CH_4, CO_2, N_2O, CO, NO_x, SO_x, particulate matter (PM), PAHs, volatile organic compounds (VOCs), and more. For a given fuel, emissions of individual pollutants can vary over orders of magnitude depending on the combustion apparatus and pollution control. Also in certain combustion processes, some pollutants are effectively independent of the type of fuel used such as CO emissions in cement kilns depending entirely on combustion temperature [7].

5.3 UELO as fuel

One liter of used oil contains about 8 MJ or enough to operate a 100 W light bulb for 24 hours. Used oil can be burned in various types of boilers and burners and recycling it as fuel recovers nearly 100% of the oil [21]. However, it creates potentially significant localized air pollution depending on used oil quality [16]. Since 65 vol. % of used oil is UELO, this review differentiates between used oil as fuel and UELO as fuel. UELO usually contains less contamination than used oil and as a result, less reprocessing and flue-gas treatment is required for combustion [10].

Used oil is mostly burned in industrial-scale processes such as power stations and cement kilns. Combustion of used oil in cement kilns is most common today because little pretreatment is required due to extremely high combustion temperatures. In 1999, over 50% of recycled used oils in France were burned in cement kilns [10]. Over 400 million kg of used oils are burned in cement kilns in Europe [16]. However, not all countries allow the burning of used oils in cement kilns: while France, Germany, Italy, and the UK allow it, Denmark, Finland, and the Netherlands do not [17].

Cement is made from a base substance called clinker (a raw material containing limestone, clay, and iron oxide). In a rotating cement kiln, clinker is heated to 1500 to 1600 °C and the hot gas residence time in the kiln is 6 seconds. With such intensive heat, dehydration, clay decomposition, limestone decarbonization, and clinkerization reactions occur in the kiln. Principal fuels used in cement kilns include solid fuels such as petroleum coke, coal, coal shale, and used tires, and liquid fuels such as heavy fuel oils,

waste solvents, and waste oils [10]. Contaminants such as sulfur, metal oxides, and chlorine are trapped in the mineral mass of the cement kiln. As well, the severe conditions of temperature and residence time do not allow the production of unwanted toxic compounds such dioxins and furnaces in the emissions. In fact, the controlled destruction in cement kilns is suggested when used oil is highly contaminated with polychlorinated biphenyls (PCBs) and polychlorinated terphenyls (PCTs) because temperatures are high enough to destroy organic compounds, neutralize acid compounds, and reduce metal content in the combustion residues [29].

Used oil destined for asphalt plants, road stone drying, large marine engines, power stations, or blending with other fuels requires simple reprocessing. Water and particulates are removed with physical treatments such as settling, filtration, or centrifugation to ensure it does not clog burners, foul boiler tubes, or cause sediment build-up in tanks [15]. The treatments typically do not deal with heavy metals, halogens, and sulfur [16]. At industrial-scale combustion the flue gas is treated to reduce CO, SO_2, aldehydes, NO_x, dust, and metal emissions [10]. For road stone plants, reprocessed used oils are burned to dry limestone and hard stone in the manufacture of road surface materials. Reprocessed used oils are also used as start-up fuel for pulverized coal power stations. With respect to fuel blending, reprocessed used oils are mixed with other heavy streams into fuel oil which is sold as bunker fuel [17].

Some basic fuel properties of UELO are compared to diesel fuel and heavy fuel in Table 5-2 below.

Table 5-2: Comparison of properties for diesel, heavy fuel, and UELO [10]

Property	Diesel Fuel	Heavy Fuel	UELO
Viscosity at 40 °C (cSt)	1.9-5.5	-	80-125
Viscosity at 100 °C (cSt)	-	9-50	10-17
Sulfur (wt. %)	0.5	-	0.4-0.9
Heating value (MJ/kg)	43	40.3	40

UELO does not contain a heavy residual hydrocarbon fraction like heavy fuel oil. UELO has a low viscosity that makes injection in a standard burner possible at 70 °C and storing and pumping possible at 10 °C. As a comparison, heavy fuel oils require 130 °C for injection and 50 to 60 °C for storage and pumping. UELO has a low sulfur content of less than 1.0 wt%, which is comparable to low sulfur fuel oil, and a high heating value, which is comparable to diesel fuel oil. While UELO is not equivalent to diesel oil in terms of viscosity, distillation curve, Conradson carbon, and sulfur content, UELO is more favorable than heavy oil in terms of viscosity, Conradson carbon, sulfur content, and asphaltene contents [10].

Combustion of UELO in small-scale space heaters is an economic heating source for garages, workshops, and greenhouses where used oil can be disposed of at the point of generation. As well, regulations for burning used oil in small-scale heaters vary from one region to another. In Europe, it is carried out on a small scale except for in the UK where it is illegal [16]. The USA EPA allows burning of used oil in used oil-fired space heaters [81]. In Canada, only the region of Southern Ontario has banned burning used oil in space heaters in 2009 [82]. The rest of Canada allows burning of used oil in space heaters or small waste oil furnaces [12].

In the USA, the Air Pollution Control Regulations (APCR) and the Hazardous Waste Management Regulations (HWMR) both regulate combustion of all used oils. The HWMR establishes allowable levels of arsenic, cadmium, chromium, lead, flash point, and total halogen and the APCR establishes allowable levels for PCBs, total organic halogens, total inorganic chloride, lead, net heat of combustion, and flash point [22].

A 1996 study by the USA EPA sampled UELO from 21 locations (vehicle maintenance facilities as well as do-it-yourself drop off sites) and met requirements for direct burning outlined by the APCR and HWMR. Barium, beryllium, nickel, zinc, PCBs, nitrogen, and sulfur were not a significant concern. Only concentrations of lead, halogens, cadmium, and chromium were significant enough to warrant further study [22]. Contaminations of UELO, virgin engine lubricating oil, and various heating fuel oils are in Table 5-3 [22].

Table 5-3: Contamination of UELO, virgin engine oil, and heating fuels [22]

Contaminant	Used gasoline engine oil	Used diesel engine oil	Virgin engine oil	Diesel fuel	Heavy fuel
Arsenic (ppm)	--	--	--	--	--
Barium (ppm)	2.73	3.39	< 1.00	<1.00	< 1.00
Beryllium (ppm)	< 0.02	< 0.02	< 0.02	<0.02	< 0.02
Cadmium (ppm)	< 1.51	2.34	< 0.25	<0.25	< 0.25
Chromium (ppm)	3.19	3.91	< 2.00	<2.00	< 2.00
Lead (ppm)	47.23	57	< 20.00	<10.00	<10.00
Nickel (ppm)	< 1.40	1.85	< 1.20	< 1.20	8.34
Zinc (ppm)	1,161	1,114	1,210	5	9.05
Ash (wt. %)	0.54	0.46	0.135	0.13	0.55
PCBs (ppm)	< 5	< 5	< 5	< 5	< 5
Total Halogens (ppm)	< 350	<234	< 300	< 200	< 200
Total Organic Halogens (ppm)	< 301	< 217	< 292	< 200	< 200
Sulfur (wt. %)	0.36	0.25	0.36	0.12	0.19
Nitrogen (wt. %)	0.04	0.02	0.02	<0.01	0.03

The same study characterized emissions from UELO combustion in small waste oil furnaces (less than 500,000 BTU per hour). As shown in Table 5-4, UELO shows higher pollution emissions than diesel fuel [22].

Table 5-4: Emission testing from diesel fuel and UELO [22]

Fuel	HCl (mg/min)	Particulate (mg/min)	Arsenic (mg/min)	Cadmium (mg/min)	Chromium (mg/min)	Lead (mg/min)
Diesel fuel	2.3	0	<0.02	<0.03	0.02	0.03
UELO	34.6	466.6	<0.03	<0.08	0.17	2.09

Average HCl emissions from UELO combustion are 15 times higher than diesel fuel combustion, particulate matter averages 467 mg/min compared to negligible amounts in diesel fuel, and chromium and lead emissions are 8.5 and 70 times higher from UELO emissions than diesel fuel. However, despite higher emission rates, waste oil furnaces complied with the ambient standards [22].

CO and CH_4 emissions are more dependent on the type of combustion device than on fuel composition. Metal, CO_2, and SO_x emissions are related to fuel composition. CO_2 emissions are calculated based on fuel carbon content assuming 99% conversion of carbon. SO_x emissions are calculated by considering that all sulfur present in the fuel is converted to SO_2 [7].

A 2017 life cycle analysis study compared combustion emissions of used oil, reclaimed used oil, heavy fuel, and light fuel. There was no basis to suggest a difference in CH_4, N_2O, and CO emissions so they were assumed to be equal for all fuels compared. NO_x emissions are dependent on fuel-bound nitrogen conversion as well as thermal fixation

from air-bound nitrogen. Since the fuels compared contained negligible nitrogen content, thermal fixation was the dominant mechanism and used oil and diesel fuel showed equal NO_x emission factors. Particulate matter was comparable to fuel ash content and similarly to the 1996 USA study, particulate matter in used oil emissions was much higher than in either heavy fuel oil or diesel oil. Metal emissions were estimated based on composition of the metals in the fuels [7].

5.4 Fish oil as fuel

Five studies study combustion and emission characteristics of fish oil as fuel. Fish oil properties from the studies mentioned in this section are shown in Table 5-5.

Table 5-5: Comparison of fish oil properties from various studies [61, 83, 84]

Properties	Steigers [61]	Blythe [83]	Wang et al. [84]	Ushakov et al. [85]
Density at 15 °C (kg/m^3)	922.5	923.7	876.9	871[a]
Heating value (MJ/kg)	39.4	37.4	40.0	40.10
Flash point (°C)	110	166	145	161
Pour point (°C)	-	-9.4	3	-3
Cloud point (°C)	-	-	3.2	-
Acid number (mg KOH/g)	-	8.63	-	-
Kinematic viscosity (cSt)	-	33 (38°C) 22.4 (50°C)	5.42 (25 °C) 4.18 (40 °C)	3.83 (40 °C)
Initial boiling point (°C)	-	161	-	-
Cracking temperature (°C)	-	297	-	-
Moisture content (wt. %)	-	-	0.05	
Carbon (wt. %)	-	78.92	77.21	76.53
Hydrogen (wt. %)	-	11.59	12.08	12.34
Sulfur (wt. %)	0.0084	0.004	0.0034	0
Nitrogen (wt. %)	-	-	0.003	-
Oxygen (wt. %)	-	-	10.39	11.13
Ash content (wt. %)	-	0.0032	< 0.001	-

[a] Measured at 20 °C

A pollock oil demonstration project conducted by Steigers demonstrated the feasibility of using blends of fish oil and low sulfur diesel fuel in medium speed, 2.3 MW two-cycle generators. Exhaust emissions and engine durability and maintainability were measured at fuel blends of 100/0, 50/50, and 0/100 vol. % at different engine load conditions [61]. They observed wearing in fuel injectors and fuel pumps, and hard deposits in exhaust

components such as piston ring seating grooves, exhaust ports, exhaust turbine inlet rings. The suspended and insoluble protein content in fish oil resulted in increased load on fuel purifiers and filters. An increase in engine-mounted fuel filter pressure differentials was observed due to the higher viscosity and lower thermal capacity of the fish oil. Start-up was easier with fish oil and fish oil/diesel blends than with pure diesel and no difficulties occurred during shut-downs. Engine lubricating oil was tested at 24-hour intervals and did not show unusual contamination or consumption rates. There are limitations to the applicability of the study due to the rare engine design used. Even so, suggestions for future cases of fish oil and diesel blending were inline blending as opposed to batch blending and pre-purification of fish oil before use by centrifugal fuel purifiers or other suitable filtration equipment [61].

Blythe used pollock oil from surimi plants as an alternative to diesel fuel for electricity generation in medium speed, two-cycle, 6-cylinder engines. Blends of fish oil and diesel fuel between 0% and 100% at 10% increments were tested at multiple engine load conditions. Fish oil contained less volatiles compared to the blends, which was seen by a decrease of the onset temperature of cracking with increasing fish oil because the initial boiling point of pure fish oil was lower than pure diesel fuel [83]. Engine performance tests across all load settings showed an increase of fuel consumption with increasing fish oil in the blend due to fish oil having a lower heating value than diesel fuel. Fish oil and fish oil blends showed no difference compared to diesel fuel in ignition delay characteristics, combustion pressure, and heat release. Only the level of hard deposits on the upper piston section after 37 hours of operation was higher with fish oil and fish oil

blends than with diesel fuel. In general, except for slight increases in hard deposits, fish oil and fish oil blends performed comparably to diesel fuel in terms of ignition and combustion characteristics [83].

Wang et al. studied combustion and emission characteristics of boilers and furnaces using Alaskan fish oil. Blends of fish oil, diesel fuel, and heavy fuel were tested and tribological properties, combustion emissions, and flame stability were measured. Pure fish oil and blends with 5% and 10% fish oil were tested in 30 and 150 kW oil-fired residential boilers and blends with 50% fish oil were tested in industrial furnaces. The study demonstrated that fish oil could be used with no adverse affects. However, the study suggested removal of impurities such as proteins, waxes, and water because of potential adverse conditions in engines and during storage. Fish oil had higher flash and pour points but lower heating value compared to petroleum fuels. Kinematic viscosity was lower than heavy fuel but higher than diesel fuel, which decreases pump load and the need for preheating requirements. Density, heating value, kinematic viscosity and carbon, hydrogen, nitrogen, and ash contents of the fish oil were all more similar to diesel fuel than to heavy fuel [84].

Ushakov et al. studied combustion and emission characteristics of fish oil fuel in a heavy-duty diesel engine. Pure residual fish oil and a 50/50 vol. % blend with low-sulfur marine gas oil (MGO) was combusted in a four-stroke, turbocharged, intercooled, direct-injection heavy-duty diesel engine. Combustion properties of fish oil and MGO were similar and no additional deposits, clogging or engine wear were observed when running on fish oil [85].

Table 5-6 below shows the difference in emissions of pure fish oil and fish oil blends compared to pure diesel for two studies mentioned above.

Table 5-6: Difference of emissions of fish oil blends compared to diesel fuel [61, 84]

Study	**Wang et al. [84]**	**Steigers [61]**	
Combustion device	**Industrial furnace**	**900-rpm diesel engine**	**720-rpm diesel engine**
Fuel blend	**50% fish oil 50% diesel**	**50/50 vol. % fish oil/diesel**	**50/50 vol. % fish oil/diesel**
CO_2	4%	5%	5%
CO	-6%	-5 to 6%	-16 to -20%
PM	-	-18%	-40%
SO_2	-40%	-30%	-30%
NO_x	11%	6 to 7%	2 to 6%
Fuel blend	**100% fish oil**	**100% fish oil**	**100% fish oil**
CO_2	4%	5%	5%
CO	-25%	-10 to 16%	-28 to -33%
PM	-	-78%	-78%
SO_2	-96%	-80%	-80%
NO_x	14%	6 to 7%	2 to 5%

Wang et al. measured CO, NO_x, CO_2, PM, and SO_2 emissions in an industrial furnace. CO_2 increased 4% and NO_x increased 11% and 14% with 50/50 vol. % fish oil/diesel fuel blends and pure fish oil, respectively. On the other hand, the 50% mixture showed decreases in CO of -6% and in SO_2 of -40%, and pure fish oil showed large decreases in CO of -25% and in SO_2 of -96% compared to pure diesel fuel. Increases in NOx emissions were said to be due to volatility of fish oil and subsequent reactions with air-bound nitrogen [84]. Steigers measured CO, NO_x, CO_2, and PM emissions and estimated SO_2 emissions from fuel-bound sulfur content. Pure fish oil emissions showed decreases of up to 78% PM, 33% CO, and 80% SO_2, and increases of less than 7% in both NO_x and

CO_2 compared to diesel fuel. The 50/50 vol. % fish oil/diesel fuel blend emissions showed decreases of up to 40% PM, 20% CO, and 30% SO_2, and increases of less than 7% in both NO_x and CO_2 compared to diesel fuel [61].

Ushakov et al. measured NO_x, CO, CO_2, THC, and PM emissions. NO_x emissions were not more than 6% higher for fish oil than for MGO. Higher NO_x emissions from oxygen-rich bio-fuels were reported and in previous studies [61, 84] were associated with an increase in flame temperature during the combustion process due to presence of fuel-bound oxygen. However, Ushakov et al. suggested high fuel-bound oxygen can also reduce the amount of fuel burned in the premixed combustion phase and decrease the peak burning temperature, which in turn reduces the NO_x emissions. CO emissions from fish oil were significantly lower than for MGO because the presence of fuel-bound oxygen facilitates complete combustion and reduces CO formation. CO_2 emissions from fish oil and MGO were very similar. THC emissions from pure fish oil showed reductions of up to 70% and fish oil/MGO blends showed reductions of up to 37% when compared to MGO. Reductions were attributed to the lack of PAHs and increased fuel-bound oxygen in fish oil. Total PM emission concentrations decreased by up to 36% for fish oil/MGO blends and by up to 67% for pure fish oil compared to MGO. However, this was due to a shift of mean particle diameters from large in MGO combustion to small in fish oil combustion [85].

5.5 Pyrolysis oil as fuel

Due to the complex nature of pyrolysis oil, modifications to equipment are needed before pyrolysis oil can used as fuel in furnaces and boilers, diesel engines, and gas turbines. Supplemental fuel must be added to facilitate ignition and depending on the composition and quality of the fuel, emissions during combustion will vary [64]. Consistent quality pyrolysis oil can be used as an alternative fuel in modified combustion equipment however use as a transportation fuel is limited due to its high acidity, low thermal stability, low heating value, high water content, and high viscosity [74, 79].

There are two distinct stages in the combustion process of pyrolysis oil. The first is evaporation and combustion of water and light components and the second is combustion of the heavier components. During combustion, heavy component droplets may fly outside of the hot flame environment unvaporized and unburned to create “sparks” and coke formation on the walls of the chamber. Water content of pyrolysis oil, atomization technology, and combustion conditions affect the amount of sparks generated. When combustion conditions are ideal and the atomization burner is properly adjusted, the flame is uniform, symmetrical, and stable, emissions decrease, and only ash will be transported from the combustion area. However, challenges arise with smaller combustors, poor quality oil, and lack of expertise in bio-oil combustion. In those cases, the oil may not be properly combusted and deposits may build up in the chamber and boiler tubes [86].

Preheating and blending with lighter fuels are recommended when using pyrolysis oil as fuel. Preheating improves atomization and performance of the combustion system by reducing viscosity and surface tension. However, in contrast to heavy petroleum oil, which is typically preheated in the storage tank, pyrolysis oil should be preheated prior to combustion in the fuel line due to its tendency to polymerize when exposed to moderate heat over an extended period of time. Pre-heat temperatures of 40 to 80 °C result in viscosity as low as 4 cSt in smaller combustion systems and 25 cSt in larger systems [72]. Preheating primary atomization air decreases its density and increases its velocity, which leads to improved combustion and reduced emissions [86].

Combustion research has been conducted with pure pyrolysis oil and its blends and emulsions with biodiesel and petroleum diesel fuels in various diesel engines. The main concerns are ignition difficulty, corrosivity, and coking of injector nozzles. A solution is blending with a lighter fuel such as ethanol and methanol or alcohol such as methanol or ethanol decreases the surface tension and density of the pyrolysis oil and increases overall volatility, heating value, and air/fuel ratio in combustion [86]. Blends of 72% pyrolysis oil, 24% methanol, and 4% cetane-improving additives have been used with success in diesel engines [69].

In general the combustion emissions of pyrolysis oil are between those of light oil and heavy oil. High particulate emissions and high CO emissions are offset by practically no SO_x emissions and little NO_x emissions. NO_x emissions are mainly due to the conversion of nitrogen bound in the fuel. Therefore NO_x emissions are dominated by NO and nitrogen emissions increase with increasing nitrogen content in the fuel [86].

5.6 Blends of UELO with fish oil or pyrolysis oil

Little to no research has been conducted on the combustion and emission properties of blends of UELO with fish oil or pyrolysis oil. Nonetheless identifying research with pyrolysis oil and fish oil blended with diesel fuel or heavy fuel for use in furnaces or boilers is worthwhile since UELO is comparable to diesel fuel or heavy fuel.

UELO is currently used as fuel for small-scale to industrial scale furnaces and boilers as well as in diesel engines and research in UELO recycling is trending towards re-refining UELO into base oil. On the other hand, current methods of using bio-oils such as fish oil or pyrolysis oil as fuel requires pretreatment and preheating to improve combustion properties, blending with other fuels (such as diesel fuel, heavy fuel, or MGO) to improve fuel properties, and sometimes flushing of the combustion equipment with clean fuel to prevent corrosion and scaling [87].

Krutof and Hawboldt have conducted a literature review of pyrolysis oil and fish oil blends with petroleum and other bio-based fuels. Pyrolysis oil or its emulsions has been blended with vegetable oil, biodiesel, and petroleum with the help of non-polar liquids such as liquid hydrocarbons [5].

Fish oil has been blended with diesel fuel at 20 and 50% and heavy fuel at 10 and 50% and it was found that all blends burn easily in tunnel furnaces and residential-scale boilers. The addition of 50% fish oil decreased the kinematic viscosity at 40 °C of heavy fuel from 602 to 19 cSt. In the same blend, the atomization and handling improved significantly compared to heavy fuel. With the exception of NO due to high protein

content in the fish oil, emissions of the blends were lower than of the pure fuel oils. [88]. Adeoti et al. investigated the thermal and flow properties of fish oil blended with diesel fuel oil and observed that viscosity and flash point are decreased in the blends compared to diesel fuel oil [4].

Emulsifications of pyrolysis oil and diesel fuel blends can be miscible with the help of surfactants. However there are many drawbacks including high cost of surfactants, high energy required for the emulsification process, high level of corrosion in the combustion equipment, high water content in the pyrolysis oil, formation of micro-emulsions, poor thermal stability of the emulsions, and the necessity of fresh pyrolysis for the production of emulsions [5].

PART 2 – BLENDING AND COMBUSTION EXPERIMENTS

6 EXPERIMENTAL METHODOLOGY

A first set of experiments assesses physical, chemical, and thermal properties of nine oil/blends: neat reclaimed-UELO (R-UELO), neat salmon fish oil, neat pyrolysis oil, three blends of R-UELO and fish oil (20:80, 50:50, and 80:20 v/v), and three blends of R-UELO and pyrolysis oil (20:80, 50:50, and 80:20 v/v). The selection of properties and characteristics to test was based on studies by Krutof and Hawboldt [5], Adeoti and Hawboldt [4], and Jayasinghe and Hawboldt [6].

In a second set of experiments the combustion and emission characteristics of R-UELO and bio-fuel blends were tested in a pilot scale multi-fuel furnace. The furnace setup was designed and built with the help of Technical Services at Memorial University. The selection of combustion and emission properties to measure was based on studies by Martin and Boateng [89] and Steigers [61], and a 1996 study from the Vermont Agency of Natural [22].

Since this study includes multiple, separate experiments, design of experiment is described in the methodology of each experiment to insure the establishment of validity, reliability, and replicability. The majority of experiments in this study are single factor, single response experiments and are performed in triplicates.

6.1 Production of reclaimed UELO

R-UELO originated from the quick lube oil change operator, Pit Crew Drive Thru Inc. Two Pit Crew locations in St. John's, NL generate 72,000 to 120,000 L of UELO annually. A portion of UELO collected is burned on-site in multi-fuel furnaces, but the majority is reclaimed on-site and sold as low-grade fuel. A flow diagram of the process is shown in Figure 6-1.

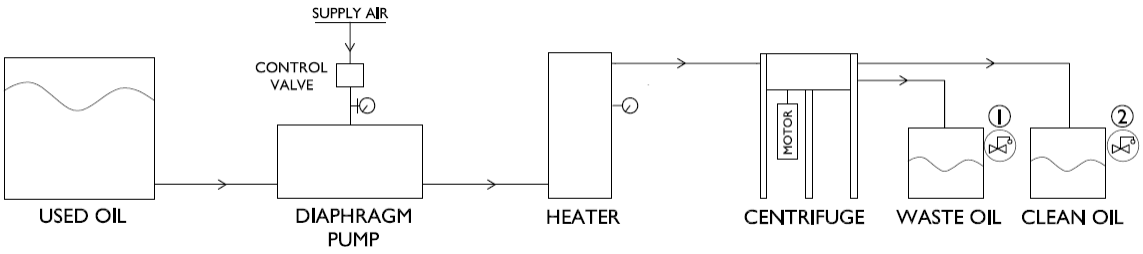

Figure 6-1: Flow diagram of UELO reclamation process at the Pit Crew

Vehicles enter the garage and UELO is emptied into 100 L holding pans. UELO is transferred to and stored in 1040 L international bulk containers, pumped via diaphragm pump past a strainer and in-line heater (100 °C), and fed into a 6000 G centrifuge as shown in Figure 6-2 below.

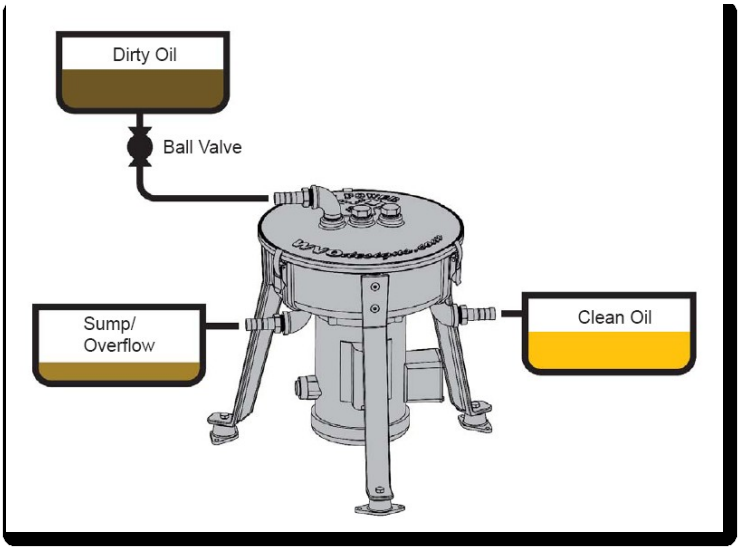

Figure 6-2: Flow diagram of UELO centrifugal separation at the Pit Crew

Heated UELO or "dirty oil" is fed at a constant rate into the centrifuge and separates into four different components: vaporized volatiles, heavy liquid or "sump/overflow", sludge and solid particles, and reclaimed UELO or "clean oil". UELO contains a small percentage of water and gasoline which evaporate when heated. These volatiles either exit through a vent in the centrifuge or condense and drip into the sump container. High density liquids (such as water, glycol, brake fluid, and glycerol) and suspended solids stay in the spinning bowl of the centrifuge until the automatic periodic shut-down every 100 L when they drain out of the centrifuge in to the sump container. Sludge and solid particles accumulate on the walls of the centrifuge, are scrapped off, and are discarded every 1000 L. Reclaimed UELO or "clean oil" exits the spinning bowl due to the lower density compared to the heavy liquid and continuously flows into a final IBC container.

Centrifugal separation is based on separation by density difference. A solid particle under the acceleration of a centrifuge in a liquid phase accelerates until a terminal velocity is

reached, where the acceleration force and the opposing force resulting from frictional drag of the surrounding medium are equal in magnitude. Terminal velocity or settling velocity for small spherical particles is described by, Stokes' law in Equation 6.1.

$$\boldsymbol{v_s = \frac{\Delta \rho d^2 \omega^2 r}{18 \mu}} \qquad \textbf{Equation 6.1}$$

$v_s =$ settling velocity; $\Delta\rho = \rho_S - \rho_L =$ density difference of the solid particle and the liquid; $d =$ diameter of the solid particle; $\omega =$ angular velocity of the particle; $r =$ radius; $\mu =$ absolute viscosity of the medium [90]. Two most important factors in centrifugation are density difference ($\Delta\rho$) and viscosity (μ). Specific gravities of many contaminants are higher than engine oil as shown in Table 6-1.

Table 6-1: Specific gravity of various components of UELO [10]

Component	Specific Gravity
Engine Oil	0.88
Water	1.00
Propylene Glycol	1.04
Brake Fluid	1.05
Ethylene Glycol	1.10
Glycerol	1.13
Calcium	1.55
Magnesium	1.738
Zincdiakyldithiophosphate	1.60
Teflon	2.20
Iron	7.85
Copper	8.96
Lead	11.4

6.2 Production of pyrolysis oil from woody biomass

Softwood pyrolysis oil used in this blending experiment was produced via fast-moderate pyrolysis in a pilot-scale auger reactor at MUN.

The Sexton Lumber sawmill in Bloomfield, NL, provided shavings from balsam fir and the required particle size of 0.1-2.0 mm was achieved with a mill. Since initial moisture content of feedstock was more than 30 wt. %, it was dried for two days at ambient temperature and overnight in an oven at 70 °C, which reduced moisture content to approximately 10 wt. %. The dried feedstock was fed to the auger reactor at 4 kg/h with a pyrolysis temperature of 450 °C. The produced oil was then stored in mason jars at -4°C. Aging of this oil has previously been investigated by Alsbou and Helleur [91].

6.3 Production of fish oil from salmon fish waste

Fish oil used in experiments was produced via the fishmeal process carried out at the Marine Institute (MI) marine bio-processing facility in St. John's NL under the supervision of Wade Murphy and Julia Pohling. Approximately 60 L or 45 kilograms of salmon waste in the form of guts or viscera sourced from a fish processing plant in Harbour Breton, NL was used as feedstock for the oil production. The fish waste was stored in three 55-gallon buckets at -30 °C until ready for the fishmeal process. Thawing the fish waste was accomplished in two steps, 48 hours in -10 °C walk-in fridge and 24 hours at room temperature. The fishmeal process is represented with a process flow diagram in Figure 6-3 and is described in further detail below.

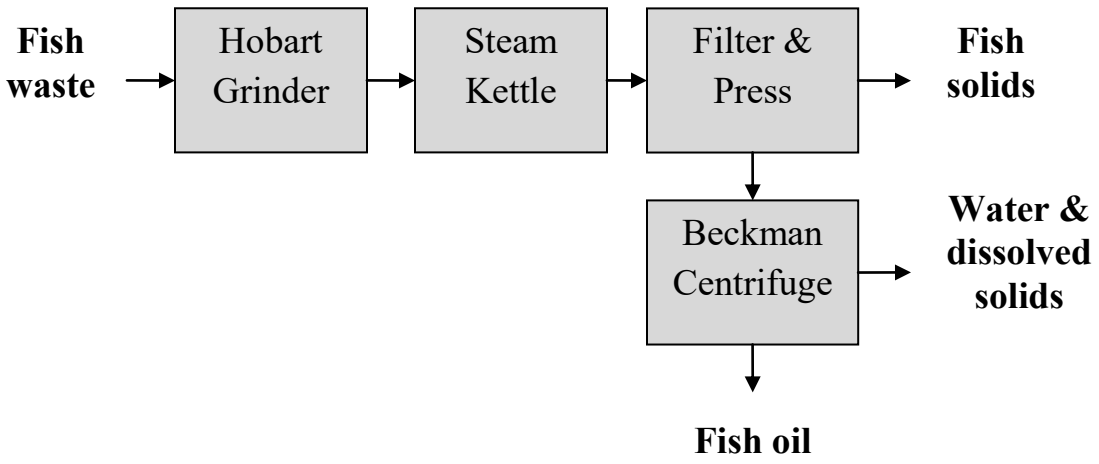

Figure 6-3: Process flow diagram of fish waste processing procedure

Thawed, wet fish waste is put through the Hobart grinder (Model 4146) for homogenization. The Hobart grinder is designed to grind fresh or tempered frozen meats above 26 °F and forces the waste through a 1/8 inch plate using a screw conveyor. The 5-

horsepower, 215-rpm conveyor motor has a magnetic starter and the entire grinder is shown in Figure 6-4 below.

Figure 6-4: Hobart grinder model 4146 at the MI bio-processing facility

In the "cooking" phase of the fishmeal process, homogenized fish waste is heated to 70 °C in a GROEN jacketed mixing kettle (Model RA) from Design and Processing Resources Inc. The direct steam heated kettle is designed to process products that require heating and light to moderate duty mixing. Mixing is accomplished with an agitator that scrapes the entire jacketed interior surface. Shown in Figure 6-5 below, the GROEN kettle has a capacity of 40 gallons and mixing speed of 34 rpm.

Figure 6-5: GROEN jacked mixing kettle model RA at the MI bio-processing facility

Once heated to 70 °C in the kettle, the fish waste is pressed by hand through cheesecloth and a sieve as seen in Figure 6-6 below. The press liquor contains fish oil and is kept for further separation, while the press solids remaining are discarded. Approximately two 5-gallon buckets of press liquor are left from the original three buckets.

Figure 6-6: Cooked fish waste pressed at the MI bio-processing facility

The final separation of fish oil from suspended solids and water is accomplished using the Beckman centrifuge (Model J2-21M/E). The press liquor is reheated to 60 °C and poured into six 500 mL Beckman centrifuge containers. In order to prevent overflowing of the agitated liquid during centrifugation, the containers are filled to approximately two-thirds volume as shown in Figure 6-7 below.

Figure 6-7: Press liquor placed in containers designed for the Beckman centrifuge

The Beckman centrifuge in Figure 6-8 below has a maximum speed of 21,000 rpm, a maximum force of 50,400 times gravity, and a total capacity of 3 L. In this process, the centrifuge is set to 15,000 rpm for 15 minutes and three visible phases are produced: a large volume of oil phase, a small volume of water phase, and an even smaller volume of solid sludge phase. Without disturbing the water and solid phases beneath, the oil phase is poured directly into jars as crude fish oil. The remaining oil with the water phase is poured into funnel separators in order to extract as much oil as possible as shown in Figure 6-9 and the solid phase is discarded.

Figure 6-8: The Beckman centrifuge at MI bio-processing facility

Figure 6-9: Separation funnel at the MI bio-processing facility

The water-oil mixture in the separation funnels are left to settle and the water phase is removed from the bottom. In total, approximately 11 L of crude salmon fish oil is produced from the fishmeal process and placed in mason jars as shown in Figure 6-10.

Figure 6-10: Crude fish oil produced at the MI bio-processing facility

Finally, the fish oil jars are placed in cold storage at -30 °C until they are needed for testing or experiments.

6.4 Blending

Different volume fractions of R-UELO were blended with fish oil and pyrolysis oil to produce six blends: 20:80, 50:50, and 80:20 v/v of both R-UELO and fish oil, and R-UELO and pyrolysis oil. Table 6-2 and Table 6-3 below show concentrations of the six blends and the neat oils. A volume of 500 mL of each blend was produced by stirring the mixture for 20 min at room temperature and phase separation of each blend was observed after 24 hours of refrigeration at 8 °C. All mixtures were stored in a freezer at -30 °C.

Before each experiment, the blends were thawed and shaken thoroughly for 5 minutes at room temperature. Heating the blends to ensure mixing was not implemented as to avoid the aging and degradation reactions of both fish oil and pyrolysis oil [5].

Table 6-2: R-UELO and fish oil blends

Mixture	R-UELO (vol. %)	Fish oil (vol. %)
R-UELO	100	0
F20	80	20
F50	50	50
F80	20	80
F100	0	100

Table 6-3: R-UELO and pyrolsis oil blends

Mixture	R-UELO (vol. %)	Pyrolysis oil (vol. %)
R-UELO	100	0
P20	80	20
P50	50	50
P80	20	80
P100	0	100

6.5 Physical properties

6.5.1 Density (specific gravity)

Density is a fundamental physical property which is used to determine mass-volume relationships. Density was determined by a method similar to ASTM D1217 “Standard Test Method for Density and Relative Density (Specific Gravity) of Liquids by Bingham Pycnometer”. However, a 10 mL Gay-Lussac pycnometer (shown in Figure 6-11) was used instead of a 25 mL Bingham type pycnometer and a ThermoScientific Microprocessor Controlled 280 Series Water Bath used for temperature control was accurate to intervals of 0.1 °C instead of 0.01 °C. An error of ±0.013 °C therefore resulted in an error of ±0.00001 in density for most hydrocarbons (ASTM D1217).

Figure 6-11: Gay-Lussac pycnometer filled with pyrolysis oil

Liquid sample is introduced into the pycnometer at a temperature of 15, 20, 40, or 60 °C, and weighed. The density ρ_s is calculated from the mass m_s and the volume of the pycnometer V_p as shown in Equation 6.2.

$$\boldsymbol{\rho_s(T) = \frac{m_s(T)}{V_p(T)}} \qquad \textbf{Equation 6.2}$$

The volume of the pycnometer V_p is obtained by calibrating the pycnometer with distilled water at different temperatures. The mass of the water in the pycnometer at 15, 20, 40, and 60 °C is divided by the density at the same temperature as seen in Equation 6.3. The density of the distilled water is taken from ASTM D1217.

$$\mathbf{V_p(T) = \frac{m_w(T)}{\rho_w(T)}} \qquad \textbf{Equation 6.3}$$

Note that the mass is not corrected for air temperature in the balance, barometric pressure, or relative humidity as is recommended in ASTM D1217. Moreover, the correction of the cubic coefficient of thermal expansion of borosilicate glass for the mass of the pycnometer at a certain temperature is neglected and the pycnometer is not allowed to cool down to room temperature completely before weighing.

6.5.2 Kinematic viscosity

ASTM standard D7544 recommends measuring kinematic viscosity according to ASTM D445 “Standard Test Method for Kinematic Viscosity of Transparent and Opaque Liquid (and Calculation of Dynamic Viscosity)” because kinematic viscosity measurements are

more reproducible versus dynamic viscosity measurement [73]. However, a rheometer is used to measure dynamic viscosity μ which is then transformed to kinematic viscosity ν through division by density ρ as shown in Equation 6.4.

$$\nu = \frac{\mu}{\rho} \qquad \textbf{Equation 6.4}$$

The rheometer is a Brookefield DV-III Ultra Programmable Rheometer V 6.0 LV. Samples are kept at 20, 40 and 60 °C using a RM3 water circulator from LAUDA-Brinkmann Model S-1 as shown in Figure 6-12. The cylindrical sample cup is filled with 6.7 mL of sample and spindle SC4-18/13RP is used without the spindle guard leg. Rotational speed is increased from 10 rpm in increments of 10 rpm until torque reading exceeded 100%. Accuracy of the measurement is 1% at torque 100%. Therefore, relative error is 1% at a torque of 100% and 10% at a torque of 10%.

Figure 6-12: Rheometer and water bath circulator

6.6 Chemical properties

6.6.1 Water content

Water content (free water and water of hydration) of neat fish oil and neat pyrolysis was determined by Karl Fischer titration previous to this work. Alsbou and Helleur determined water content of ash pyrolysis oil [91]. Water content of R-UELO is very low because a preflash is involved in reclamation. Water content of fish oil from fishmeal process is also very low because water is separated by centrifugation during the production process. Only water content of R-UELO is measured as the water content of neat fish oil and neat pyrolysis oil are known from previous work. Water content of R-UELO and fish oil is negligible compared to water content of pyrolysis oil which is between 20 and 30 wt. % [72].

Water content was determined using a Mettler Toledo C20 Compact Karl Fischer Coulometer according to ASTM E203 "Standard Test Method for Water using Volumetric Karl Fischer Titration". The range of water content measured is 1 ppm to 5 wt. % and the reactions during titration the titration are:

$$2H_2O + SO_2 + I_2 \rightarrow {SO_4}^{2-} + 2I^- + 4H^+$$

$$CH_3OH + SO_2 + RN \rightarrow (RNH) \cdot (CH_3OSO_2)$$

$$(RNH) \cdot (CH_3OSO_2) + I_2 + H_2O + 2RN \rightarrow (RNH) \cdot (CH_3OSO_3) + 2(RNH) \cdot I$$

$$H_2O + I_2 + SO_2 + CH_3OH + 3RN \rightarrow [RNH]SO_4CH_3 + 2[RNH]I$$

where RN is a base.

6.6.2 Elemental analysis and sulfur content

The weight percent of carbon, hydrogen, nitrogen, sulfur, and oxygen were determined using a Thermo Flash 2000 Elemental Analyzer for CHNS and Oxygen. Samples of neat R-UELO and neat fish oil were sent to the analytical and instrumentation laboratory of the University of Alberta, Department of Chemistry. The elemental analysis of pyrolysis oil was determined in a previous work by Alsbou and Helleur [91].

To perform elemental analysis with the Thermo Flash 2000, a sample is placed in a tin capsule and positioned in an oxidation/reduction reactor at a temperature of 900 – 1000 °C. A precise amount of oxygen required for optimal combustion is delivered which reacts with the tin capsule and generates an exothermic reaction which raises the temperature to 1800 °C for a few seconds. At this high temperature both organic and inorganic substances are converted into elemental gases which, after further reduction, are separated in a chromatographic column and finally detected by a highly sensitive thermal conductivity detector (TCD).

Sulfur content can be determined alone according to ASTM D4294 “Standard Test Method for Sulfur in Petroleum and Petroleum Products by Energy Dispersive X-ray Fluorescence Spectrometry”. The sulfur content of neat R-UELO, neat fish oil, and pyrolysis oil are not measured by this method in this study.

6.7 Thermal properties

6.7.1 Heating value

Heat available by a fuel is determined by heat of combustion. It is essential in calculations of thermal efficiency for equipment producing either power or heat. Heating value or heat of combustion is a requirement in most fuel standards.

The method used to determine gross heat of combustion of R-UELO, fish oil, pyrolysis oil, and their blends is ASTM D240 "Standard Test Method for Heat of Combustion of Liquid Hydrocarbon Fuels by Bomb Calorimeter". The measurement is carried out in a Parr B41 calorimeter with the 1108 Oxygen Combustion Bomb and a Model 6775 Digital Thermometer.

The bomb is pressurized with oxygen to 29 bar for each run. The heat of combustion of the fuse wire ΔU_{Wire} is 1400 cal/g or 5.8576 kJ/g. In order to prevent the loss of volatiles, combustion is carried out using two-piece Parr Gelatin Capsules for all samples instead (Capsule Size 00, CAS# 9000-70-8, capacity 0.9 mL). Heat of combustion of the flattened capsules is determined in triplicates and subtracted from heat of combustion of the sample. Parr Benzoic Acid Standard CAS# 65-85-0 with a heat of combustion ΔU_{BA} of 26.454 MJ/kg is used to determine W: the energy equivalent of the calorimeter. Three tests with a mass of benzoic acid standard m_{BA} of about 1 g of benzoic acid are carried out to determine W. The energy equivalent W is determined according to Equation 6.5.

$$\boldsymbol{W = \frac{\Delta U_{BA} \cdot m_{BA} + e_1 + e_3}{\Delta T}}$$ **Equation 6.5**

where e_1 is the correction for heat of formation of nitric acid (MJ) and e_3 is the correction for heat of combustion of firing wire (MJ).

Heat of formation of nitric acid is neglected and the correction for heat of combustion of firing wire e_3 is calculated by multiplication of heat of combustion of the wire ΔU_{Wire} with mass of combusted wire m_{Wire} as shown in Equation 6.6 below.

$$\mathbf{e_3 = \Delta U_{Wire} \cdot m_{Wire}}$$ **Equation 6.6**

Corrected temperature rise ΔT is calculated according to Equation 6.7 below.

$$\mathbf{\Delta T = T_c - T_a - r_1 \cdot (b - a) - r_2 \cdot (c - b)}$$ **Equation 6.7**

Where a is time of firing, b is time when temperature rise reaches 60% of total rise, and c is start time of the period after combustion in which the rate of temperature change with time is constant. Temperatures at time a and time c are T_a and T_c, respectively and rate at which temperature changes during the 5 min period before firing r_1 in °C/min is determined by the slope of temperature over time. Rate in °C/min at which temperature changes after time c is r_2. To determine time b when temperature rise reaches 60% of total rise, temperature at this time is first calculated as shown in Equation 6.8 below.

$$\mathbf{T_b = [0.6 \cdot (T_c - T_a)] + T_a}$$ **Equation 6.8**

If temperature T_b at time b is known, time b is calculated by linear interpolation between the measurement before temperature T_b at time b_{-1} and after temperature T_b at time b_{+1} as shown in Equation 6.9 below.

$$\mathbf{b = b_{-1} + (b_{+1} - b_{-1}) \frac{T_b - T_{b-1}}{T_{b+1} - T_{b-1}}} \qquad \textbf{Equation 6.9}$$

After determining energy equivalent of calorimeter W in MJ/°C according to Equation 6.5, heat of combustion of gelatin capsules $\Delta U_{Capsule}$ is measured from Equation 6.10.

$$\mathbf{\Delta U_{Capsule} = \frac{\Delta T \cdot W - e_3}{1000 \cdot m_{Capsule}}} \qquad \textbf{Equation 6.10}$$

Finally, gross heat of combustion of sample at constant volume ΔU_g in MJ/kg is calculated according to Equation 6.11 below.

$$\mathbf{\Delta U_g = \frac{\Delta T \cdot W - e_1 - e_2 - e_3}{1000 \cdot m_S}} \qquad \textbf{Equation 6.11}$$

where e_1 (correction for heat of formation of nitric acid) and e_2 (correction for heat of formation of sulfuric acid) are neglected. Weight of each sample m_s is about 0.5 g for each run (ASTM D7544 – 12).

Lower heating value or net heat of combustion at 25 °C or $\Delta U_n(\text{net, } 25\,°C)$ can be calculated by Equation 6.12 below.

$$\mathbf{\Delta U_n(net, 25\,°C) = \Delta U_g(gross, 25\,°C) - 0.2122 \cdot H} \qquad \textbf{Equation 6.12}$$

where H is mass percentage of hydrogen in the sample (ASTM D240).

6.7.2 Thermo-gravimetric analysis (TGA) and ash content

A TGA Q500 from TA Instruments was used according to ASTM E1131 "Standard Test Method for Compositional Analysis by Thermogravimetry".

Triplicates of a 15 mg sample are heated at 20 °C/min to 800 °C on a platinum pan. Furnace is purged with 50 mL/min of nitrogen and at 600 °C, gas is switched over from nitrogen to 50 mL/min of oxygen until the remaining carbon burns and ash is left. The temperature at which gas is switched is chosen when a mass loss plateau is established. If gas is switched from nitrogen to oxygen at a higher temperature, carbon in the samples slowly burns off because the furnace cannot be sealed from ambient oxygen completely. Described in Table 6-4, mass loss is divided into highly volatile matter, medium volatile matter, combustible material, and ash. Ash content is an important property of a fuel. Depending on size and type e.g. sand, or char, the particles can contribute to the wear of burner pumps and valves and decrease fuel efficiency by fouling heat exchanger surfaces.

Table 6-4: Division of groups of matter as per ASTM E1131

Components	Description of term as per ASTM E1131
Highly volatile matter	moisture, plasticizer, residual solvent or other low boiling point components (200 °C or less)
Medium volatile matter	oil and polymer degradation products in the range of 200 to 750 °C
Combustible material	oxidizable material not volatile at 750 °C, or some stipulated temperature dependent on the material
Ash	non-volatile residues in an oxidizing atmosphere which may include metal components, filler content or inert reinforcing materials

The equations below and temperatures X, Y, and Z equation are used in order to calculate the weight percentage of the four component divisions. Temperature X is taken in the center of the first mass loss plateau or, if no plateau exists, at an agreed upon temperature value less than 200 °C. Temperature Y corresponds to the mass loss plateau between 200 and 800 °C and is close to or before the temperature used for switching from inert to reactive atmospheres. Temperature Z corresponds to the residual weight after the evolution of carbon dioxide and is not necessarily the final temperature because the ash components of some materials slowly oxidize and gain weight at high temperatures. Equation 6.13, Equation 6.14, Equation 6.15, and Equation 6.16 are used to calculate the amount of highly volatile matter, medium volatile matter, combustible material, and ash content, respectively.

$$\boldsymbol{V = \frac{W - R}{W} \times 100\%} \qquad \textbf{Equation 6.13}$$

where V = highly volatile matter (wt. %), W = original mass of sample (mg), and R = mass of sample at Temperature X (mg).

$$\boldsymbol{O = \frac{R - S}{W} \times 100\%} \qquad \textbf{Equation 6.14}$$

where O = medium volatile matter (wt. %), R = mass of sample at Temperature X (mg), S = mass of sample at Temperature Y, and W = original mass of sample (mg).

$$\boldsymbol{C = \frac{S - T}{W} \times 100\%} \qquad \textbf{Equation 6.15}$$

where C = combustible material (wt. %), S = mass of sample at Temperature Y, T = mass of sample at Temperature Z (mg), and W = original mass of sample (mg).

$$\boldsymbol{A = \frac{T}{W} \times 100\%} \qquad \textbf{Equation 6.16}$$

where A = ash content (wt. %), T = mass of sample at Temperature Z (mg), and W = original mass of sample (mg).

6.7.3 Flash point

Flash point is the maximum temperature at which oil can be stored and handled without serious fire hazard (ASTM D7544). Flash point is measured in accordance with ASTM D93 "Standard Test Method for Flash Point by Pensky-Martens Closed Cup Tester". The sample is heated and stirred in a covered brass cup and an ignition source is directed into the test cup at regular temperature intervals. Flash point is observed when a flash is seen in the test cup. Water content of R-UELO and fish oil is close to zero and therefore flash point can be determined without problems. However, flash point of pyrolysis oil is reportedly difficult to measure due to high water content and does not correlate with ignition properties as it does for mineral oil [72]. Although pyrolysis oil is ignited above 500 °C, a low flash point is observed when volatile compounds are present but evaporated water extinguishes the flame instantly [5].

For these experiments, only flash point of neat R-UELO is measured as neat fish oil and pyrolysis oil were determined from previous works of Alsbou and Helleur and Krutof and Kelly [91, 5].

6.8 Pilot-scale multi-fuel furnace experiments

A custom-built pilot-scale multi-fuel furnace was used to determine combustion and emission characteristics for R-UELO and bio-fuel blends with diesel fuel as the reference fuel. Physical, chemical, and thermal properties of R-UELO and bio-fuel blends determined previously are applied to screen the suitability of combusting the blends in the furnace. Exhaust gas color, start-up and ignition characteristics, and combustion residues were observed during the combustion. Fuel flow rate, fuel pre-heat temperature, combustion chamber and exhaust gas temperatures, and O_2, CO, H_2S, and CH_4 concentrations in the exhaust gas were measured during combustion. Finally, a GC-TCD was used to analyze the concentration of the exhaust gas.

Construction and commissioning using diesel fuel of the furnace was completed with help from Dennis Cramm at MUN Technical Services, Dr. Peter Fransham at Abritech Inc., Dmitry Chebotarenko at Nortec Pro, Hubert Alacoque at Newfoundland Energy Services Limited, and work term students Joachim Urbanek and Chanciee Ossihou.

The entire furnace sits on a trailer bed and includes a 20-L day tank, a lifting unit, a Nortec WB 40 multi-fuel burner, and a combustion chamber as shown in Figure 6-13 below. Fuel is drawn from the day tank to the burner by the lifting unit and is heated in the preliminary fuel heating box before being mixed with compressed air and sent through the air atomizing nozzle. The burner flame shoots into the combustion chamber and flue gases exit the stack fitted with a spark arrester.

Figure 6-13: The custom-built pilot-scale multi-fuel furnace

The 20-L horizontal cylindrical day tank sits on the movable aluminum cart attached via 6-foot cables to the furnace. During combustion, the day tank is moved at least six feet away from the furnace for safety. Fuel is dispensed into the tank through a removable

cover and exits via gravity from a one-inch hole at the bottom. As shown in Figure 6-14, the day tank outlet is equipped with ball valves on the pump line and a drain.

Figure 6-14: 20-L day tank equipped with two ball valves

As shown in Figure 6-15 below, the lifting unit is an electric gear pump with a fuel filter attachment connected via flexible tube.

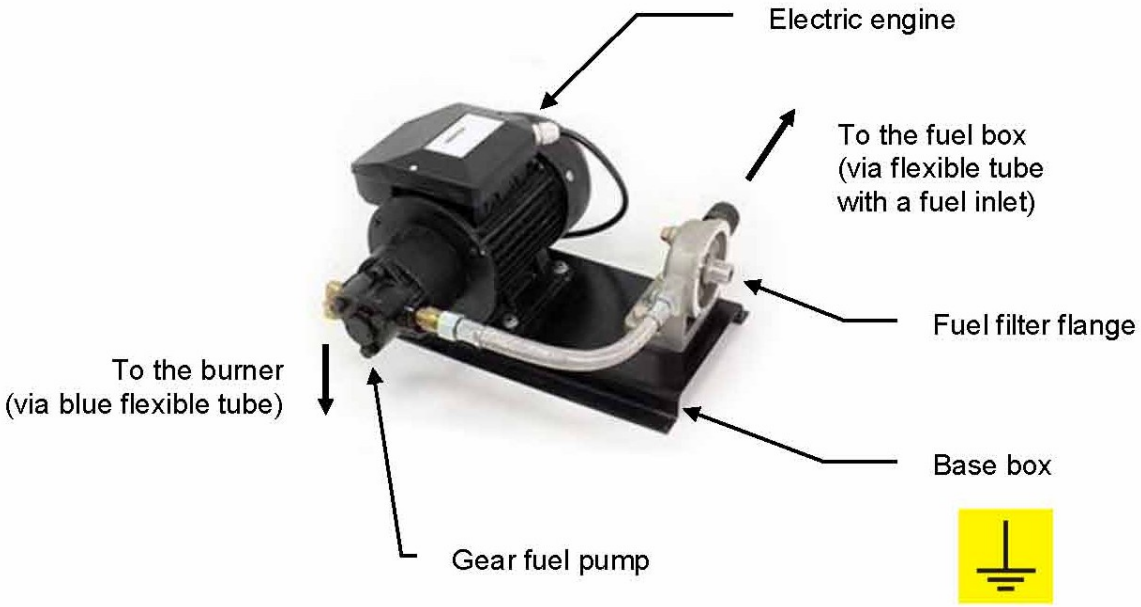

Figure 6-15: Gear pump with disposable fuel filter

Fuel is pre-heated in the preliminary fuel heating box equipped with two immersion heated controlled by two thermostat dials (T1 and T2). Compressed air is regulated by a valve and is pre-heated by passing through a copper pipe inside the fuel heating box. Fuel and air are sent through the atomizing nozzle and are ignited with an electric spark. The burner continues to combust fuel until the photocell sensor indicates a lack of flame or until there is no more fuel in the preliminary fuel heating box. The burner (shown in Figure 6-16) directs the flame into the combustion chamber made of refractory lined steel and exhaust gases exit the 8-foot high by 6-inch diameter stack fitted with temperature probes, gas analyzer ports, and a spark arrester.

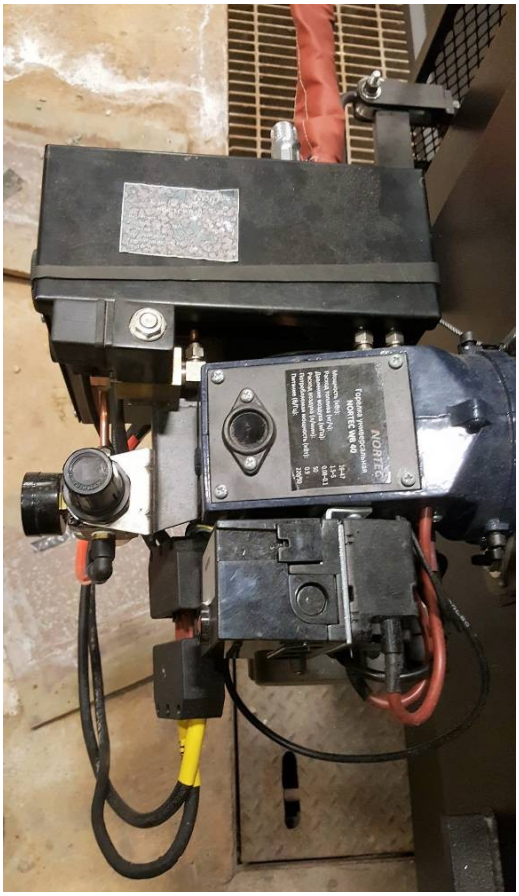

Figure 6-16: Nortec WB 40 burner

Primary air atomizing pressure (5 to 15 psi), secondary air intake opening (0 to 10 cm), and pre-heat temperatures (T1 and T2) are determined for each new fuel so that complete combustion is attained. Occurrence of complete combustion is established by observing exhaust gas color and measuring O_2 exhaust gas concentration in the stack. Exhaust gas during complete combustion is transparent in color instead of smoking dark or white. O_2 exhaust gas concentration during complete combustion is between 3% and 6%.

The Testo 325-1 flue gas analyzer monitors composition and conditions of exhaust gas in a furnace. The device measures oxygen (vol. %), carbon monoxide (ppm), and

temperature with a probe inserted into the stack. Oxygen measurement range is 0 to 21 vol. % with a resolution of 0.1 vol. % and temperature measurement range is -40 to 600 °C with a resolution of 0.1 °C. Figure 6-17 shows the flue gas analyzer.

Figure 6-17: Testo 325-1 flue gas analyzer (testo.com)

The Gas Alert MicroClipXT (Figure 6-18) is a detector that warns of hazardous gas at levels above user-defined set points. Calibrated with a gas mixture of 100 ppm CO, 25 ppm H_2S, 2.5 vol. % methane, and 18 vol. % oxygen, detection ranges are 0 to 500 ppm for CO, 0 to 100 ppm for H_2S, 0 to 5 vol. % for methane, and 0 to 30 vol. % for oxygen.

Figure 6-18: Gas Alert MicroClip XT (gasalertmicroclipxt.com)

Two type K thermocouple probes measure the temperatures in the chamber and the stack. One is placed in the side of the combustion chamber approximately 50 centimeters below stack entrance and the other is placed half-way up the stack with the probe tip in the center of the stack. Temperature measurements provide an indication of efficiency and of operating temperature for each fuel. The portable RDXL4SD 4-channel Omega data logger (Figure 6-19) is a handheld thermometer and data logger with thermocouple inputs, backlight display, and is capable of saving data on an SD memory card with a sampling time of one measurement per second.

Figure 6-19: 4-Channel Omega Handheld Thermometer (omega.com)

The furnace test run protocol begins with warming up the refractory lined chamber with diesel oil or R-UELO until stack temperatures are measured above 400 °C. In winter conditions with ambient temperatures of around 0 °C, this warm-up process takes up to two hours. The furnace is shut off, the tank is switched to the fuel used in the run, and the furnace is restarted. When measured temperatures have once again reached 400 °C, exhaust gas is extracted from the stack into a sample gas cylinder and analyzed with an Agilent 490 Micro Gas Chromatograph (GC). The sample gas cylinder as shown in Figure 6-20 below is connected to one of the ports in the stack while the furnace is running. On the other end, negative pressure is created with an electric vacuum pump in order to pull the emissions from the stack into the cylinder.

Figure 6-20: Sample gas cylinder used to capture emission gases

The Micro GC uses a thermal conductivity detector (TCD) to analyze the sample. GC-TCDs detect and produce voltages proportional to the difference in thermal conductivity between the column effluent flow (carrier gas + sample components) and the reference flow of carrier gas alone. The Micro GC is a equipped with heated injectors and samples lines, both set to 110 °C, to eliminate any clod spots and prevent possible condensation of moisture, and to ensure the integrity of the sample is maintained throughout the sample flow path. The gas sample passes through two parallel columns with helium as the inert carrier gas: the 10-meter PoraPLOT U heated column and the 8-meter CP-Sil 5 CB heated column. The PoraPLOT U column is used to separate carbon dioxide from the composite air peak and can also analyze methane, ethane, and propane.

The 8-meter CP-Sil 5 CB is used to analyze hydrocarbons from C1 to C10. The setup parameters for the columns are found in the table below.

Table 6-5: Setup parameters for Micro GC columns

Column Parameter	PoraPLOT U, 10 m	CP-Sil 5 CB, 8 m
Carrier gas	helium, 22 psi	helium, 22 psi
Column temperature	150°C	50 °C
Injector temperature	100 °C	100 °C
Injection time	240 ms	240 ms
Backflush time	0 sec	-
Run time	120 sec	120 sec

Chromatographic data is presented as a graph of detector response (volts) against retention time (seconds) which is called a chromatogram. The height of a peak and the area under a peak is proportional to the amount of that molecule present in the sample. Therefore, by using the Agilent computer software to draw and integrate peaks, the concentration of a specific molecule in the original sample can be determined. In interpreting the results, peak heights can vary due to non-Gaussian distortion of the peak shapes such as the broadening, fronting, or tailing. The area under a peak is calculated by the software based on integration and is more accurate for quantitative chromatographic estimation. Peak area is used in this study and duplicates for each sample are analyzed by the Micro GC.

7 RESULTS AND DISCUSSION

7.1 Blending

No phase separation is observed in R-UELO/fish oil blends or in R-UELO/pyrolysis oil blends as shown in Table 7-1 below.

Table 7-1: Phase separation of R-UELO/fish oil and R-UELO/pyrolysis oil blends

Mixture	% Volume R-UELO	% Volume fish oil	% Volume pyrolysis oil	Phase separation
F20	80	20	-	NO
F50	50	50	-	NO
F80	20	80	-	NO
P20	80	-	20	NO
P50	50	-	50	NO
P80	20	-	80	NO

A lack of phase separation indicates miscibility in R-UELO/fish oil blends because neat R-UELO and neat fish oil are contrasting in color (black and orange respectively). Figure 7-1 below shows the 50/50 vol. % blend of R-UELO and fish oil. Furthermore, previous studies show salmon and other fish oil is miscible with similar petroleum-based fuels such as diesel and bunker fuels [4, 61, 5].

However a lack of phase separation does not indicate miscibility in R-UELO/pyrolysis oil blends because neat R-UELO and neat pyrolysis oil are the same color and phase separation is impossible to observe as shown in Figure 7-2. Previous research on pyrolysis oil shows that it contains a polar phase that is immiscible with similar petroleum-based fuels such as diesel [5].

Figure 7-1: 50/50 vol. % blend of R-UELO and fish oil

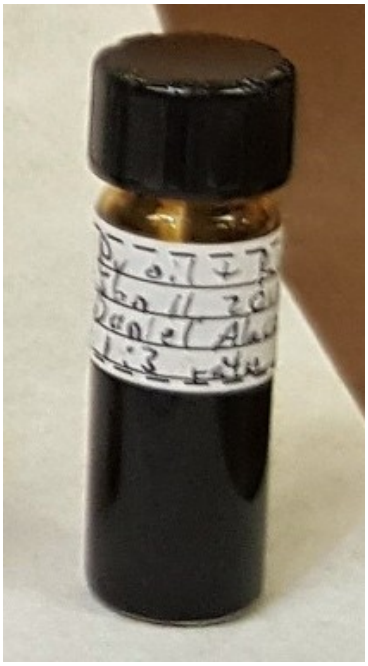

Figure 7-2: 3:1 by mass of pyrolysis oil:R-UELO

7.2 Physical properties

7.2.1 Density

A summary of the results of the density measurements at 25, 40, and 60 °C for neat R-UELO, neat fish oil, neat pyrolysis oil, and all blends are shown in Figure 7-3 below.

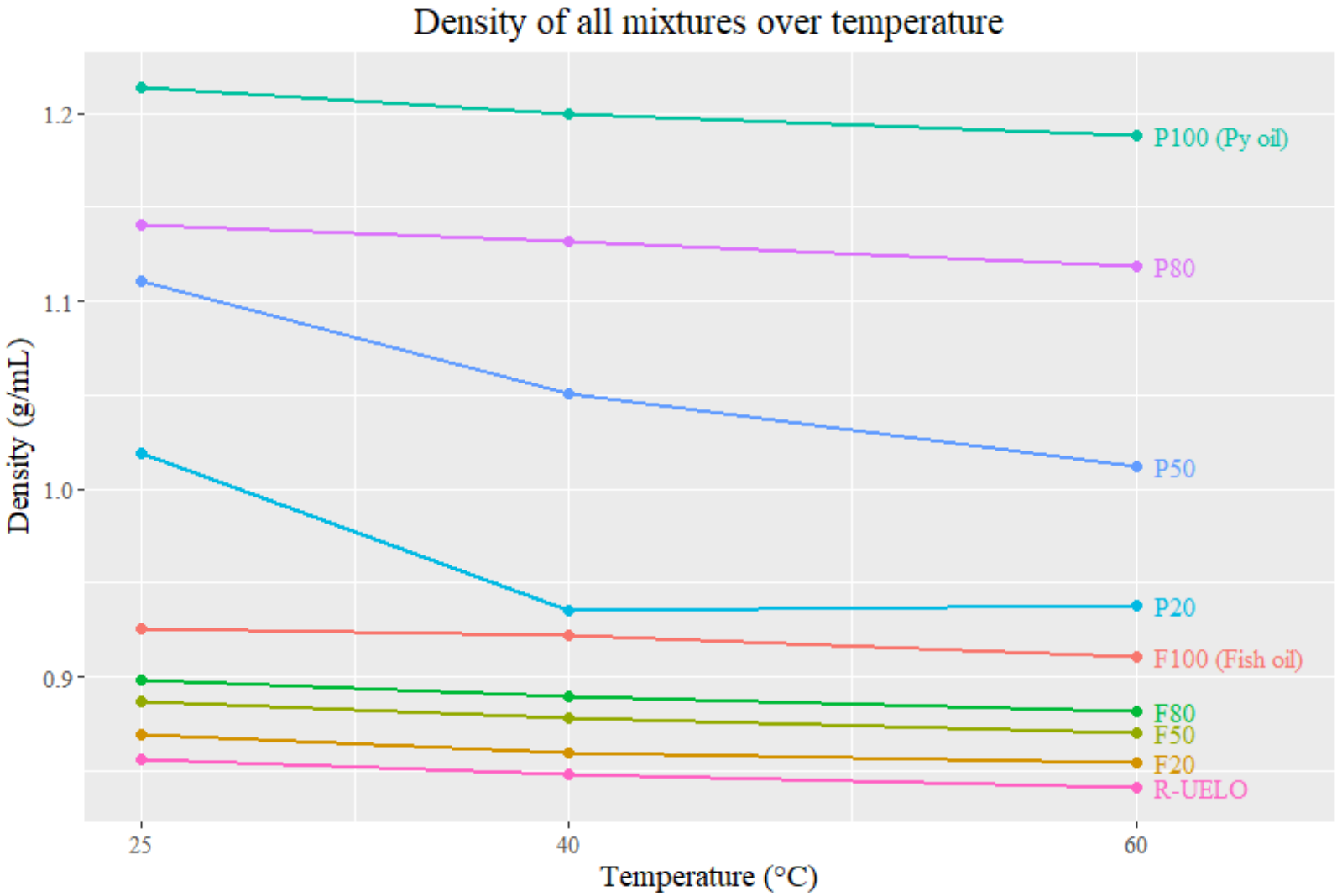

Figure 7-3: Density measurements for all mixtures for three different temperatures

The densities of neat R-UELO (0.841 to 0.856 g/ml) are closer in value to neat fish oil (0.911 to 0.926 g/ml) than neat pyrolysis oil (1.188 to 1.214 g/ml). A large difference in density is one of the reasons why pyrolysis oil is immiscible with R-UELO. Figure 7-4 and Figure 7-5 show densities over volume fraction of R-UELO/fish oil mixtures and R-UELO/pyrolysis oil mixtures respectively.

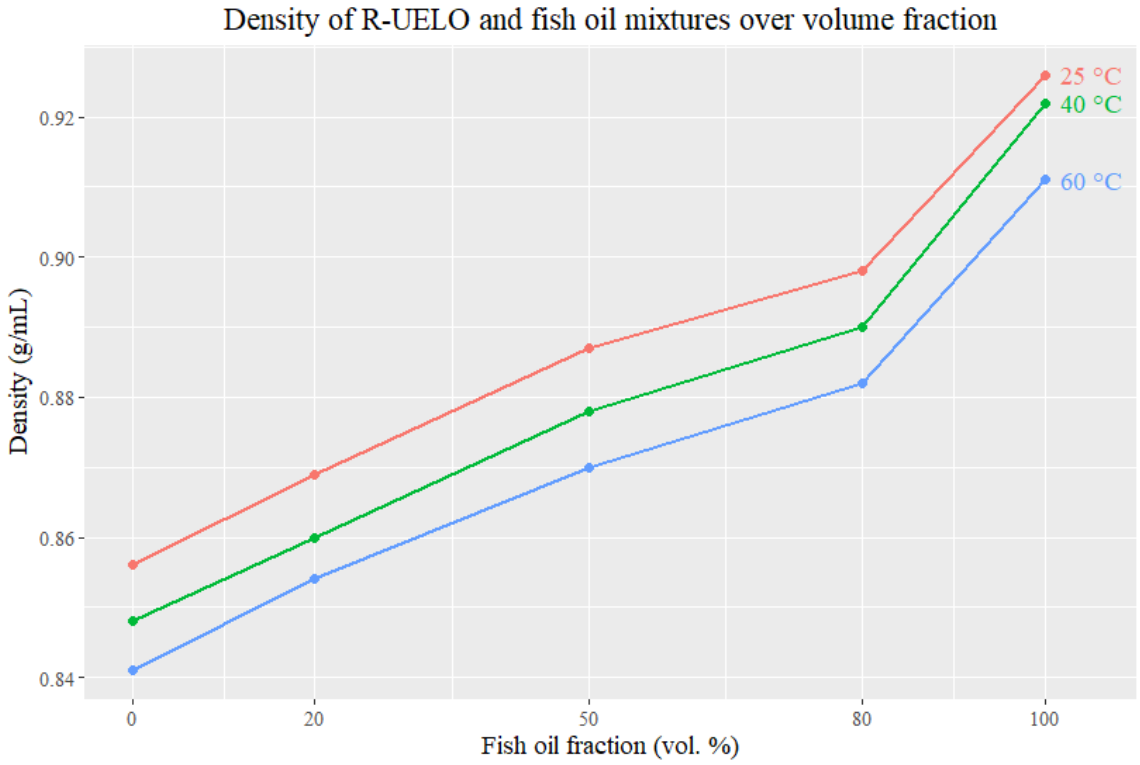

Figure 7-4: Densities of R-UELO/fish oil mixtures at different volume fractions

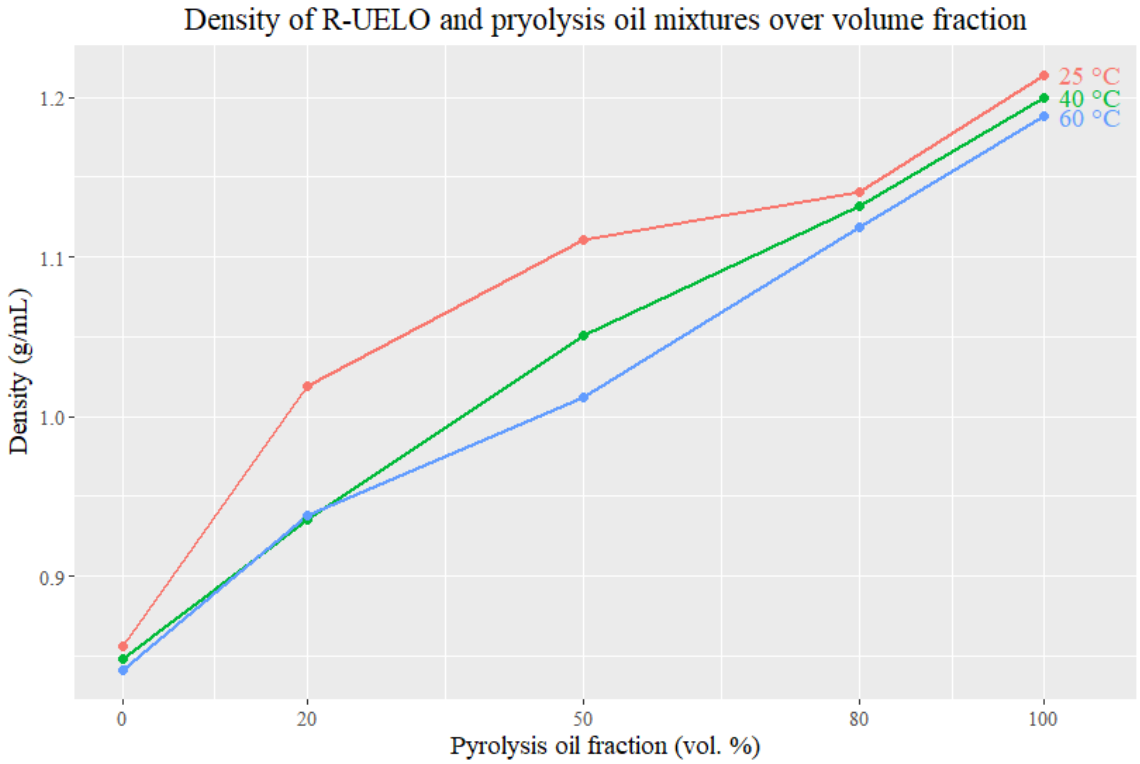

Figure 7-5: Densities of R-UELO/pyrolysis oil mixtures at different volume fractions

Following the assumption of miscibility in all R-UELO/fish oil blends, the lines in Figure 7-4 are expected to be completely linear. However, the 80 vol. % fish oil fraction is skewed off-linear by the same amount at all three temperatures, indicating human measurement error involved in creating that specific blend. The actual fish oil fraction is likely less than 80 vol. %.

As seen in Figure 7-5, the densities for the 20 and 50 vol. % pyrolysis oil fractions are also non-uniformly skewed off-linear. One explanation is the presence of emulsions in samples before being poured into the pycnometer. Although samples are mixed thoroughly at room temperature, it is likely 20 and 50 vol. % pyrolysis oil fractions have more difficulty homogenizing their emulsions than 80 vol. % pyrolysis oil fraction.

7.2.2 Kinematic viscosity

The kinematic viscosities of neat R-UELO, fish oil, and pyrolysis oil are shown in Table 7-2 below.

Table 7-2: Kinematic viscosities of the neat oil mixtures

Temperature (°C)	R-UELO (cSt)	Fish oil (cSt)	Pyrolyis oil (cSt)
20	121.28	75.49	68.60
40	48.06	31.35	20.90
60	23.24	3.58	8.87

In general, R-UELO has a higher kinematic viscosity than fish oil and pyrolysis oil. Furthermore, the difference of kinematic viscosity between R-UELO and fish oil increases as temperature increases with the largest difference being observed at 60 °C.

On the following page, Figure 7-6 and Figure 7-7 show kinematic viscosity over temperature and volume fraction for R-UELO/fish oil mixtures and R-UELO/pyrolysis oil mixtures respectively. Appendix 10.1 shows the raw viscosity data with statistical error.

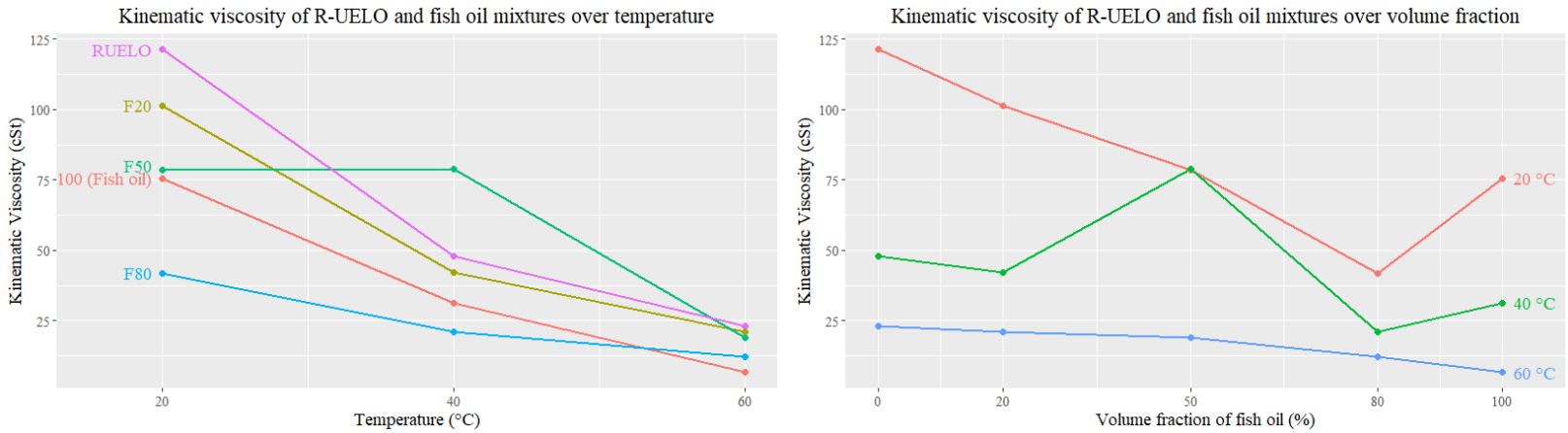

Figure 7-6: Kinematic viscosity of R-UELO/fish oil mixtures at various temperatures

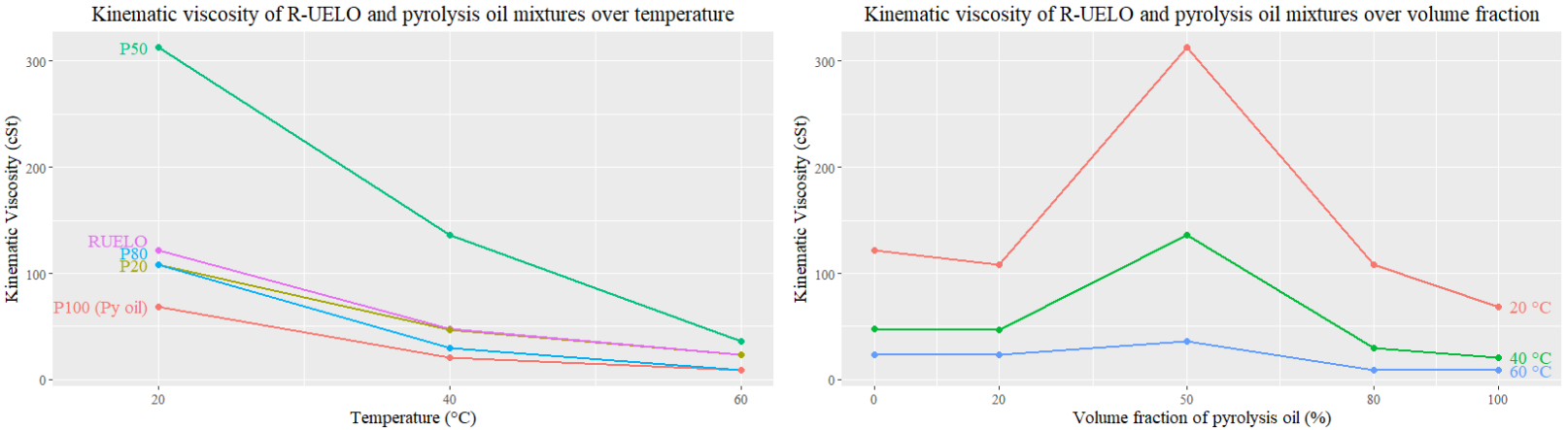

Figure 7-7: Kinematic viscosity of R-UELO/pyrolysis oil mixtures at various temperatures

Addition of fish oil to R-UELO lowers kinematic viscosity in almost all cases as shown on the right graph of Figure 7-6. Kinematic viscosities of R-UELO/fish oil mixtures at 60 °C are close to linear with respect to volume fraction. However, kinematic viscosities of R-UELO/fish oil mixtures at 20 and 40 °C show non-linearity with respect to volume fraction as can be seen from kinematic viscosity of the 50/50 vol. % R-UELO/fish oil blend at 40 °C (green line). Duplicates for this specific mixture resulted in an error of ±0.28 cSt and the result is likely due poor miscibility of the 50/50 vol. % R-UELO/fish oil blend at 40 °C. As shown in Figure 7-7, the 50/50 vol. % R-UELO/pyrolysis oil blend shows an unexpectedly high kinematic viscosity at all temperatures and especially at 20 °C. These spikes are likely from disturbances in the spinning mechanism of the rheometer caused by emulsions in the mixture from poor miscibility. Emulsions could have resulted in abnormal shear forces and therefore viscosity. Krutof and Hawboldt (2016) and Adeoti et al. (2014) observed similar anomalous measurements with a Brookfield rheometer for a 50/50 vol. % fish oil/pyrolysis oil blend and a 50/50 vol. % fish oil/petroleum fuel blend [5, 4].

7.3 Chemical properties

7.3.1 Water content

Table 7-3 below shows water content of neat R-UELO, fish oil, and pyrolysis oil.

Table 7-3: Water content of neat fuels using Karl Fischer

Neat fuel	Water content
R-UELO	0.16 wt. %
Fish oil [a]	0.05 wt. %
Pyrolysis oil [a]	between 20 and 30 wt. %

[a] known from previous reference [5, 4]

Water is mostly immiscible in R-UELO and fish oil so it can be removed with simple physical and thermal separation techniques such as centrifugation and heating [10, 5]. Water content of R-UELO is low because water is separated with heat and centrifugation in the reclamation process and water content of fish oil is low because water is separated by centrifugation in the production process. Water is difficult to remove from pyrolysis oil because the aqueous emulsion is miscible with water.

Krutof and Hawboldt (2016) show that compared to neat pyrolysis oil, fish oil and pyrolysis oil blends have lower water content which result in higher heating value and higher viscosity [5]. It is expected that R-UELO and pyrolysis oil blends show the same characteristics.

7.3.2 Elemental analysis and sulfur content

Elemental analysis for neat R-UELO and neat fish oil obtained from the analytical laboratory of the University of Alberta are shown in Table 7-4 below. Carbon, hydrogen, nitrogen, and sulfur are measured directly, and oxygen is calculated by difference.

Table 7-4: Elemental analysis results for R-UELO, fish oil, and pyrolysis oil

Neat fuel	Carbon	Hydrogen	Nitrogen	Sulfur	Oxygen
R-UELO	84.3 wt. %	13.9 wt. %	0.26 wt. %	0.22 wt. %	1.06 wt. %
Fish oil	77.4 wt. %	11.3 wt. %	0.00 wt. %	0.00 wt. %	11.3 wt. %
Pyrolysis oil [a]	41.4 wt. %	4.3 wt. %	0.2 wt. %	0.00 wt. %	25.5 wt. %

[a] known from previous reference [91]

Carbon and hydrogen content of neat R-UELO is higher than neat fish oil and pyrolysis oil which likely accounts for higher heating values because carbon has a higher heating value than the other elements. Low sulfur content is desired for combustion to avoid formation of SO_x products in emissions [22]. The high oxygen content (25.5 wt. %) in neat pyrolysis oil is due to high amounts of water (up to 30 wt. %), aldehydes (up to 20 wt. %), acids (up to 15 wt. %), and alcohols (up to 5 wt. %) [68, 70].

7.4 Thermal properties

7.4.1 Heating value

Table 7-5 shows heating value or HHV of neat R-UELO, fish oil, and pyrolysis oil.

Table 7-5: HHV results of neat fuels

Neat fuel	Heating value (HHV)
R-UELO	45.39 MJ/kg
Fish oil	36.76 MJ/kg
Pyrolysis oil	18.55 MJ/kg

Heating value of neat fish oil and pyrolysis oil is lower than neat R-UELO and correspond to values obtained from previous studies [92, 5]. Heating value of neat pyrolysis oil is much lower than neat R-UELO because of high water content in the pyrolysis oil. Figure 7-8 shows heating values for R-UELO/fish and R-UELO/pyrolysis oil blends. As heating value of blends is approximately the fractional average of the individual components, it is expected that blends of R-UELO and fish oil have higher heating values than blends of R-UELO and pyrolysis oil. The heating value of the 80/20% vol. blend of R-UELO/pyrolysis oil is very close to neat R-UELO likely because of lack of miscibility and difficulty mixing between R-UELO and pyrolysis oil. Heating values of R-UELO/fish oil blends are more suitable for combustion.

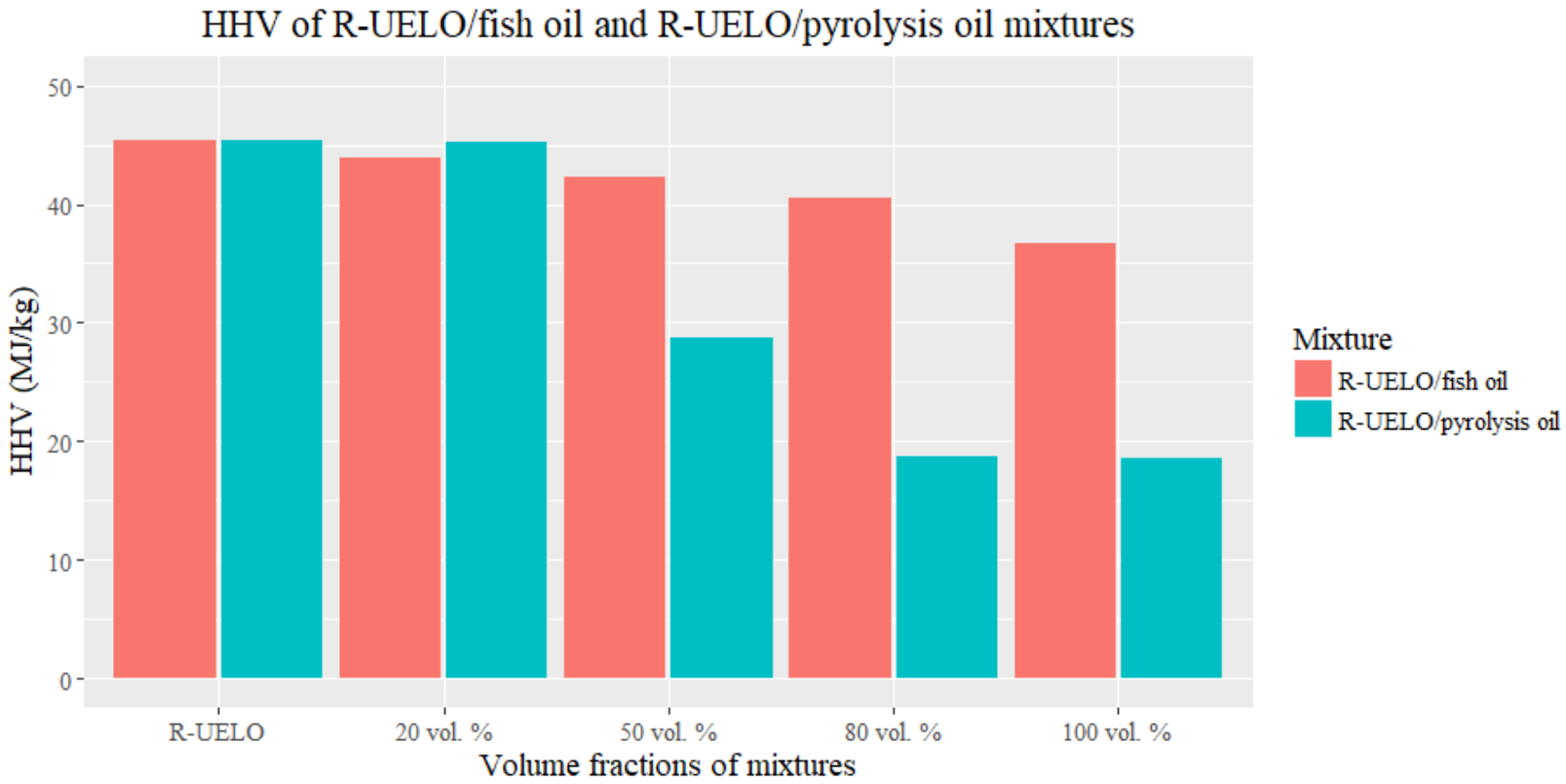

Figure 7-8: Heating value (HHV) of R-UELO/fish oil and R-UELO/pyrolysis oil blends

7.4.2 Thermo-gravimetric analysis (TGA) and ash content

Figure 7-9 and Figure 7-10 show the TGA curves for R-UELO/fish oil mixtures and R-UELO/pyrolysis oil mixtures respectively.

Neat R-UELO is stable up to around 250 °C, neat fish oil is stable up to around 200 °C, and neat pyrolysis oil begins to thermally degrade immediately due to the high amount of volatiles and water. R-UELO decomposes rapidly until 400 °C where approximately 7 wt. % remains and then slowly until oxygen is added at 600 °C. Fish oil decomposes rapidly until 300 °C where approximately 57 wt. % remains and from 300 to 500 °C, the rate of decomposition decreases. At 500 °C, approximately 11 wt. % remains and decomposition nearly stops completely until oxygen is added at 600 °C. Fish oil and R-UELO have a cross-over point at 335 °C when fish oil decomposition becomes slower than R-UELO decomposition. Pyrolysis oil decomposes rapidly until 300°C where approximately 50 wt. % remains. The rate of decomposition continually decreases until 500 °C where approximately 16 wt. % remains and increases again from 500 °C until the addition of oxygen at 600 °C. Pyrolysis oil and R-UELO have a cross-over point at 370 °C when pyrolysis oil decomposition becomes slower than R-UELO decomposition.

The blends of R-UELO and fish oil (F20, F50, and F80) roughly fit the predicted curves in between the curves of neat R-UELO and fish oil. However, the blends of R-UELO and pyrolysis oil (P20, P50, and P80) are not equally spaced between the curves of neat R-UELO and pyrolysis oil. This is likely due to the immiscibility of R-UELO and pyrolysis oil resulting in emulsions in the 5 mL syringe.

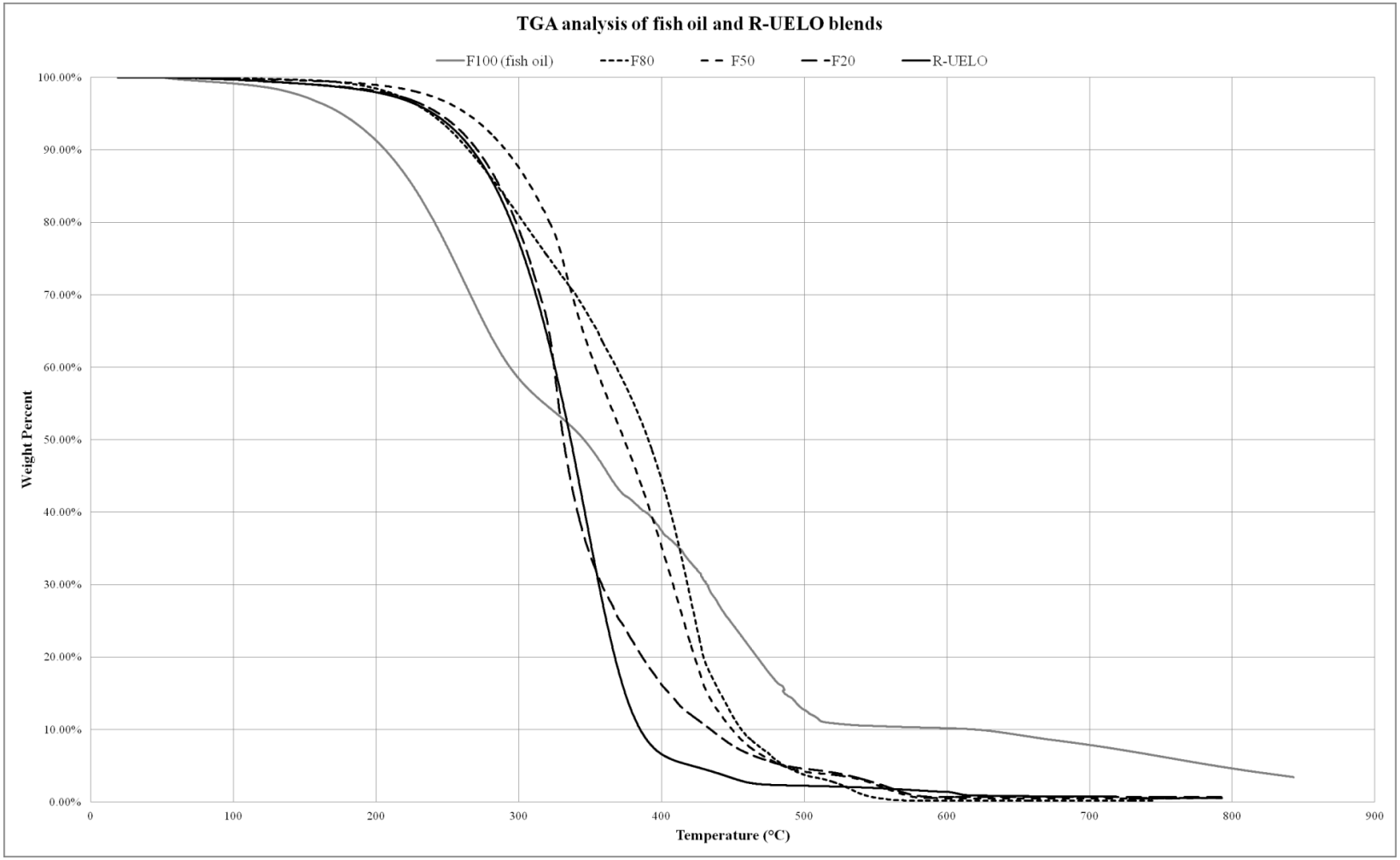

Figure 7-9: TGA analysis of fish oil and R-UELO blends under nitrogen and air atmosphere

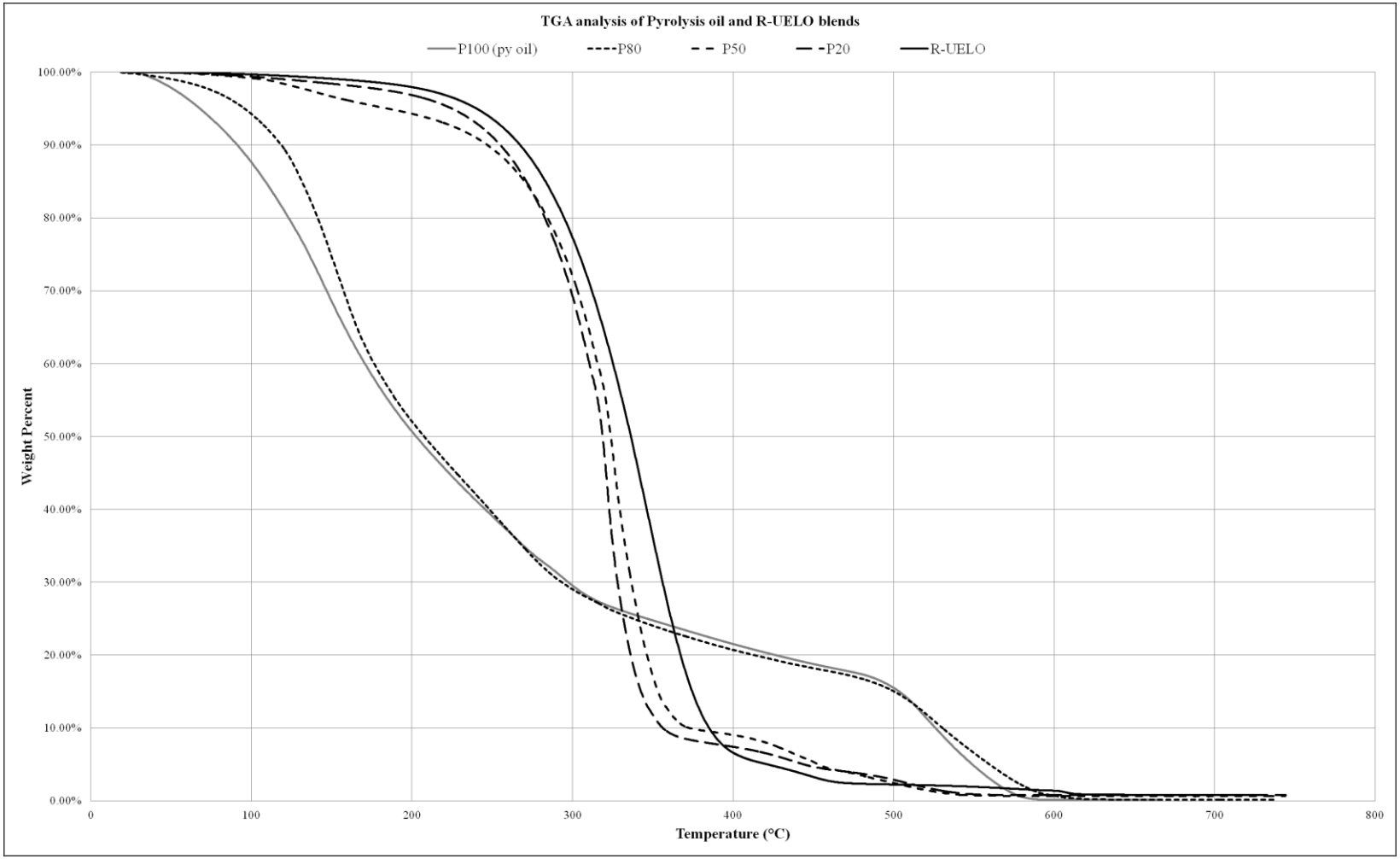

Figure 7-10: TGA analysis of pyrolysis oil and R-UELO blends under nitrogen and air atmosphere

To determine composition of highly volatile matter, medium volatile matter, combustible material, and ash, temperatures X, Y, and Z are selected depending on TGA curves. Temperature X is taken at the first mass loss plateau below 200 °C therefore 150 and 200 °C are chosen for R-UELO/fish oil and R-UELO/pyrolysis oil mixtures respectively. Temperature Y is taken at the mass loss plateau between 500 and 900 °C and temperature Z corresponds to the ash remaining near the final temperatures. To keep constancy within mixtures, two different sets of X and Y temperatures are used for TGA analysis of R-UELO (R-UELO-1 and R-UELO-2). More details can be found in Appendix 10.2. Results of TGA analysis for R-UELO/fish oil mixtures are shown in Table 7-6.

Table 7-6: TGA results for R-UELO and fish oil blends (wt. %)

Segment	R-UELO1	F20	F50	F80	F100 (fish oil)
Highly volatile matter (< 150 °C)	0.90	1.00	0.43	0.44	2.34
Medium volatile matter (150 to 500/550 °C)	96.87	94.63	95.38	95.23	89.98
Combustible material (500/550 to 700 °C)	1.46	3.76	3.70	4.13	3.47
Ash content (> 700 °C)	0.77	0.61	0.49	0.20	4.21
Total	100	100	100	100	100

Neat R-UELO, neat fish oil, and their blends have similar amounts of highly volatile matter, medium volatile matter, and combustible material. However, the fish oil TGA curve in Figure 7-9 is markedly different than the curves of R-UELO and R-UELO and fish oil blends. This could be due to the nature of thermally resistant compounds of the fish oil. Fish oil contains phospholipids, metals, minerals, FFAs, and peroxides, and

forms oxidation products such as more peroxides, dienes, FFAs, carbonyls, and aldehyes [62]. In a previous study by Adeoti et al., fish oil was more thermally stable than heavy fuel in the TGA between 200 and 450 °C [4].

Ash content decreases with the addition of fish oil for all the R-UELO/fish oil blends except for neat fish oil which shows an abnormally high ash content (4.21 wt. %). Unrefined salmon fish oil from the fishmeal process in a previous study shows a TGA ash content of 0.6 wt. % [4]. One possible reason is that metal compounds of the ash oxidize under oxygen atmosphere and result in higher ash content in the TGA.

Results of TGA analysis for the R-UELO/pyrolysis oil mixtures are shown in Table 7-7.

Table 7-7: TGA results for R-UELO and pyrolysis oil blends (wt. %)

Segment	R-UELO2	P20	P50	P80	P100 (pyrolysis oil)
Highly volatile matter (< 200 °C)	2.06	3.16	5.72	47.97	49.33
Medium volatile matter (200 to 600 °C)	96.56	96.05	93.63	51.33	50.54
Combustible material (600 to 700 °C)	0.61	0.03	0.04	0.53	0
Ash content (> 700 °C)	0.77	0.76	0.61	0.17	0.13
Total	100	100	100	100	100

Neat R-UELO, neat pyrolysis, and their blends have similar amounts of combustible material and ash content. Water and light organic molecules in pyrolysis oil likely accounts for the large differences between highly volatile matter and medium volatile matter.

7.4.3 Flash point

Flash point of neat R-UELO is 136 °C. Non-reclaimed UELO containing gasoline is known to have a flash point of less than 100 °C [22]. The UELO reclamation process increases the flash point by separating out the volatiles. Flash points of neat fish oil and pyrolysis oil were studied previously. Adeoti et al. determined that bunker fuel oil, waste fish oil, and unrefined salmon oil have flash points of 130, 203.5, and 208.5 °C respectively [4]. Flash point of pyrolysis oil can be less than 150 °C when volatile compounds in pyrolysis oil are present. However, the evaporating high content of water distinguishes the flame as seen by flashes without ignition [64].

7.5 Pilot-scale multi-fuel furnace experiments

Physical, chemical, and thermal properties of R-UELO/bio-oil blends obtained in Section 7.2, Section 7.3, and Section 7.4 are used to screen blends for further combustion testing. During combustion, exhaust gas color, ignition characteristics, and combustion residues are observed. Fuel flow rate, fuel pre-heat temperature, chamber and exhaust gas temperatures, and exhaust gas O_2, CO, H_2S, and CH_4 concentrations are measured and GC-TCD is used to analyze exhaust gas samples.

7.5.1 Selection of blends to proceed to furnace experiments

Neat R-UELO, neat fish oil, and the 50/50 vol. % R-UELO/fish oil blend are selected to proceed to furnace experiments. Physical, chemical, and thermal properties of diesel fuel, R-UELO, fish oil, the 50/50 vol. % R-UELO/fish oil blend, and pyrolysis oil are summarized in Table 7-8.

Table 7-8: A summary of physical, chemical, and thermal properties

Property	Diesel	R-UELO	50/50 vol. % R-UELO/fish oil blend	Fish oil	Pyrolysis oil
PHYSICAL PROPERTIES					
Density 25 °C (g/ml)	0.831[a]	0.856	0.887	0.926	1.21
Density 40 °C (g/ml)	0.818[a]	0.848	0.878	0.922	1.20
Density 60 °C (g/ml)	0.804[a]	0.841	0.870	0.911	1.19
Viscosity 20 °C (cSt)	4.15[a]	121.3	78.50	75.49	68.60
Viscosity 40 °C (cSt)	2.70[a]	48.06	78.92	31.35	20.90
Viscosity 60 °C (cSt)	1.92[a]	23.24	19.12	6.576	8.870
CHEMICAL PROPERTIES					
Water Content (wt. %)	0.00[a]	0.16	-	0.05[a]	30.3[a]
Ash Content (wt. %)	0.10[a]	-	-	0.12[a]	0.74[a]
Carbon content (wt. %)	86.23[a]	84.3	-	77.4	41.4[a]
Hydrogen content (wt. %)	13.77[a]	13.9	-	11.3	4.3[a]
Nitrogen content (wt. %)	0.00[a]	0.26	-	0	0.2[a]
Sulfur content (wt. %)	0.004[a]	0.22	-	0	0[a]
Oxygen content (wt. %)	0.00[a]	1.06	-	11.3	25.5[a]
THERMAL PROPERTIES					
Heating Value (MG/kg)	45.7[a]	45.39	42.26	36.76	18.55
TGA - Highly Volatile Matter (wt. %)	-	0.90-2.06[b]	0.43	2.34	49.33
TGA - Medium Volatile Matter (wt. %)	-	96.56-96.87[b]	95.38	89.98	50.54
TGA - Combustible Matter (wt. %)	-	0.61-1.46[b]	3.70	3.47	0
TGA - Ash content (wt. %)	-	0.77	0.49	4.21	0.13
Flash point (°C)	131[a]	136	-	209[a]	> 150

[a] Results are taken from previous works [91, 5, 93, 94, 89]

[b] See Section 7.4.2 for explanation for range of TGA values

R-UELO/fish oil mixtures are selected over R-UELO/pyrolysis oil mixtures due to better miscibility. Superior fuel homogeneity in R-UELO/fish oil blends means the mixture does not have to be continually mixed which is critical for storage in the day tank and preliminary fuel heating box. R-UELO and fish oil are miscible because they are largely non-polar in nature. R-UELO contains up to 90 wt. % non-polar base oil with

hydrocarbon chain lengths of 20 to 40 carbon molecules [8, 10]. In a previous study, unrefined salmon fish oil from the fishmeal process contained between 82.8 and 91.6 wt. % lipids and between 43.2 and 63.4 wt. % TAGs which are also non-polar and have carbon lengths varying between 14 and 22 [6]. Due to the similar polarity and molecule size of lubricating base oil and fish oil lipids, R-UELO and fish oil have similar densities (0.856 and 0.926 g/ml at 25°C) and water content (0.16 and 0.05 wt. %).

As shown in Table 4-1, pyrolysis oil contains a large concentration of polar compounds such as water (up to 30 wt. %), aldehydes (up to 20 wt. %), carboxylic acids (up to 15 wt. %), and alcohols (up to 5 wt. %) [68, 70]. R-UELO and pyrolysis oil are immiscible due to unmatched polarity and different densities (0.856 and 1.21 g/ml at 25°C, respectively). From characterization tests in this study and a previous study by Krutof et al., it is apparent that the high water content in pyrolysis oil (30.3 wt. %) lowers heating value (18.55 MJ/kg), increases oxygen in elemental analysis (25.5 wt. %), and increases amount of highly volatile matter in TGA (49.33 wt. %) [5]. Combustion and emission properties of neat R-UELO or UELO and neat fish oil are known from this study and others as discussed in Chapter 5 [22, 88, 61, 7, 95, 5].

7.5.2 Combustion observations and measurements

Combustion of R-UELO, the 50/50 vol. % R-UELO/fish oil blend, and fish oil did not require modifications to the burner or nozzle. In fact, the burner starts easier and ignites faster with neat R-UELO, neat fish oil, and the 50/50 vol. % R-UELO/fish oil blend than with diesel. Steigers similarly noticed that fish oil and fish oil blends started without

difficulty and started easier than diesel in a stationary diesel engine but offered no explanation [61]. One possible explanation is that the Nortec multi-fuel burner nozzle is designed with high tolerances for dense and viscous fuels and the low viscosity of diesel makes it difficult to atomize in a larger nozzle. Inspection of deposit build-up after combustion in the interior chamber walls and the burner nozzle revealed no unusual uncombusted particles or hard deposits. However, deposit build-up is not expected due to the limited total furnace run-time (less than 50 hours).

Primary air pressure, pre-heat temperature, and secondary air are set so for complete combustion as per the furnace test run protocol described in Section 6.8. Table 7-9 shows the burner settings and the fuel and exhaust gas properties for each fuel.

Table 7-9: Burner settings and combustion properties for each fuel

Setting or property	Diesel	R-UELO	50/50 vol. % R-UELO/fish oil blend	Fish oil
BURNER SETTINGS				
Primary air pressure (psi)	5 – 10	15 – 20	15 – 20	10 – 15
Pre-heat temperature T2 (°C)	20	60	60	60
Secondary air (cm)	4/10 open	6/10 open	6/10 open	6/10 open
FUEL PROPERTIES				
Fuel flow rate (kg/h)	2.4	2.7	3.4	3.9
Actual fuel temperature (°C)	15	55	55	55
Viscosity at temperature (cSt)	5.2	29.4	26.5	18.8
EXHAUST GAS PROPERTIES				
Exhaust gas temperature (°C)	350 – 400	350 – 400	350 – 375	325 – 350
O_2 in exhaust gas (vol. %) [a]	2.5 – 3	2.5 – 6	2.5 – 6	2.5 – 6
CO in exhaust gas (ppm) [a]	100	200 – 400	200 – 400	200 – 400
H_2S in exhaust gas (ppm) [a]	0	0	0	0
CH_4 in exhaust gas (vol. %) [a]	0	0	0	0
Exhaust gas color [b]	clear	clear	clear	clear

[a] measured using combustion analyzers described in Section 6.8

[b] visual measurement as per protocol described in Section 6.8

Primary air atomization pressure required for combustion depends on fuel viscosity which is directly related to pre-heat temperature. Fuel flow rate is a function of primary air pressure and therefore fuel viscosity at pre-heat temperature. Fuel flow rate, fuel temperature, and corresponding viscosity for each fuel are shown in Table 7-9. Diesel fuel is pre-heated to 15 °C and has a kinematic viscosity of 5.2 cSt at that temperature. Combustion with primary air pressure between 5 and 10 psi results in a fuel flow rate of 2.4 kg/hr. R-UELO, the 50/50 vol. % R-UELO/fish oil blend, and fish oil are all pre-heated to 55 °C with corresponding kinematic viscosities of 29.4, 26.5, and 18.8 cSt respectively. Due to the higher viscosity of R-UELO and the 50/50 vol. % R-UELO/fish oil blend, the primary air needed for atomization is between 15 and 20 psi compared to between 10 and 15 psi for fish oil.

Secondary air intake opening is set by observing exhaust gas color and by measuring O_2 concentrations of exhaust gas in the stack. One difficulty is that new fuel is pumped from the day tank to the preliminary fuel box every 4 L and the preliminary fuel box thermostats measure a drop in temperature. Then, the burner shuts off in order to re-heat fuel to the set temperature before restarting ignition. Intermittent restarts occur more frequently with R-UELO, fish oil, and the 50/50 vol. % R-UELO/fish oil blend than with diesel fuel due to higher set pre-heat temperatures. Due to this difficulty, measured O_2 and CO concentrations in the exhaust gas as well as chamber and stack temperatures fluctuate between 2 and 6 vol. % for O_2, 200 and 400 ppm for CO, and Appendix 10.4 shows temperature fluctuations. H_2S or CH_4 measurements of 0 ppm and 0 wt. % on the MicroClipXT could be due to operation error. One explanation is that high exhaust gas

temperatures interfered with the device sensors. Another explanation is that condensed water from the exhaust gas interfered with the device sensors.

7.5.3 Theoretical exhaust gas calculations

In this section, common exhaust gas emissions are discussed. O_2, CO_2, H_2O, and N_2 are estimated for diesel fuel, R-UELO, and fish oil using stoichiometric combustion calculations. Studies that look at combustion of neat UELO and fish oils give insight into emissions such as NO_x, SO_2, CH_4, N_2O, CO, and PM.

Stoichiometric combustion calculations based on Equation 7.1, Equation 7.2, and CHNO elemental concentrations can estimate combustion and emission characteristics (Appendix 10.5).

$$C_{elemental} + O_2 \rightarrow CO_2 \qquad \textbf{Equation 7.1}$$

$$H_2 + 0.5\,O_2 \rightarrow H_2O \qquad \textbf{Equation 7.2}$$

Table 7-10 shows the results with theoretical concentrations of O_2, CO_2, H_2O, and N_2 for 0 % excess air and 3 kg fuel/hour and 15 % excess air and experimental fuel flow rates.

Table 7-10: Exhaust gas concentration from theoretical calculations

Diesel fuel								
	Excess air = 0 %, 3 kg fuel/hr				**Excess air = 15 %, 2.4 kg fuel/hr**			
	kg/h	kmol/h	v% wet	v% dry	kg/h	kmol/h	v% wet	v% dry
O_2	-	-	-	-	1.2	0.04	2.5%	2.9%
CO_2	9.5	0.22	12.7%	15.2%	7.6	0.17	11.1%	13.1%
H_2O	5.0	0.28	16.4%	-	4.2	0.23	14.9%	-
N_2	33.6	1.20	70.9%	84.8%	30.9	1.10	71.4%	84.0%
Wet total	48.1	1.69	100.0%	-	43.9	1.55	100.0%	-
Dry total	43.1	1.42	83.6%	100.0%	39.7	1.31	85.1%	100.0%
R-UELO								
	Excess air = 0 %, 3 kg fuel/hr				**Excess air = 15 %, 2.7 kg fuel/hr**			
	kg/h	kmol/h	v% wet	v% dry	kg/h	kmol/h	v% wet	v% dry
O_2	-	-	-	-	1.4	0.04	2.5%	2.9%
CO_2	9.3	0.21	12.6%	15.1%	8.3	0.19	11.1%	13.0%
H_2O	5.0	0.28	16.7%	-	4.7	0.26	15.2%	-
N_2	33.1	1.18	70.7%	84.9%	34.3	1.22	71.3%	84.1%
Wet total	47.4	1.67	100.0%	-	48.7	1.72	100.0%	-
Dry total	42.4	1.39	83.3%	100.0%	44.0	1.46	84.8%	100.0%
Fish Oil								
	Excess air = 0 %, 3 kg fuel/hr				**Excess air = 15 %, 3.9 kg fuel/hr**			
	kg/h	kmol/h	v% wet	v% dry	kg/h	kmol/h	v% wet	v% dry
O_2	-	-	-	-	1.7	0.05	2.5%	2.9%
CO_2	8.5	0.19	13.5%	16.1%	11.1	0.25	11.9%	13.9%
H_2O	4.1	0.23	16.0%	-	5.6	0.31	14.6%	-
N_2	28.3	1.01	70.5%	83.9%	42.3	1.51	71.1%	83.2%
Wet total	40.9	1.43	100.0%	-	60.6	2.12	100.0%	-
Dry total	36.8	1.20	84.0%	100.0%	55.0	1.81	85.4%	100.0%

Stoichiometric air-to-fuel ratios of diesel fuel, R-UELO, and fish oil are 14.59, 14.38, and 12.28 respectively. Although fish oil has a lower air-to-fuel ratio, there is no difference in air supply pressure combustion compared to R-UELO in the experiments. This is likely due to the low viscosity of fish oil, which results in more fish oil exiting the burner

nozzle for the same air supply pressure. Diesel fuel and R-UELO have similar CHNO elemental concentration and therefore have similar theoretical exhaust gas concentrations. Fish oil has lower carbon content and higher oxygen content which results higher theoretical CO_2 and lower H_2O concentrations compared to diesel fuel due to a lower fuel-to-air ratio. Increased CO_2 in fish oil emissions compared to diesel fuel corresponds with previous experimental studies [61, 88]. O_2 combustion analyzer measurements from this study correspond to theoretical estimations of O_2 at experimental flow rates. CO_2, H_2O, and N_2 are not directly measured in this study.

There are two possible mechanisms of NO_x formation during combustion. The thermal or Zeldovich mechanism of NO_x formation is an oxidation of molecular nitrogen in the post-flame zone and the fuel-bound mechanism of NO_x formation is an oxidation of nitrogen-containing compounds in the fuel [96]. Unlike the fuel-bound mechanism, the thermal mechanism of NO_x formation is very sensitive to the peak flame temperature and independent of fuel type. Higher flame temperatures result in more NO_x formation from the thermal mechanism. Adiabatic flame temperatures are calculated for each fuel (appendix 10.4) and compared in Table 7-11 with fuel-bound nitrogen concentrations.

Table 7-11: Adiabatic flame temperature of each fuel

	Diesel fuel	R-UELO	50/50 vol. % R-UELO/fish oil	Fish oil
Adiabatic flame temperature (°C)	2104[a]	2102	2048[b]	1994
Nitrogen content (wt. %)	0.00	0.21	-	0.00

[a] adiabatic flame temperature is found in literature [94]
[b] adiabatic flame temperature is estimated from the neat fuels

Preto et al. showed that NO_x emissions do not vary significantly with the fraction of fish oil in blends with diesel and heavy fuel and that pure fish oil has 14 wt. % more NO_x diesel fuel [88]. Steigers observed a marginal increase (up to 7%) in fish oil NO_x emissions compared to diesel fuel with little explanation as to why [61]. Mrad et al. and Ushakov et al. show marginal increases NO_x emissions and explain that NO_x in diesel engines are highly dependent on in-cylinder temperature, oxygen concentration, and residence time [95, 85]. R-UELO has similar adiabatic flame temperature to diesel fuel and fuel-bound nitrogen content is negligible. Diesel fuel and used oil are assumed to have the same NO_x emissions because thermal formation of NO_x is the dominant mechanism [7]. NO_x is not directly measured in this study.

SO_x emissions are dependent on the elemental sulfur content in the fuel and are often estimated by elemental sulfur content [7]. As shown in Table 7-8, the sulfur content of diesel fuel, neat R-UELO and neat fish oil are 0.004, 0.22, and 0 wt. % respectively. In a previous study, the SO_x emissions for used oil are 320% higher than diesel fuel and are 2.2 and 0.69 wt. % respectively [7]. Studies on fish oil combustion show drastically reduced SO_2 emissions for neat fish oil. Preto et al. showed that diesel fuel emissions have around 30 times more SO_2 than fish oil emissions. Steigers saw reductions of up to 80% for pure fish oil and up to 30% for a 50/50 vol. % fish oil/diesel fuel blend compared to pure diesel fuel in a diesel engine [88, 61]. SO_x is not directly measured in this study.

CH_4, N_2O, and CO emissions vary with both the fuel type and the firing configuration. A previous life cycle analysis showed no difference of these emissions between diesel fuel,

heavy fuel, and used oil [7]. Studies on fish oil combustion show reduction of CO emissions between -6 and -33% compared to diesel fuel [88, 61, 95]. It is likely that lower CO emissions with fish oil compared to diesel fuel are related to the lower air-to-fuel ratio of fish oil since fish oil receives more oxygen per kg of fuel with identical air supply during combustion. While CH_4 and CO are measured in this study, operating errors produced no conclusive values.

Carbon particles such as soot or ash present in the exhaust are referred to as particulate matter (PM). Due to the high levels of ash and soot present in R-UELO, PM emissions are generally much higher than in diesel fuel. Once study measured R-UELO PM emissions to be 500 times more than diesel fuel and almost twice more than heavy fuel [7]. The Vermont used oil study showed that particulate matter in used oil emissions is 467 mg/min compared 0 mg/min for diesel fuel. Steigers shows with a diesel engine that PM emissions decrease 78% for pure fish oil and 40% for a 50/50 vol. % fish oil/diesel fuel blend compared to diesel fuel [61]. Mrad et al. show that PM emission for bio-fuel is lower compared to diesel fuel in a diesel engine [95]. Ushakov et al. showed a reduction of up to 67% when fish oil was used alone in a heavy-duty diesel engine compared to MGO [85]. PM emissions are not measured in this study.

7.5.4 Micro GC analysis

The Micro GC uses a TCD with helium as a carrier gas and elutes components roughly according to thermal conductivity between carrier gas and component. However, elution

is not necessarily in order thermal conductivity as methane usually elutes after oxygen and nitrogen [97]. Thermal conductivities of various gases are shown in Table 7-12.

Table 7-12: Thermal conductivity of various gases [98]

Gas	Thermal conductivity (mW/mK)	Difference from Helium (mW/mK)
Hydrogen	471.1	95.0
Helium	376.1	-
Methane	89.3	-286.8
Oxygen	68.2	-307.9
Nitrogen	65.7	-310.4
Carbon monoxide	63.9	-312.2
Ethane	58.3	-317.8
Ethene	55.0	-321.0
Propane	48.4	-327.7
Argon	45.5	-330.6
Carbon dioxide	43.8	-332.3
n-Butane	43.4	-332.7

Lamb et al. describe a GC-TCD method with two columns for analyzing exhaust gas in diesel engines with helium as the carrier gas. Elution order of gases in the GC-TCD is H_2, N_2, O_2, A, CO, NO, CH_4, CO_2, N_2O, ethylene, acetylene, water, ethane, propylene, propane, butane-1, trans-butene-2, butadiene-1,3, iso-butene, cis-butene-2, n-butane, iso-pentane, and n-hexane. The first column was cooled to -78 °C and the second was heated to 160 °C which was similar to the column temperature used in the Micro GC. Lamb et al. observed a composite air peak co-eluting H_2, N_2, O_2, A, CO, and NO, as well as CH_4, CO_2, N_2O, ethylene, acetylene, and water eluting within less than one minute in a 60 minute analysis [99].

The primary challenge in the Micro GC analysis is a lack of accurate calibration data. Only column 1 is calibrated with an external calibration sample of natural. Natural gas is very different in composition than exhaust emissions and for the components that are similar, the concentrations are very different. We were unable to obtain a calibration gas that better represented the exhaust gas. Table 7-13 shows calibration data for the external calibration natural gas sample.

Table 7-13: Calibration data for Micro GC Column 1

Compound	Fraction (vol. %)	Ret. Time (sec)	Window (sec)	Min. (sec)	Max. (sec)
Nitrogen [a]	0.33	-	-	-	-
Methane	46.2	31.19	1.56	29.63	32.75
CO_2	40.61	32.59	1.63	30.96	34.22
Ethane	5.08	33.59	1.68	31.91	35.27
Propane	4.58	38.35	1.92	36.43	40.27
Iso-butane	0.6	47.25	2.36	44.89	49.61
N-butane	1.47	50.83	2.54	48.29	53.37
Iso-pentane	0.29	75.70	4.20	71.50	79.90
N-pentane	0.4	82.04	4.10	77.94	86.14
N-hexane [a]	0.33	-	-	-	-
N-heptane [a]	0.06	-	-	-	-
N-octane [a]	0.05	-	-	-	-

[a] peak data not calibrated for these compounds

Column 1 is a 10-meter PoraPLOT U designed to separate CO_2 from the composite air peak and can also analyze methane, ethane, and propane. The analysis takes approximately 120 seconds and all of the peaks eluted within 47.5 seconds. Figure 7-11 to Figure 7-14 show the chromatographs for diesel, R-UELO, the 50/50% blend, and fish oil.

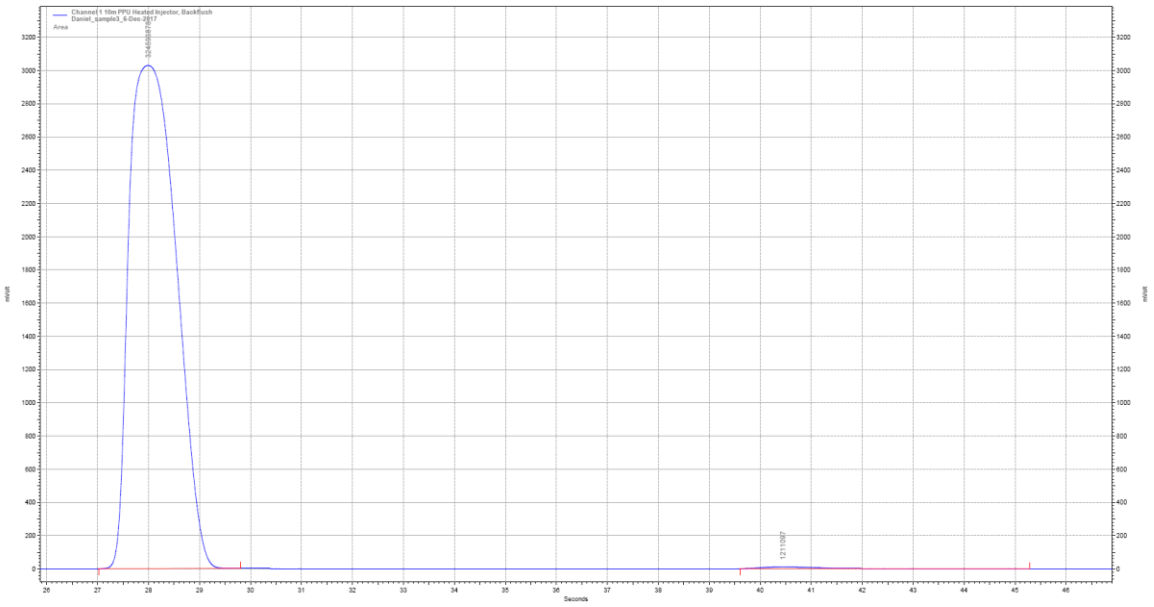

Figure 7-11: Column 1 results for diesel fuel

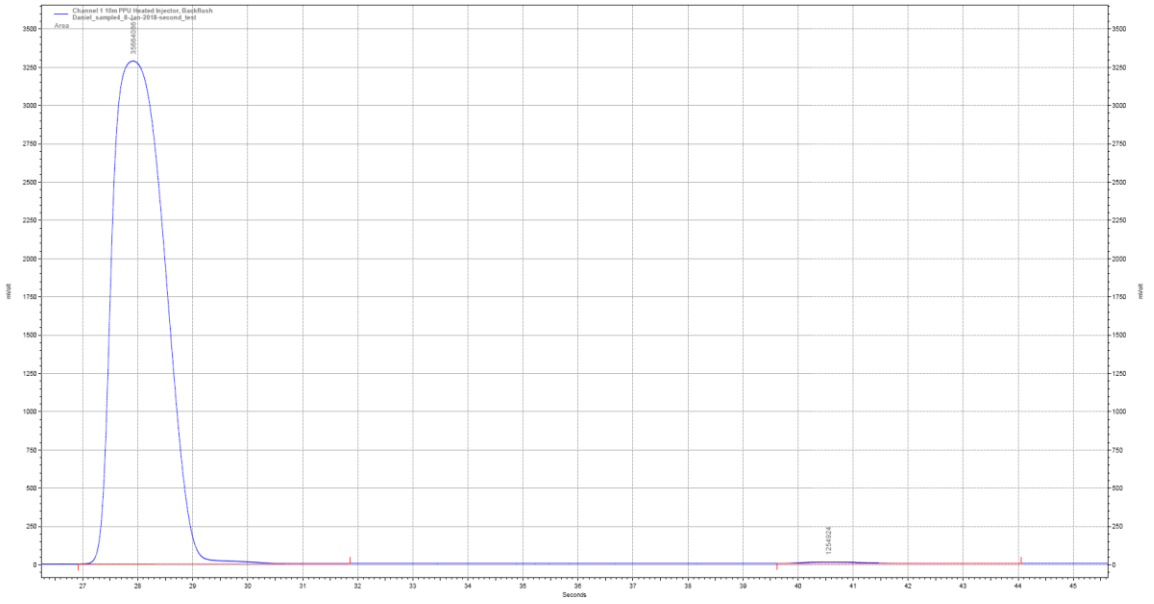

Figure 7-12: Column 1 results for R-UELO

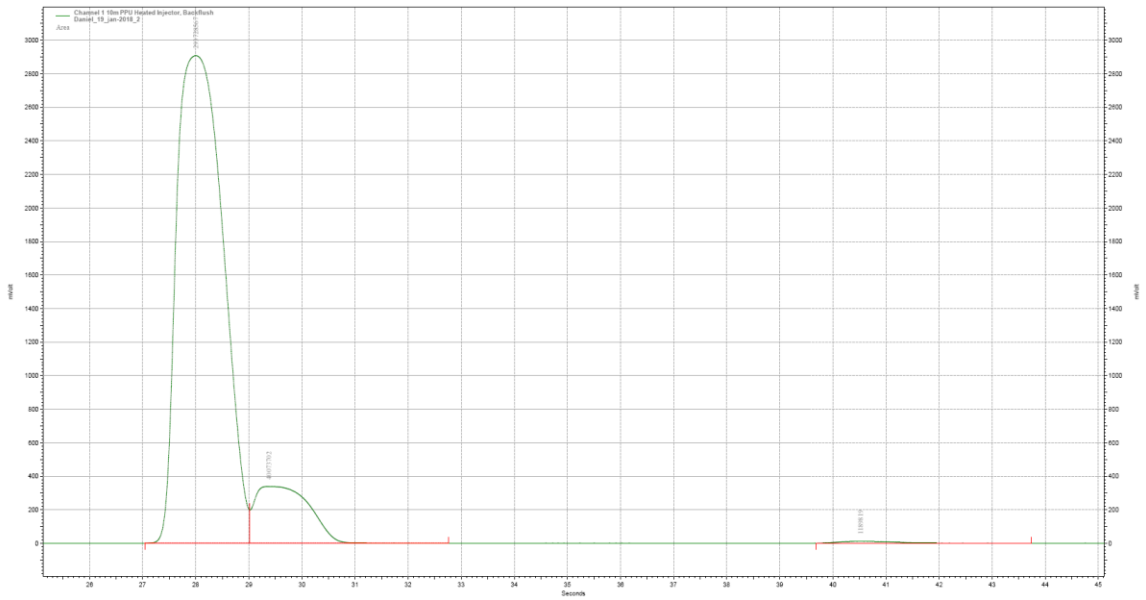

Figure 7-13: Column 1 results for 50/50% R-UELO/fish oil blend

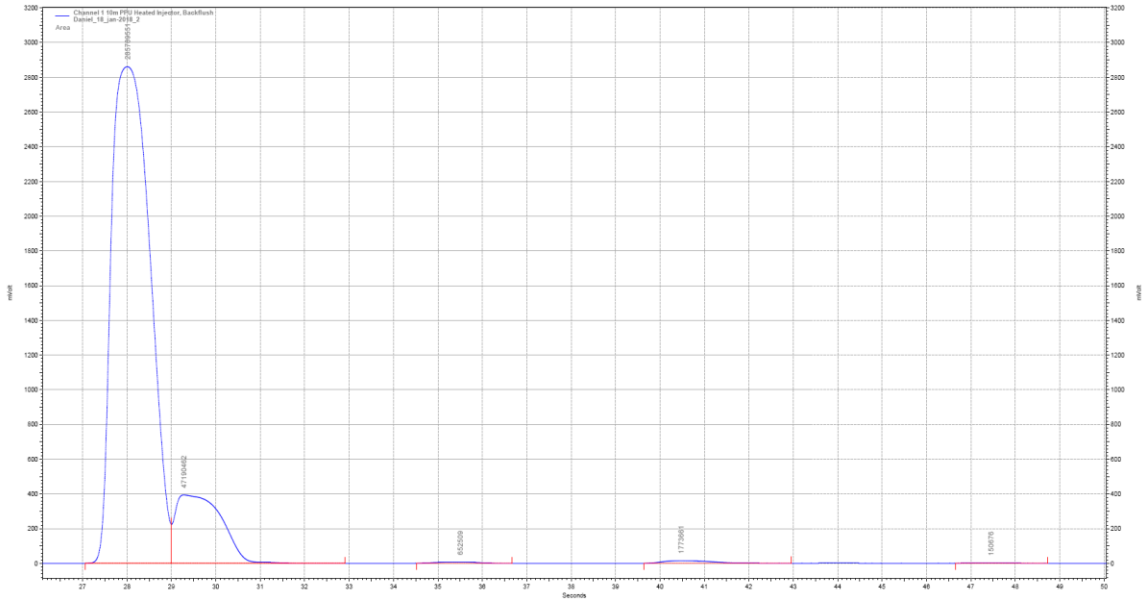

Figure 7-14: Column 1 results for 100% fish oil

Table 7-14 shows the integration results for column 1. The EZChrom integration software calculates voltage area and area % for each peak.

Table 7-14: Micro GC Column 1 PoraPLOT U results

Peak #	Retention time (sec)	Units	Diesel	R-UELO	50/50 %	Fish oil
1	27.1 – 29.0 Composite air	volts area %	337.10 99.5%	356.64 99.6%	293.96 87.7%	285.79 85.2%
2	29.0 – 32.9 CH_4 and CO_2	volts area %	- -	- -	39.70 11.9%	47.19 14.1%
3	34.5 – 36.6 Propane derivatives	volts area %	- -	- -	- -	0.65 0.19%
4	39.7 – 42.9 Propane derivatives	volts area %	1.58 0.47%	1.25 0.35%	1.20 0.36%	1.77 0.53%
5	46.7 – 48.8 iso-butane	volts area %	- -	- -	- -	0.15 0.04%
Total	-	volts area %	338.68 100.0%	357.90 100.0%	334.86 100.0%	335.56 100.0%

Peak #1 at 27.1 – 29.0 is the composite air peak and is likely composed of H_2, N_2, O_2, A, CO, and NO [99]. The retention time of peak #2 at 29.0 to 32.9 seconds corresponds to both CH_4 and CO_2 in the calibration sample, however peak #2 may also include N_2O, ethylene, acetylene, and water [99]. Peak #2 is difficult to qualify because of partial co-elution with the composite air peak and because the peak is broad without a clearly defined peak apex as shown in the chromatographs of the 50/50 vol. % R-UELO/fish oil blend and fish oil (Figure 7-13 and Figure 7-14). Assuming peak #2 is 100% CO_2, the area % (roughly equal to volume fraction) is 14.0% for fish oil which corresponds to the theoretical CO_2 emission concentration of 13.9 vol. % using 15% excess air and the experimental flow rate of 3.9 kg/hr. The 11.8 area % of peak #2 in the 50/50 vol. % R-UELO/fish oil blend is slightly less than neat fish oil and corresponds to lower theoretical CO_2 emissions from R-UELO. Retention times of peak #3 and peak #4 roughly

correspond to the propane peak in the external calibration sample and may include related compounds such as propylene [99]. Uncombusted or partially combusted organic molecules with similar thermal conductivity may also be included in this peak for neat fish oil or the 50/50 vol. % R-UELO/fish oil blend. Peak #3 is largest for fish oil (0.53% + 0.19% = 0.72%) followed by diesel (0.47%), the 50/50 vol. % R-UELO/fish oil blend (0.36%), and R-UELO (0.35%). Peak #5 only shows up in fish oil emissions and corresponds to iso-butane in the calibration sample but may be uncombusted or partially combusted organic molecules with similar thermal conductivity and other derivatives such as butane-1, trans-butene-2, butadiene-1,3, iso-butene, and cis-butene-2 [99].

Column 2 is an 8-meter CP-Sil 5 CB designed to analyze hydrocarbons from C1 to C10. Figure 7-15 to Figure 7-18 show chromatographs for diesel, R-UELO, the 50/50% blend, and fish oil.

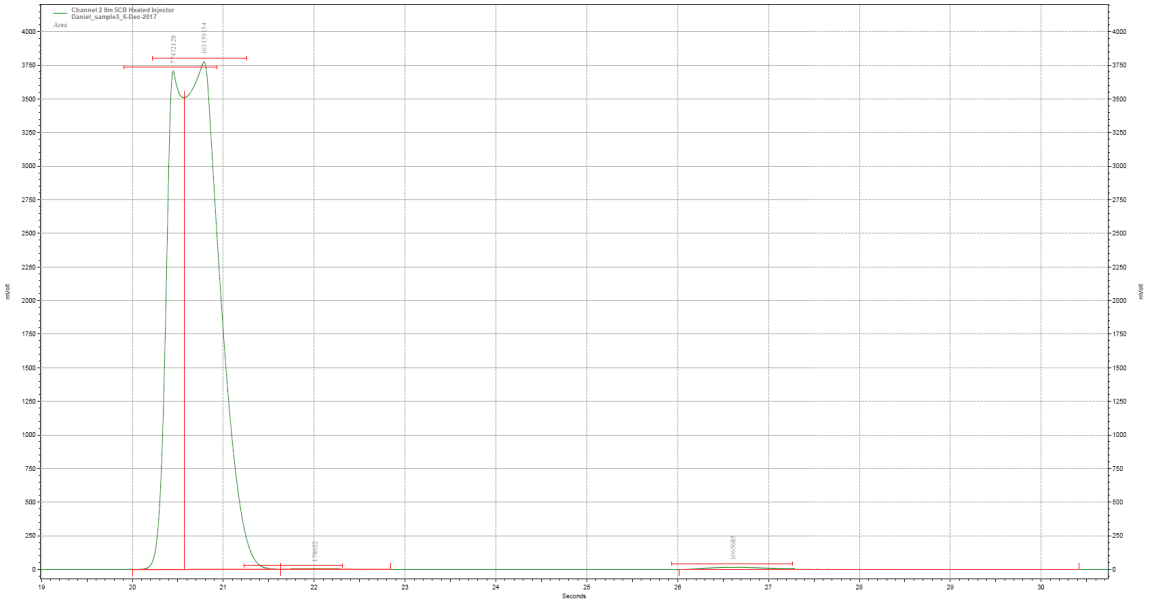

Figure 7-15: Column 2 results for diesel fuel

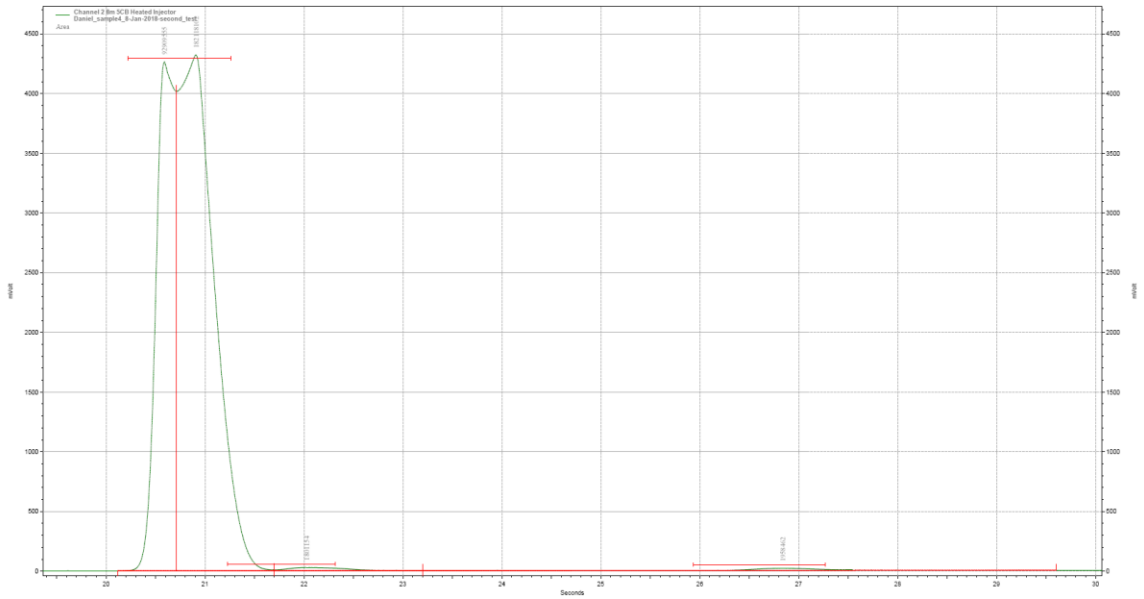

Figure 7-16: Column 2 results for R-UELO

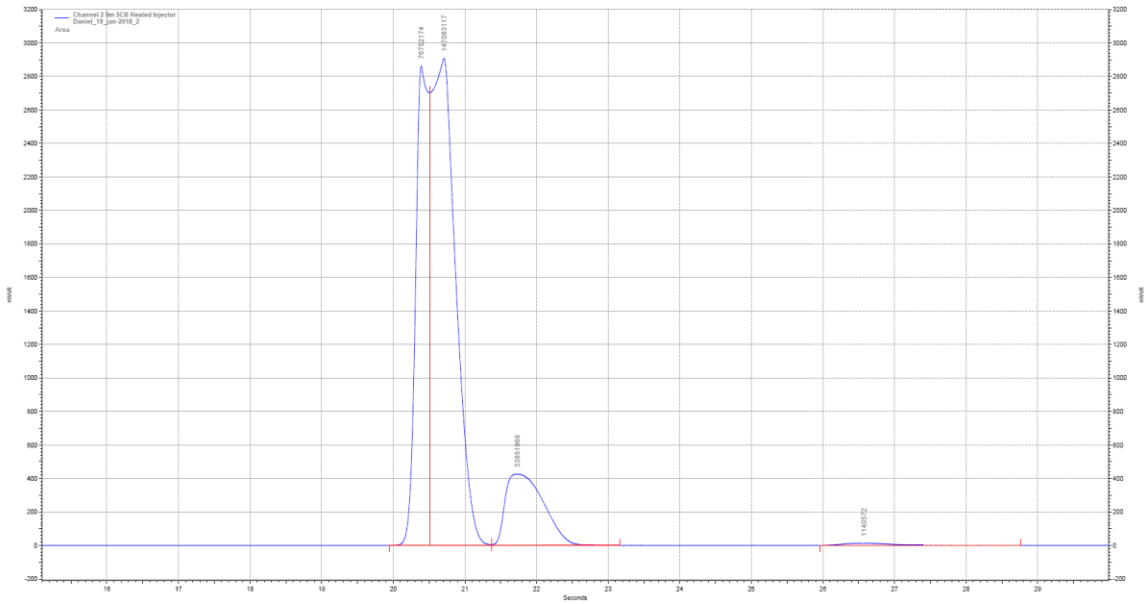

Figure 7-17: Column 2 results for 50/50% R-UELO/fish oil blend

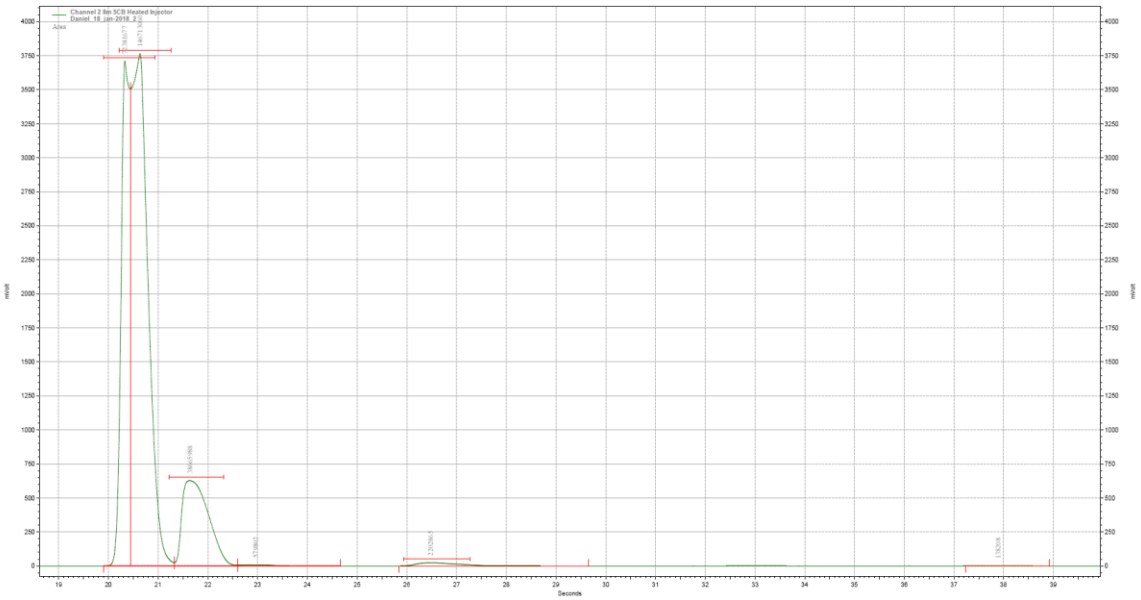

Figure 7-18: Column 2 results for 100% fish oil

Table 7-15 shows the integration results for column 1. The EZChrom integration software calculates voltage area and area % for each peak.

Table 7-15: Micro GC Column 2 CP-Sil 5 CB results

Peak #	Retention time (sec)	Units	Diesel	R-UELO	50/50 %	Fish oil
1	19.9 - 20.5 Composite air	volts area %	86.27 34.0%	91.58 33.1%	75.87 29.4%	72.38 27.8%
2	20.5 – 21.4 Composite air	volts area %	164.88 65.4%	181.65 65.6%	147.74 57.2%	146.71 56.3%
3	21.4 – 23.2 CH_4 and CO_2	volts area %	0.25 0.10%	1.80 0.65%	33.47 13.0%	38.67 14.8%
4	22.6 – 24.6	volts area %	- -	- -	- -	0.58 0.22%
5	25.9 – 29.6	volts area %	1.37 0.55%	1.92 0.69%	1.15 0.45%	2.20 0.85%
6	37.2 – 38.9	volts area %	- -	- -	- -	0.14 0.05%
Total	-	volts area %	252.77 100.0%	276.95 100.0%	258.24 100.0%	260.68 100.0%

Peak #1 and peak #2 are both part of the composite air peak, which is likely composed of H_2, N_2, O_2, A, CO, and NO [99]. Peak #3 is similar in peak size to peak #2 of column 1 and is likely CH_4 and CO_2, however, may also include N_2O, ethylene, acetylene, and water [99]. Peak #3 is co-eluted with the composite air peak for diesel and R-UELO (Figure 7-15 and Figure 7-16) and is separate and clearly defined in the 50/50 vol. % R-UELO/fish oil blend and fish oil (Figure 7-17 and Figure 7-18). Once again assuming peak #3 is 100% CO_2, the area % (roughly equal to volume fraction) is 14.8% for fish oil which corresponds to the theoretical CO_2 emission concentration of 13.9 vol. % using 15% excess air and experimental flow rate of 3.9 kg/hr. The area % of peak #3 in the 50/50 vol. % R-UELO/fish oil blend is slightly smaller than fish oil at 13.0%. Peak #4 only appears on the chromatograph of the fish oil sample and likely co-elutes with peak #3 or the composite air peak for the other samples. Peak #5 shows a similar area % to the propane and related compounds peak in column 1. Peak #5 is largest for fish oil (0.85%) followed by R-UELO (0.69%), diesel (0.55%), and the 50/50 vol. % R-UELO/fish oil blend (0.45%). Peak #6 only shows up in fish oil emissions with an area % of 0.05% which is nearly equal to the area % of peak #5 in column 1 (0.04%). Therefore it is likely iso-butane and larger organics/hydrocarbons.

There are a number of observations from the GC analysis. Firstly, chromatographs for diesel fuel and R-UELO emissions show composite air peaks of more than 99 area % which likely co-elute H_2, N_2, O_2, A, CO, NO, CH_4, and CO_2. Chromatographs for the 50/50 vol. % R-UELO/fish oil blend and neat fish oil emissions show an additional peak

that is presumed to be CO_2. The 50/50 vol. % R-UELO/fish oil blend shows a composite air peak of 87.7 and 86.6 area % for column 1 and 2 respectively and a CO_2 peak of 11.9 and 13.0 area % for column 1 and 2 respectively. Fish oil shows a composite air peak of 85.2 and 84.1 area % for column 1 and 2 respectively and a CO_2 peak of 14.1 and 14.8 area % for column 1 and 2 respectively. Fish oil showed higher CO_2 emissions than the 50/50 vol. % R-UELO/fish oil blend likely due to a lower fuel-to-air ratio as estimated in Section 7.5.3 and as indicated by previous studies with diesel fuel and fish oil blends [61, 88]. Compared to the other fuels, fish oil combustion gases contain a higher area % of organic molecules with similar thermal conductivity to propane and butane derivatives. These molecules make up 0.76 and 0.9 area % in column 1 and column 2 respectively and are smaller for diesel (0.47 and 0.55 area %), R-UELO (0.35 and 0.69 area %), and the 50/50 vol. % R-UELO/fish oil blend (0.36 and 0.45 area %). This indicates that fish oil contains thermally resistant organic molecules that partially combust or do not combust in the furnace. Adeoti et al. showed that phospholipids, metals, minerals, FFAs, peroxides, dienes, carbonyls, and aldehyes in fish oil are thermally resistant [4]. These molecules may be the source of the organic molecules found in the fish oil emissions.

8 CONCLUSIONS AND RECOMMENDATIONS

8.1 Conclusions

The primary objectives of this study have been to determine feasibility and impact of using R-UELO and bio-oil blends as fuel through study of physical, chemical, and thermal properties of neat R-UELO, salmon fish oil, and pyrolysis oil, R-UELO/salmon fish oil blends, and R-UELO/pyrolysis oil blends. Combustion and emission properties of certain blends were also determined using a custom-built pilot-scale multi-fuel furnace.

Although studies cover individual use of UELO, pyrolysis oil, and fish oil as fuel [22, 89, 92, 3] and blending of bio-oils with petroleum fuels [5, 4], little or no research has been conducted on blending UELO with fish oil or pyrolysis oil to improve combustion properties. UELO with little to no reprocessing is either burned alone or blended with other fuel oils in small-scale space heaters, or in industrial-scale processes such as power stations and cement kilns [16, 17]. Fish oil is used as fuel for small-scale to industrial scale furnaces and boilers as well as in diesel engines [61, 95, 88]. Consistent quality pyrolysis oil can be preheated and blended with fuel oils for use in modified combustion equipment however there are still many challenges to overcome regarding its high acidity, low thermal stability, low heating value, high water content, and high viscosity [74, 79, 96].

Physical, chemical, and thermal properties were determined for all neat oils, R-UELO/fish oil blends, and R-UELO/pyrolysis oil blends. R-UELO and fish oil are

miscible because of similar molecule sizes and non-polar nature. R-UELO is made up of 90 wt. % lubricating base oil which is non-polar and is composed of hydrocarbons with carbon chain lengths of 20 to 40 [8, 10]. Similarly, unrefined salmon fish oil from the fishmeal process contains between 82.8 and 91.6 wt. % lipids and between 43.2 and 63.4 wt. % TAGs which are also non-polar and have carbon chain lengths between 14 and 22 [6]. R-UELO and fish oil have similar physical and chemical properties such as density (0.856 and 0.926 g/ml at 25°C), water content (0.16 and 0.05 wt. %), elemental concentrations (84.3 and 77.4 wt. % carbon), heating value (45.39 and 36.76 MJ/kg), and thermal stability in with TGA (96.87 and 89.98 wt. % medium volatile matter).

R-UELO and pyrolysis oil are immiscible due to density differences (0.856 and 1.21 g/ml at 25°C, respectively) and pyrolysis oil contains polar compounds such as water (up to 30 wt. %), aldehydes (up to 20 wt. %), carboxylic acids (up to 15 wt. %), and alcohols (up to 5 wt. %) [68, 70]. The high water content in pyrolysis oil (30.3 wt. %) lowers heating value (18.55 MJ/kg), increases oxygen in elemental analysis (25.5 wt. %), and increases amount of highly volatile matter in TGA (49.33 wt. %) [5].

Combustion and emission characteristics of neat R-UELO, neat fish oil, and a 50/50 vol. % R-UELO/fish oil blend were compared to diesel fuel in a pilot-scale multi-fuel furnace. Combustion of all fuel blends was accomplished and no difficulty occurred during ignition or atomization in warm or cold ambient conditions. Complete combustion and steady state parameters were determined individually for each fuel by measuring exhaust gas temperature, O_2 concentration, and color. The fuel pre-heat temperature was 15 °C for diesel and 55 °C for R-UELO and fish oil blends. R-UELO and fish oil flow rates

increased with increasing fish oil (2.7 to 3.9 kg/hr) and corresponded with decreasing fuel viscosity (29.4 to 18.8 cSt).

Emissions were analyzed using a two-column Agilent Micro GC-TCD with helium as a carrier gas. However, calibration with an external calibration sample of natural gas limited peak identification and quantification. Chromatographs for diesel fuel and R-UELO emissions co-elute H_2, N_2, O_2, A, CO, NO, CH_4, and CO_2. The chromatograph for fish oil showed higher CO_2 emissions than the chromatograph for the 50/50 vol. % R-UELO/fish oil blend due to a lower fuel-to-air ratio [61, 88]. The chromatograph for fish oil emissions shows more organic molecules with similar thermal conductivity to propane and butane derivatives compared to diesel fuel, R-UELO, and the 50/50 vol. % R-UELO/fish oil blend. This is likely due to thermally resistant compounds found in fish oil such as phospholipids, metals, minerals, FFAs, peroxides, dienes, carbonyls, and aldehyes. The thermal resistance of these molecules can also explain how in section 7.4.2, fish oil was more resistant than R-UELO to thermal decomposition above 335 °C and contained higher ash content.

Overall, blends of R-UELO with fish oil show good combustion and emission characteristics in the furnace.

8.2 Recommendations for future work

More physical, chemical, and thermal properties could be investigated for R-UELO and bio-oil blends in future work. Firstly, cold flow properties such as pour point, cloud point,

and plug point could be determined. Lipid analysis of the neat bio-oils could be accomplished and oxidation stability of the neat bio-oils and the R-UELO/bio-oil blends could be determined by peroxide or p-anisidine value. The impact of R-UELO addition on bio-oil aging could be investigated because of the high degradation of bio-oils [6]. Also, since R-UELO and pyrolysis oil were immiscible, future work can improve miscibility of pyrolysis oil with the addition of other components.

The design, construction, and commissioning of the pilot-scale multi-fuel furnace was a large part of this research and further research could be accomplished with it. A design of experiments can be used to help identify important combustion factors and how they relate to combustion characteristics in the furnace. More experiments can be performed using the furnace to determine combustion and emission characteristics of bio-oils (such as fish oil and pyrolysis oil) and blends. Quantifying emissions of R-UELO and fish oil blends can be accomplished with a GC column designed for exhaust emissions such as using a mole sieve column that separates individual H_2, N_2, O_2, A, CO, and NO peaks.

In order to evaluate the feasibility of using R-UELO and fish oil blends as heating fuel in remote locations, a life cycle analysis could be carried out.

Since fish oil is used as fuel for diesel engines [61, 95, 88], further work can be done on combustion of R-UELO and fish oil blends in diesel engine.

9 REFERENCES

[1] Z. Pawlak, W. Urbaniak, T. Kaldonski and M. Styp-Rekowski, “Energy conservation through recycling of used oil,” *Ecological Engineering,* vol. 36, pp. 1761-1764, 2010.

[2] P. Jayasinghe, “Biofuels from fish waste from remote fish processing plants in Newfoundland and Labrador,” Memorial University of Newfoundland, St. John's, Newfoundland and Labrador, Canada, 2010.

[3] P. Jayasinghe, I. A. Adeoti and K. Hawboldt, "A study of process optimization of extraction of oil from fish waste for use as a low-grade fuel," *Journal of the American Oil Chemists' Society,* no. 90, pp. 1903-1915, 2013.

[4] I. A. Adeoti, K. Hawboldt and M. R. Santos, "Thermal and flow properties of fish oil blends with bunker oil," *Fuel,* 2014.

[5] A. Krutof and K. Hawbolt, “Blends of pyrolysis oil, petroleum, and other bio-based fuels: A review,” *Renewable and Sustainable Energy Reviews,* vol. 59, pp. 406-419, 21 January 2016.

[6] P. Jayasinghe and K. Hawboldt, "A review of bio-oils from waste biomass: Focus on fish processing waste," *Renewable and Sustainable Energy Reviews,* no. 16, pp. 798-821, 2012.

[7] M. Collins, K. Schiebel and P. Dyke, “Life Cycle Assessment of Used Oil Management,” Environmental Resource Management (ERM), London, England, 2017.

[8] J. E. Denton, K. Randles, L. Mazur and C. Milanes, “A Review of the potential Human and Environmental Health Impacts of Synthetic Motor Ols,” US EPA, California, 2007.

[9] A. H. A. K. Durrani, “Strategies for Vehicle Waste-Oil Management in Pakistan,” Mehran University of Engineering & Technology, Jamshoro, Pakistan, 2010.

[10] F. Audibert, Waste Engine Oils: Rerefining and Energy Recovery, Elsevier, 2006, p. 323.

[11] J. Liu, K. Gu, H. Duan, Y. Zhao and J. Li, “Tribological and economic evaluation of recyled mineral lubricating oils,” *Science China Technological Sciences,* vol. 56, pp. 2964-2972, 2013.

[12] Environment Canada, "Follow-up Report on a PSL1 Substance For Which There Was Insufficient Information to Conclude Whether the Substance Constitutes a Danger to the Environment," Environment Canada, Canada, 2005.

[13] T. Mang and A. Gosalia, “Lubricants and Their Market,” in *Lubricants and Lubrication*, 3 ed., Hoboken, New Jersey: Wiley-VCH Verlag GmbH & Co. KGaA, 2017, pp. 1-9.

[14] A. J. Jafari and M. Hassanpour, “Analysis and comparison of used lubricants, regenerative technologies in the world,” *Resources, Conservation and Recycling,* vol. 103, pp. 179-191, 2015.

[15] M. A. Nwachukwu, J. Alinnor and H. Feng, “Review and assessment of mechanic village potentials for small scale used engine oil recycling business,” *African Journal of Environmental Science and Technology,* vol. 6, no. 12, pp. 464-475, December 2012.

[16] F. D. Giovanna, O. Khlebinskaia, A. Lodolo and S. Miertus, “Compendium of Used Oil Regeneration Technologies,” International Centre for Science and High Technology, Trieste, 2003.

[17] Taylor Nelson Sofres; Bio Intelligence Service, “Critical review of existing studies and life cycle analysis on the regeneration and incineration of waste oils,” Raylor Nelson Sofres Consulting S. A., Montrouge cedex, 2001.

[18] Y.-L. Hsu and C.-C. Liu, “Evaluation and selection of regeneration of waste lubricating oil technology,” *Environ Monit Assess,* vol. 176, pp. 197-212, 2011.

[19] U. S. EPA, “Managing Used Oil: Answers to Frequentl Questions for Businesses,” EPA, 10 April 2017. [Online]. Available: https://www.epa.gov/hw/managing-used-oil-answers-frequent-questions-businesses. [Accessed 24 October 2017].

[20] F. Awaja and D. Pavel, Design Aspects of Used Lubricating Oil Re-refining, 1 ed.,

Amsterdam: Elsevier, 2006.

[21] V. Kanokkantapong, W. Kiatkittipong and B. Panyapinyopol, "Used lubricating oil management options based on life cycle thinking," *Resources, Conservation and Recycling,* vol. 53, pp. 294-299, 2009.

[22] Vermont Agency of Natural Resources, "Vermont used oil analysis and waste oil furnace emissions study," Government of Vermont, Waterbury, Vermont, 1996.

[23] A. J. Caines, R. F. Haycock and J. E. Hillier, Automotive Lubricants Reference Book, 2nd ed., Warrendale, Pa: SAE International, 2004.

[24] T. Mang and J. Braun, "Antioxidants," in *Encyclopedia of Lubricants and Lubrication*, T. Mang, Ed., Mannheim, Springer Berlin Heidelberg, 2014, pp. 56-58.

[25] M. Harperscheid, "Engine Oils," in *Encyclopedia of Lubricants and Lubrication*, T. Mang, Ed., Berlin, Mannheim: Springer Berlin Heidelberg, 2014, pp. 486-492.

[26] I. Hamawand, T. Yusaf and S. Rafat, "Recycling of waste engine oils using a new washing agent," *Energies,* vol. 6, pp. 1023-1049, 2013.

[27] N. Zaki, "Antifoam Agents," in *Encyclopedia of Lubricants and Lubrication*, T. Mang, Ed., Kansas, Springer Berlin Heidelberg, 2014, pp. 53-56.

[28] A. Hamad, E. Al-Zubaidy and M. E. Fayed, "Used lubricating oil recycling using hydrocarbon solvents," *Journal of Environmental Management,* vol. 74, pp. 153-159, 2005.

[29] M. El-Fadel and R. Khoury, “Strategies for vehicle waste-oil management: a case study,” *Resources, Conservation and Recycling,* vol. 33, pp. 75-91, 2001.

[30] R. Irwin, M. VanMouwerik, L. Stevens, M. Seese and W. Basham, “Environmental Contaminants Encyclopedia - Oil, Used Oil Entry,” National Park Service, Water Resources Division, Fort Collins, Colorado, 1997.

[31] C. Yang, Z. Yang, G. Zhang, B. Hollebone, M. Landriault, Z. Wang, P. Lambert and C. E. Brown, “Characterization and differentiation of chemical fingerprints of virgin and used lubricating oils for identification of contamination or adulteration sources,” *Fuel,* vol. 1, no. 163, pp. 271-281, 2016.

[32] R. Beg, M. Sarker and M. R. Pervez, “Production of Diesel Fuel From Used Engine Oil,” *International Journal of Mechanical & Mechatronics Engineering,* vol. 10, no. 2, pp. 1-6, 2010.

[33] A. Hamad, E. Al-Zubaidy and M. Fayed, “Used lubricating oil recycling using hydrocarbon solvents,” *Journal of Environmental Management,* vol. 74, pp. 153-159, 2005.

[34] M. Fox, “Sustainability and environmental aspects of lubricants,” in *Handbook of Lubrication and Tribology*, New York, NY: CRC Press, Taylor and Francis, 2007.

[35] F. B. Hani and H. Al-Wedyan, “Regeneration of base-oil from waste-oil under different conditions and variables,” *African Journal of Biotechnology,* vol. 10, no. 7,

pp. 1150-1153, 14 Feburary 2011.

[36] J. Jonidi and M. Hassanpour, Used Motor Oil Management, 1st ed., Tehran: Ebadi Far, 2013.

[37] J. Rincon, P. Canizares and M. T. Garcia, "Regeneration of used lubricant oil by ethane extraction," *The Journal of Supercritical Fluids,* vol. 39, no. 3, pp. 315-322, January 2007.

[38] N. Elbashir, A. Al-Zahrani, M. A. Mutalib and A. Abasaeed, "A method of predicting effective solvent extraction parameters for recycling of used lubricating oils," *Chemical Engineering and Processing,* vol. 41, pp. 765-769, 2002.

[39] J. Rincon, P. Canizares, M. T. Garcia and I. Gracia, "Regeneration of Used Lubricant Oil by Propane Extraction," *Ind. Eng. Chem. Res.,* vol. 42, no. 20, pp. 4867-4873, 2003.

[40] J. Rincon, P. Canizares and M. T. Garcia, "Regeneration of used lubricant oil by polar solvent extraction," *Ind. Eng. Chem. Res.,* vol. 44, pp. 4373-4379, 2005.

[41] S. M. Al-Zahrani and M. D. Putra, "Used lubricating oil regeneration by various solvent extraction techniques," *Journal of Industrial and Engineering Chemistry,* vol. 19, pp. 536-539, 2013.

[42] J. L. A. Filho, L. G. M. Moura and A. C. S. Ramos, "Liquid-liquid extraction and adsorption on solid surfaces applied to used lubricant oils recovery," *Brazilian*

Journal of Chemical Engineering, vol. 27, no. 04, pp. 687-697, 2010.

[43] R. R. Mohammed, I. A. Ibrahim, A. H. Taha and G. McKay, "Waste lubricating oil treatment by extraction and adsorption," *Chemical Engineering Journal,* vol. 220, pp. 343-351, 2013.

[44] D. Gourgouillon, L. Schrive, S. Sarrade and G. M. Rios, "An environmentally friendly process for the regeneration of used oils," *Environmental Science and Technology,* vol. 34, pp. 3469-3473, 2000.

[45] R. Moliner, L. Lazaro and I. Suelves, "Valorization of Lube Oil Waste by Pyrolysis," *Energy & Fuels,* vol. 11, pp. 1165-1170, 1997.

[46] C. Nerin, C. Domeñoa, R. Moliner, M. Lázaro, I. Suelves and J. Valderrama, "Behaviour of different industrial waste oils in a pyrolysis process: metals distribution and valuable products," *Journal of Analytical and Applied Pyrolysis,* vol. 55, pp. 171-183, 2000.

[47] S. Kim and S. Kim, "Pyrolysis kinetics of waste automobile lubricating oil," *Fuel,* vol. 79, pp. 1943-1949, 2000.

[48] S.-S. Kim, B. H. Chun and S. H. Kim, "Non-isothermal pyrolysis of waste automobile lubricating oil in a stirred batch reactor," *Chemical Engineering Journal,* vol. 93, pp. 225-231, 2003.

[49] M. F. Gomez-Ric, I. Martin-Gullon, A. Fullana, J. A. Conesa and R. Font,

"Pyrolysis and combustion kinetics and emissions of waste lube oils," *Journal of Analytical and Applied Pyrolysis,* Vols. 68-69, pp. 527-546, 2003.

[50] M. Fuentes, R. Font, M. F. Gomez-Rico and I. Martin-Gullon, "Pyrolysis and combustion of waste lubricant oil from diesel cars: Decomposition and pollutants," *Journal of Analytical and Applied Pyrolysis,* vol. 79, pp. 215-226, 2007.

[51] M. Balat, M. F. Demirbas and M. Balat, "Pyrolysis of Waste Engine Oil in the Presence of Wood Ash," *Energy Sources, Part A: Recovery, Utilization, and Environmental Effects,* pp. 1494-1499, 2009.

[52] W. Manasomboonphan and S. Junyapoon, "Production of Liquid Fuels from Waste Lube Oils Used by Pyrolysis process," *2nd International Conference on Biomedical Engineering and Technology,* vol. 34, pp. 130-133, 2012.

[53] A. Demirbas, M. A. Baluabaid, M. Kabli and W. Ahmad, "Diesel Fuel From Waste Lubricating Oil by Pyrolitic Distillation," *Petroleum Science and Technology,* vol. 33, pp. 129-138, 2015.

[54] S. S. Lam, A. D. Russell and H. A. Chase, "Microwave pyrolysis, a novel process for recycling waste automotive engine oil," *Energy,* vol. 35, pp. 2985-2991, 2010.

[55] S. S. Lam, A. D. Russell and H. A. Chase, "Pyrolysis Using Microwave Heating: A sustainable Process for Recycling Car Engine Oil," *Ind. Eng. Chem. Res.,* vol. 49, pp. 10845-10851, 2010.

[56] S. S. Lam, A. D. Russell, C. L. Lee and H. A. Chase, “Microwave-heated pyrolysis of waste automotive engine oil: Influence of operation parameters on the yield, composition, and fuel properties of pyrolysis oil,” *Fuel,* vol. 92, pp. 327-339, 2012.

[57] S. S. Lam, A. D. Russell, C. L. Lee, S. K. Lam and H. A. Chase, “Production of hydrogen and light hydrocarbons as a potential gaseous fuel from microwave-heated pyrolysis of waste automotive engine oil,” *International Journal of Hydrogen Energy,* vol. 37, pp. 5011-5021, 2012.

[58] Oakdene Hollins Research & Consulting, “Improving Markets for Waste Oils,” OECD, United Kingdom, 2010.

[59] FAO, “The state of world fisheries and aquacultures,” Food and Agriculture Organization of the United Nations, Rome, 2006.

[60] AMEC, “Management of wastes from Atlantic seafood processing operations,” AMEC Earth & Environment Limited, Dartmouth, Nova Scotia, Canada, 2003.

[61] Steigers, John A., "Demonstrating the use of fish oil as fuel in a large stationary diesel engine," in *Advances in seafood byproducts conference proceedings*, Alaska Sea Grant, Fairbanks Alaska, 2002.

[62] S. Sathivel, W. Prinyawiwatkul and J. Huang, “Thermal properties and applications of the Arrhenius equation for evaluating viscosity and oxidation rates of unrefined Pollock oil,” *Journal of Food Engineering,* vol. 84, pp. 187-193, 2008.

[63] T. Skara, M. Sivertsvik and S. Bickeland, “Production of Salmon oil from filleting by-products - effects of storage conditions on lipid oxidation and content of w-3 polyunsaturated fatty acids,” *Journal of Food Science,* vol. 69, no. 8, pp. 417-421, 2004.

[64] A. Krutof, “Blending of bio-oils derived from pyrolysis of woody biomass with oil extracted from fish waste to determine applicability as a fuel oil,” Hochschule Mannheim, Mannheim, 2014.

[65] FAO, “The production of fishmeal and oil,” Food and Agriculture Organization of the United Nations, Rome, Italy, 1986.

[66] P. A. Brownsort, “Biomass pyrolysis processes: performance parameters and their influence on biochar system benefits,” University of Edinburgh, Edinburgh, England, 2009.

[67] W. N. R. W. Isahak, M. W. Hisham, M. A. Yarmo and T.-y. Y. Hin, "A review on bio-oil production from biomass by using pyrolysis method," *Renewable and Sustainable Energy Reviews,* no. 16, pp. 5910-5923, 2012.

[68] P. Basu, Biomass gasification and pyrolysis: Practical design and theory, Oxford UK: Elsevier Inc., 2010.

[69] S. Czernik and A. V. Bridgwater, "Overview of applications of biomass fast pyrolysis oil," *Energy & Fuels,* no. 18, pp. 590-598, 2004.

[70] A. Krutof, “Enhancement of pyrolysis oil fuel properties through co-pyrolysis and improved analysis,” Memorial University, St. John's, Newfoundland and Labrador, 2017.

[71] M. Garcia-Perez, J. Shen, X. S. Wang and C.-Z. Li, "Production and fuel properties of fast pyrolysis oil/bio-diesel blends," *Fuel Processing Technology,* no. 91, pp. 296-305, 2010.

[72] A. Oasmaa, D. C. Elliott and S. Müller, "Quality control in fast pyrolysis bio-oil production and use," *Environmental Progress & Sustainable Energy,* no. 28, pp. 404-409, 2009.

[73] D. C. Elliott, A. Oasmaa, F. Preto, D. Meier and A. V. Bridgwater, "Results of the IEA round robin on viscostiy and stability of fast pyrolysis bio-oils," *Energy & Fuels,* no. 26, pp. 3769-3776, 2012.

[74] R. C. Brown, Thermochemical processing of biomass: Conversion into fuels, chemicals and power, Chichester: John Wiley & Sons, Ltd., 2011.

[75] J. N. Brown and R. C. Brown, "Alternative Pyrolyzer Design: Auger Reactor," Iowa State University, 2009. [Online]. Available: http://www.cset.iastate.edu/research/current-research/alternative-pyrolyzer-design-auger-reactor/. [Accessed 6 August 2014].

[76] D. Mohan, C. U. Pittman and P. H. Steele, "Pyrolysis of wood/biomass for bio-oil: A

critical review," *Energy & Fuels,* no. 20, pp. 848-889, 2006.

[77] H. B. Goyal, S. R. C. and D. Seal, “Dio-fuels from thermochemical conversion of renewable resources: A review,” *Renewable and Sustainable Energy Reviews,* vol. 12, pp. 504-517, 2008.

[78] J. N. Brown and R. C. Brown, "Process optimization of an auger pyrolyzer with heat carrier using response surface methodology," *Bioresource Technology,* pp. 405-414, 2012.

[79] A. V. Bridgwater, "Upgrading fast pyrolysis liquids," in *Thermochemical processing of biomass: Conversion into fuels, chemicals and power*, Chichester, John Wiley & Sons Ltd., 2011, pp. 157-199.

[80] S. Papari and K. Hawboldt, “A review on the pyrolysis of woody biomass to bio-oil: Focus on kinetic models,” *Renewable and Sustainable Energy Reviews,* vol. 52, pp. 1580-1595, August 2015.

[81] Environmental Protection Agency, “Part 279 - Standards for the management of used oil,” EPA, United States, 2012.

[82] Ministry of the Environment, “A ban on the burning of used oil in space heaters,” Government of Ontario, 8 February 2007. [Online]. Available: http://www.ebr.gov.on.ca/ERS-WEB-External/displaynoticecontent.do?noticeId=MjkxMDk=&statusId=MTUwNjQ4. [Accessed 22 May 2017].

[83] N. X. Blythe, “Fish oil as an alternative fuel for internal combustion engines,” in *International Chemcial Engineering Spring Technical Conference*, 1996.

[84] J. Wang, F. Zhang and F. Preto, “A study on using fish oil as an alternative fuel for conventional combustors,” *Journal of Fuel,* vol. 87, pp. 2258-2268, 2008.

[85] S. Ushakov, H. Valland and v. Aesoy, “Combustion and emission characteristics of fish oil in a heavy-duty diesel engine,” *Energy Conversion and Management,* vol. 65, pp. 228-238, 2013.

[86] J. Lehto, A. Oasmaa, Y. Solantausta, M. Kyto and D. Chiaramonti, “Fuel oil quality and combustion of fast pyrolysis bio-oils,” VTT Technology, Espoo, Finland, 2013.

[87] D. Chiaramonti, M. Bonini, E. Fratini, G. Tondi, K. Gartner and A. V. Bridgwater, “Development of emulsions from biomass pyrolysis liquid and diesel and their use in engines. Part 1: Emulsion production,” *Biomass and Bioenergy,* no. 25, pp. 85-99, 2003.

[88] F. Preto, F. Zhang and J. Wang, "Fish oil as an alternative fuel for conventional combustors," in *The Arctic Energy Summit*, Anchorage, Alaska, 2007.

[89] J. Martin and A. Boateng, “Combustion performance of pyrolysis oil/ethanol blends in a residential-scale oil-fired boiler,” *Fuel,* vol. 133, pp. 34-44, 2014.

[90] J. Cummings, Kirk-Othmer Encyclopedia of Chemical Technology, vol. 21, A. Seidel, Ed., Hoboken, NJ: Emerald Group Publishing Limited, 2007.

[91] E. Alsbou and R. Helleur, "Accelerated Aging of Bio-oil from Fast Pyrolysis of Hardwood," *Energy & Fuels,* no. 28, pp. 3224-3235, 2014.

[92] I. A. Adeoti and K. Hawboldt, "A review of lipid extraction from fish processing by-product for us as a biofuel," *Biomass and Bioenergy,* no. 30, pp. 1-11, 2014.

[93] B. Esteban, J.-R. Riba, G. Baquero, A. Rius and R. Puig, "Temperature dependence of density and viscosity of vegetable oils," *Biomass and Bioenergy,* vol. 42, pp. 164-171, 5 April 2012.

[94] W. Cannella, C. Fairbridge, P. Arboleda, T. Bays, H. Dettman, M. Foster, R. Gieleciak, G. Gunter, D. Hager, C. Lay, S. Lewis, J. Luecke, S. Sluder and B. Zigler, "Detailed characterization of the physical and chemical properties of the reformulated FACE diesel fuels: FD2B, FD4B, and FD7B," Coordinating Research Council, Inc. (CRC), Alpharetta, GA, 2013.

[95] N. Mrad, E. G. Varuvel, M. Tazerout and F. Aloui, "Effects of biofuel from fish oil industrial residue - Diesel blends in diesel engine," *Energy,* vol. 44, pp. 955-963, 7 june 2012.

[96] V. Stamatov, D. Honnery and J. Soria, "Combustion properties of slow pyrolysis bio-oil produced from indigenous Australian species," *Renewable Energy,* vol. 31, pp. 2108-2121, 2006.

[97] C. Duvekot, "Fast refinery gas analysis using the Agilent 490 Micro GC QUAD,"

Agilent Technologies, USA, 2012.

[98] C. J. Cowper and A. J. DeRose, The analysis of gases by chromatography, vol. 7, A. W. &. C. Ltd., Ed., London: Pergamon Series, 1985.

[99] A. Lamb, K. A. Larson and E. L. Tollefson, "A gas chromatographic method for exhaust gas analysis," *Journal of the Air Pollution Control Association,* vol. 23, pp. 200-202, 1973.

10 APPENDICES

10.1 Kinematic viscosity results

Table 10-1 shows viscosity data for the Brookfield rheometer with statistical error.

Table 10-1: viscosity data from Brookfield rheometer with statistical analysis

Mixture & Temperature	Run #1 (cSt)	Run #2 (cSt)	Average (cSt)	STD DEV (cSt)	Error (α=0.1)
R-UELO 20C	121.47	121.08	**121.28**	0.28	0.29
R-UELO 40C	48.09	48.03	**48.06**	0.04	0.05
R-UELO 60C	23.29	23.18	**23.24**	0.08	0.08
Fish oil 20% 20C	101.48	101.52	**101.50**	0.02	0.02
Fish oil 20% 40C	42.14	42.08	**42.11**	0.04	0.04
Fish oil 20% 60C	21.12	21.22	**21.17**	0.07	0.07
Fish oil 50% 20C	79.33	77.65	**78.49**	1.19	1.21
Fish oil 50% 40C	79.12	78.72	**78.92**	0.28	0.28
Fish oil 50% 60C	19.09	19.15	**19.12**	0.05	0.05
Fish oil 80% 20C	42.01	41.83	**41.92**	0.13	0.13
Fish oil 80% 40C	20.92	21.04	**20.98**	0.08	0.08
Fish oil 80% 60C	12.32	12.36	**12.34**	0.03	0.03
Fish oil 100% 20C	69.76	81.23	**75.49**	8.11	8.25
Fish oil 100% 40C	34.00	28.70	**31.35**	3.74	3.81
Fish oil 100% 60C	6.79	6.36	**6.58**	0.30	0.31
Pyrolysis oil 20% 20C	106.13	110.04	**108.08**	2.77	2.82
Pyrolysis oil 20% 40C	45.44	48.74	**47.09**	2.34	2.38
Pyrolysis oil 20% 60C	21.64	25.52	**23.58**	2.74	2.79
Pyrolysis oil 50% 20C	318.63	306.15	**312.39**	8.83	8.99
Pyrolysis oil 50% 40C	127.68	143.99	**135.84**	11.53	11.74
Pyrolysis oil 50% 60C	36.40	36.53	**36.46**	0.09	0.10
Pyrolysis oil 80% 20C	108.11	108.52	**108.32**	0.29	0.29
Pyrolysis oil 80% 40C	29.00	29.66	**29.33**	0.47	0.47
Pyrolysis oil 80% 60C	8.83	8.29	**8.56**	0.38	0.39
Pyrolysis oil 100% 20C	68.12	69.08	**68.60**	0.68	0.69
Pyrolysis oil 100% 40C	20.47	21.32	**20.90**	0.60	0.62
Pyrolysis oil 100% 60C	8.91	8.84	**8.87**	0.05	0.05

10.2 TGA data

Aanalysis of the TGA results is found in chapter 7.4.2. Table 10-2 below shows nitrogen and oxygen purge rates and the switch temperature. Table 10-3 shows temperatures X, Y, and Z used for the analysis of each mixture. Figure 10-1 to Figure 10-9 are TGA curves for each mixture and contain indicators of temperatures X, Y, and Z.

Table 10-2: Experimental purge gas data for TGA

Mixture	Nitrogen rate (°C/min)	Oxygen rate (°C/min)	Temperature to switch gases (°C)
R-UELO	20.00	20.00	600
F20	20.00	20.00	600
F50	20.00	20.00	600
F80	20.00	20.00	600
F100	20.00	20.00	550
P20	20.00	20.00	600
P50	20.00	20.00	600
P80	20.00	20.00	600
P100	20.00	20.00	600

Table 10-3: Temperatures X, Y, and Z used in TGA analysis

Mixture	Temperature X	Temperature Y	Temperature Z
R-UELO-1	150 °C	500 °C	700 °C
F20	150 °C	500 °C	700 °C
F50	150 °C	500 °C	700 °C
F80	150 °C	500 °C	700 °C
F100	150 °C	550 °C	750 °C
R-UELO-2	200 °C	600 °C	700 °C
P20	200 °C	600 °C	700 °C
P50	200 °C	600 °C	700 °C
P80	200 °C	600 °C	700 °C
P100	200 °C	600 °C	700 °C

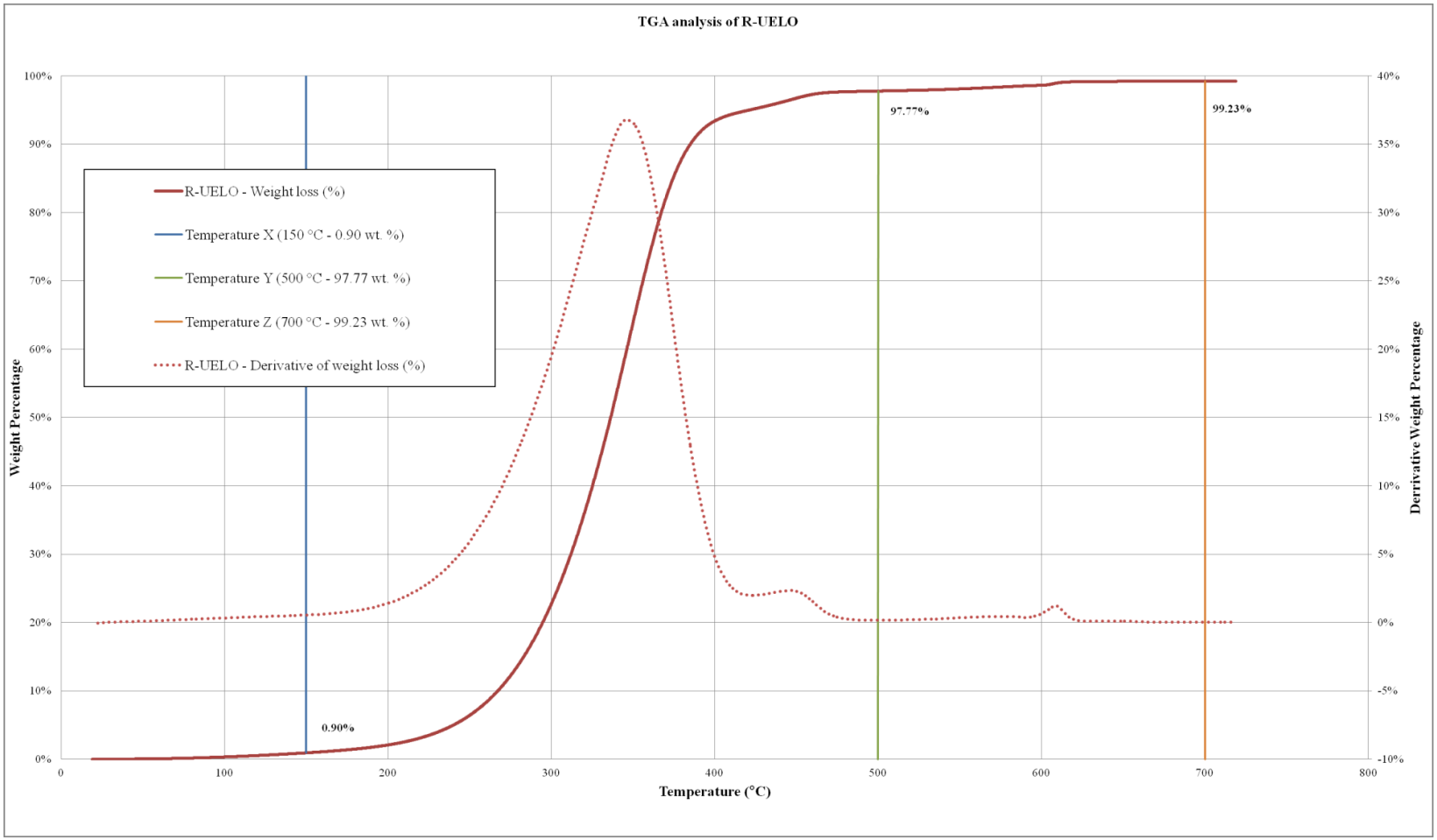

Figure 10-1: TGA curve of R-UELO with indicators of volatiles and ash content

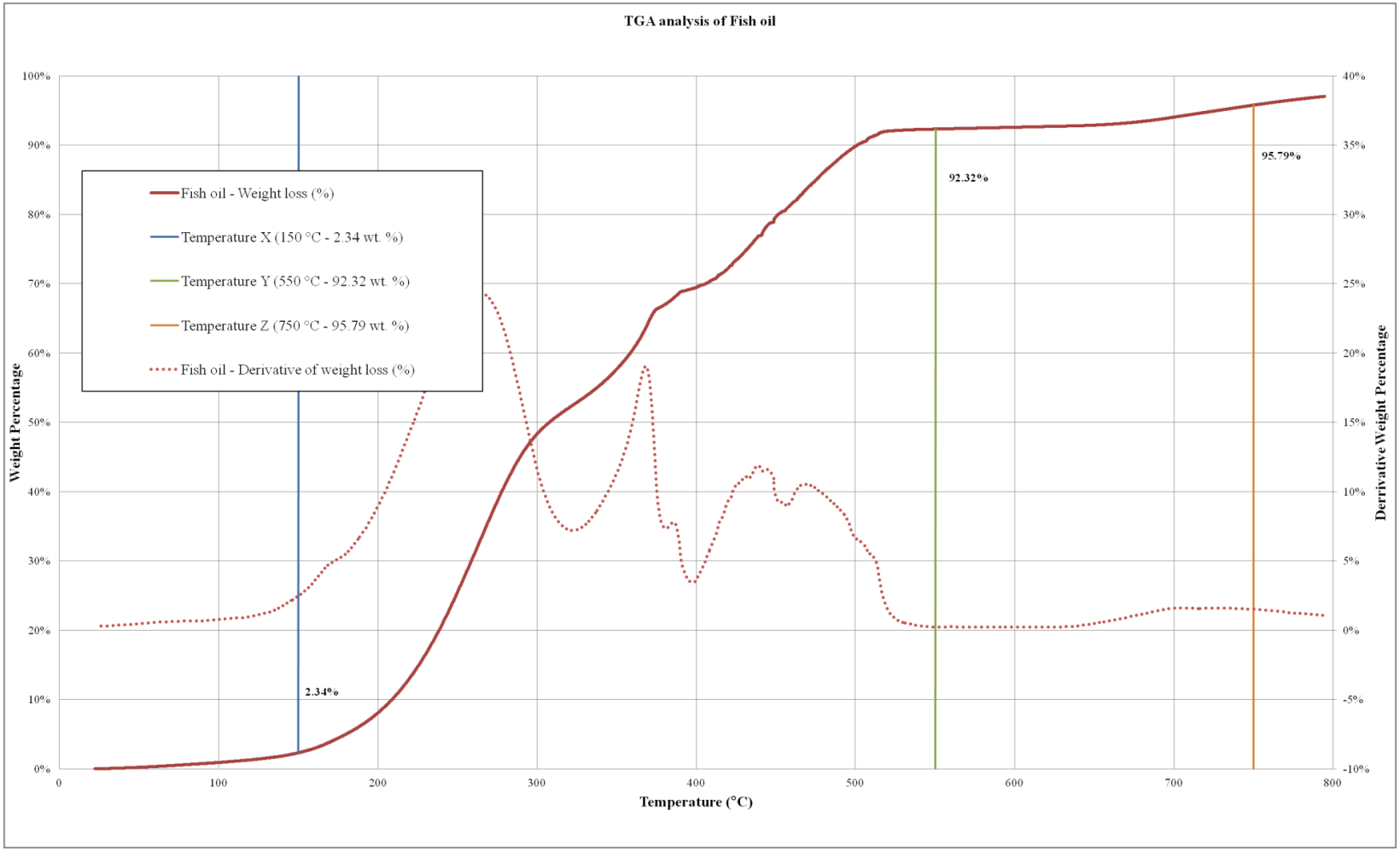

Figure 10-2: TGA curve of fish oil with indicators of volatiles and ash content

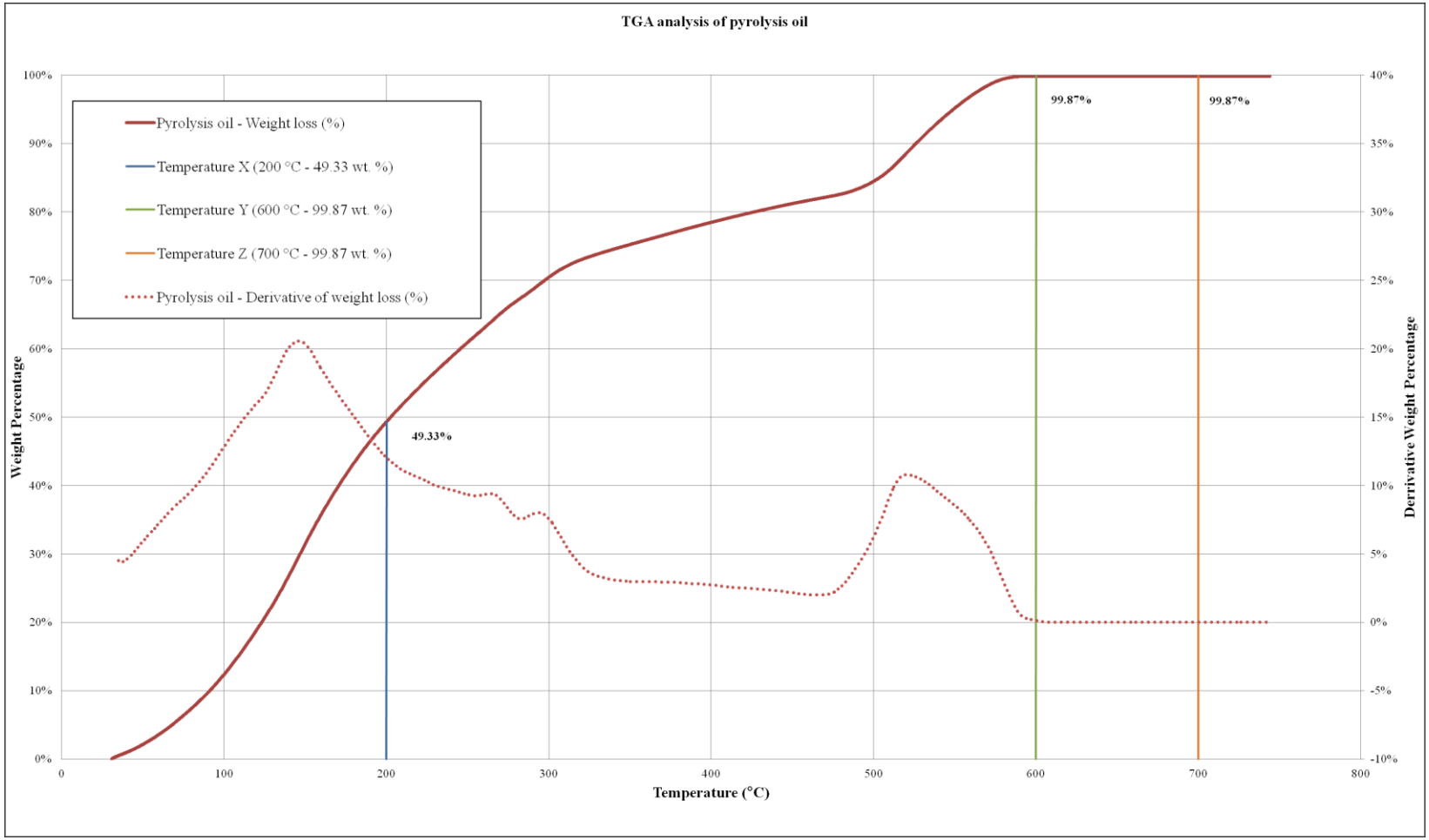

Figure 10-3: TGA curve of pyrolysis oil with indicators of volatiles and ash content

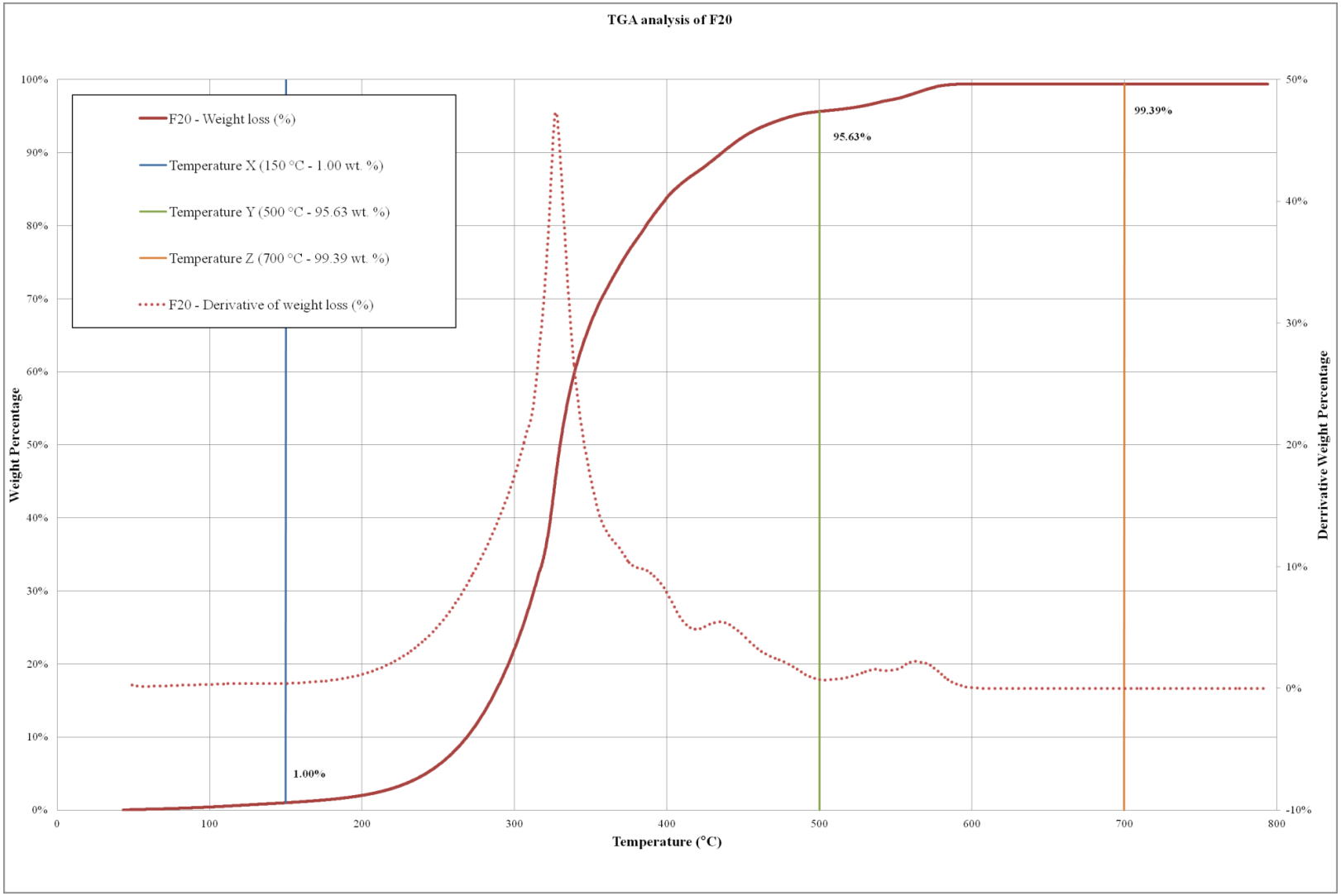

Figure 10-4: TGA analysis of F20

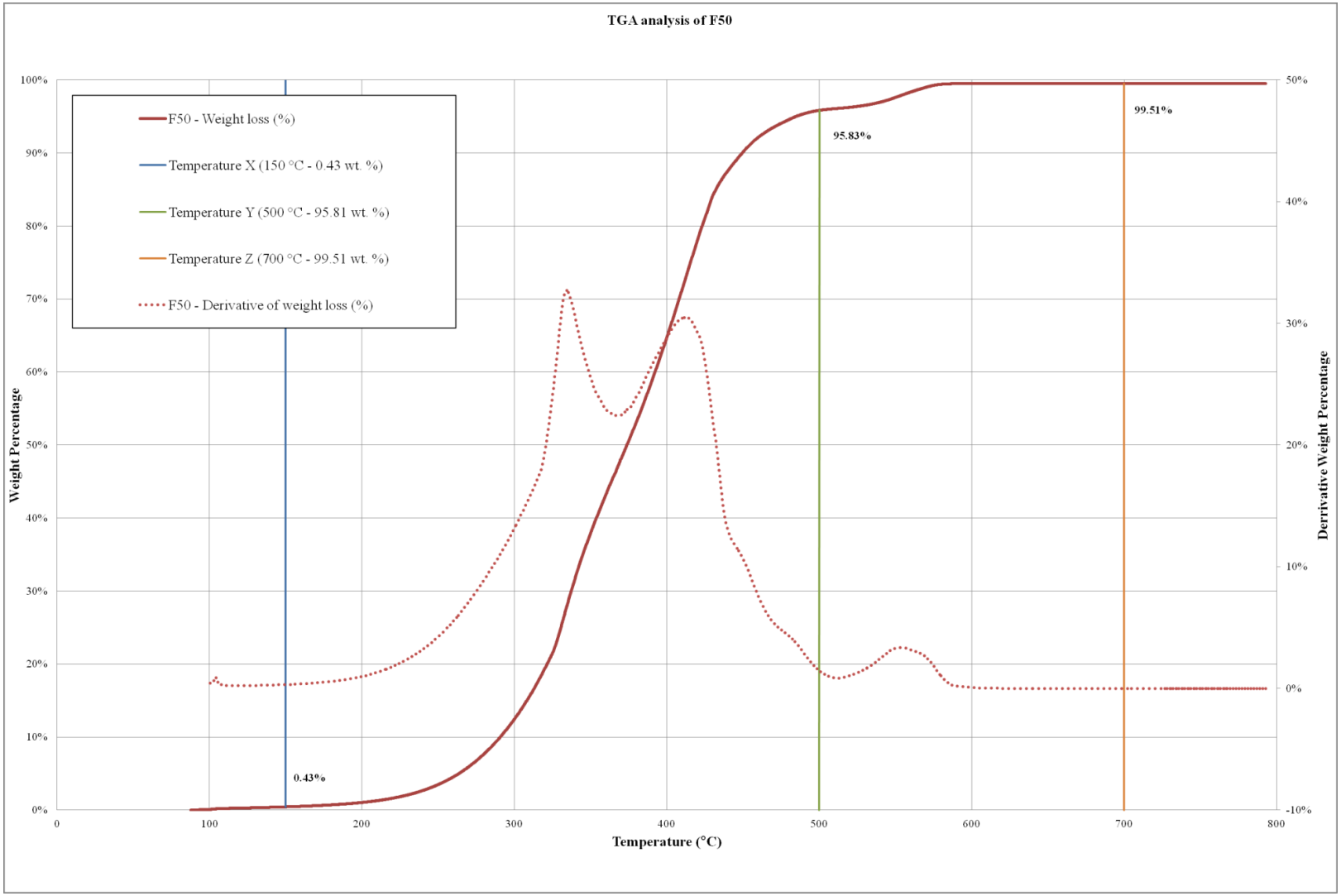

Figure 10-5: TGA analysis of F50

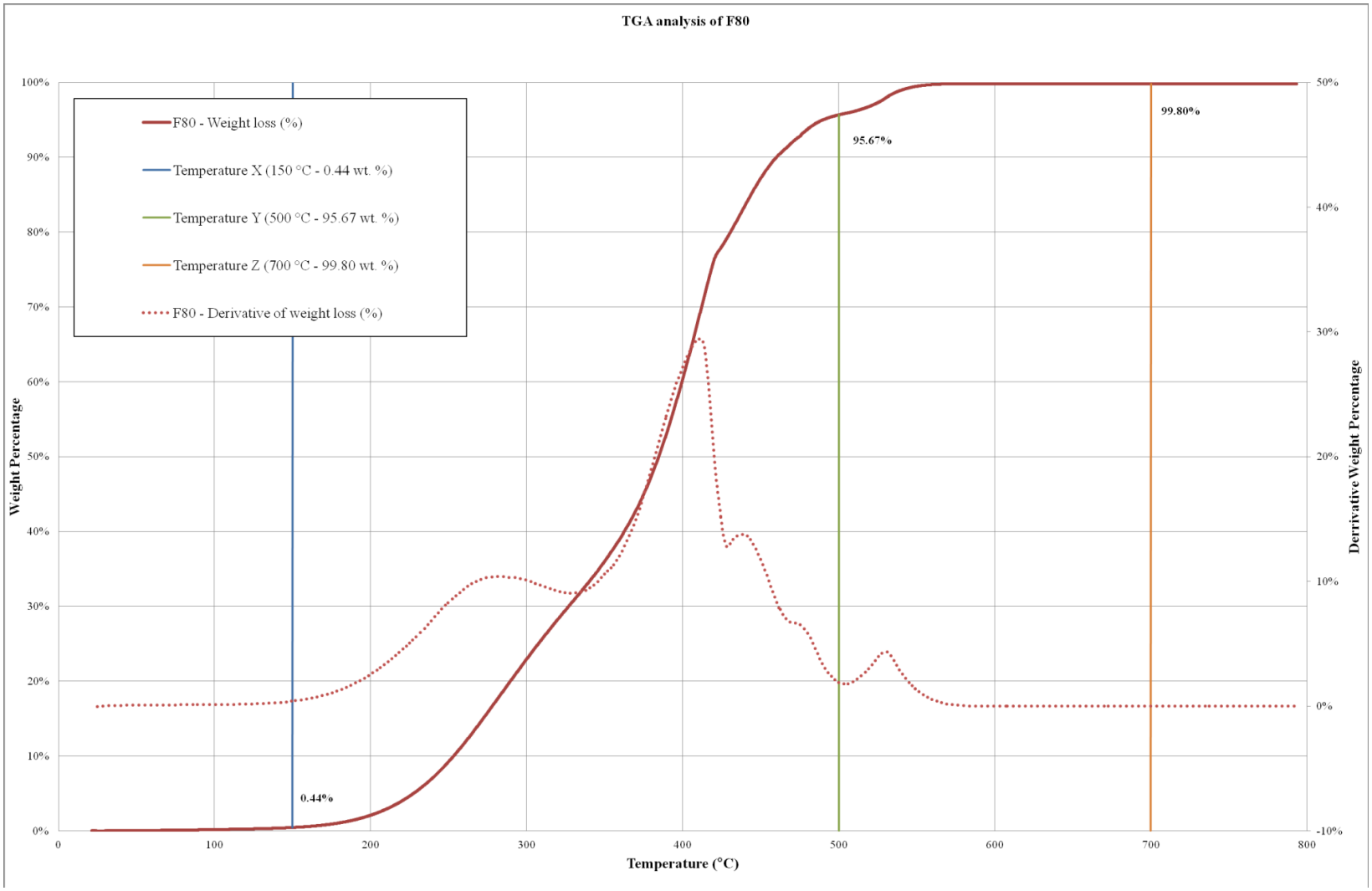

Figure 10-6: TGA analysis of F80

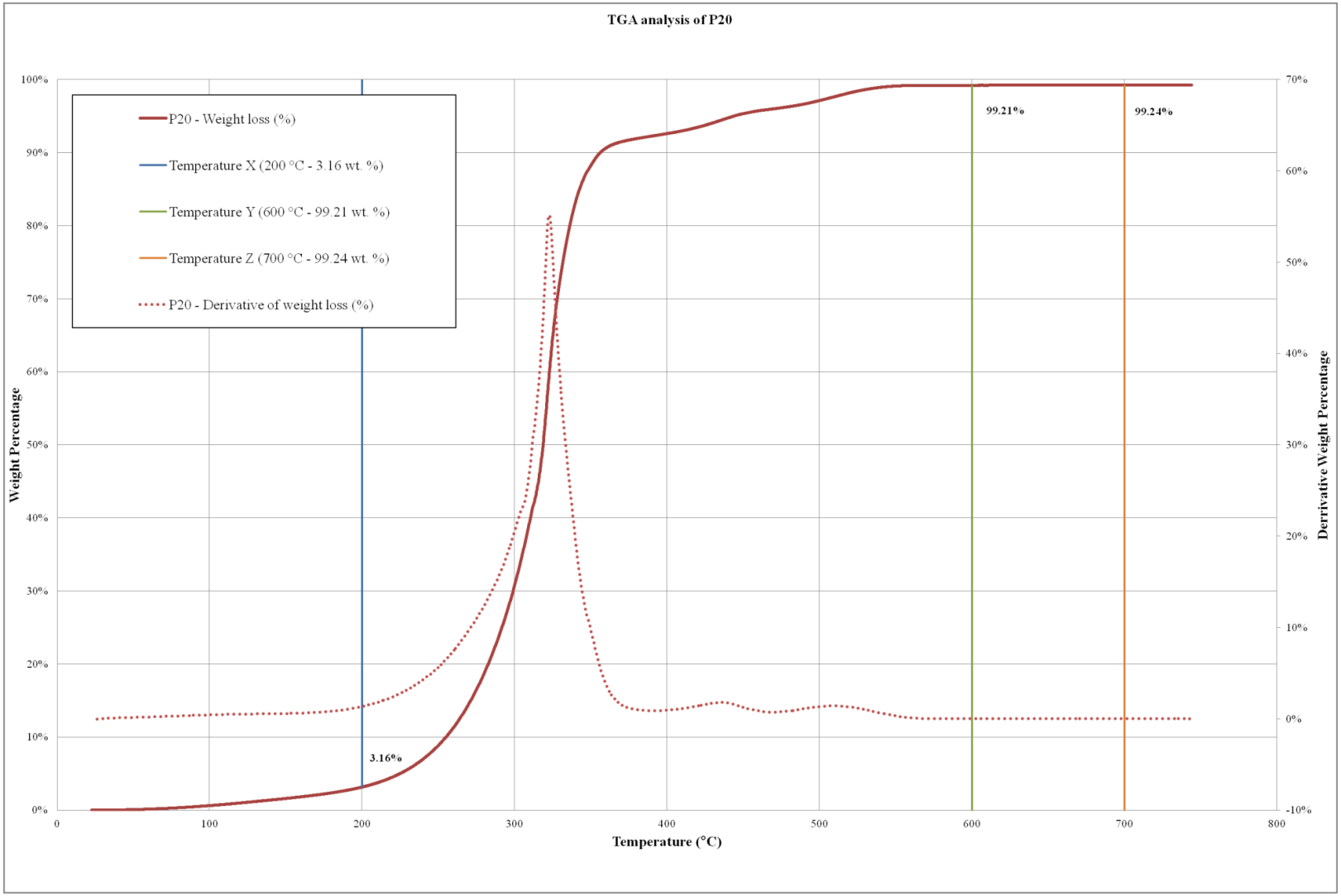

Figure 10-7: TGA analysis of P20

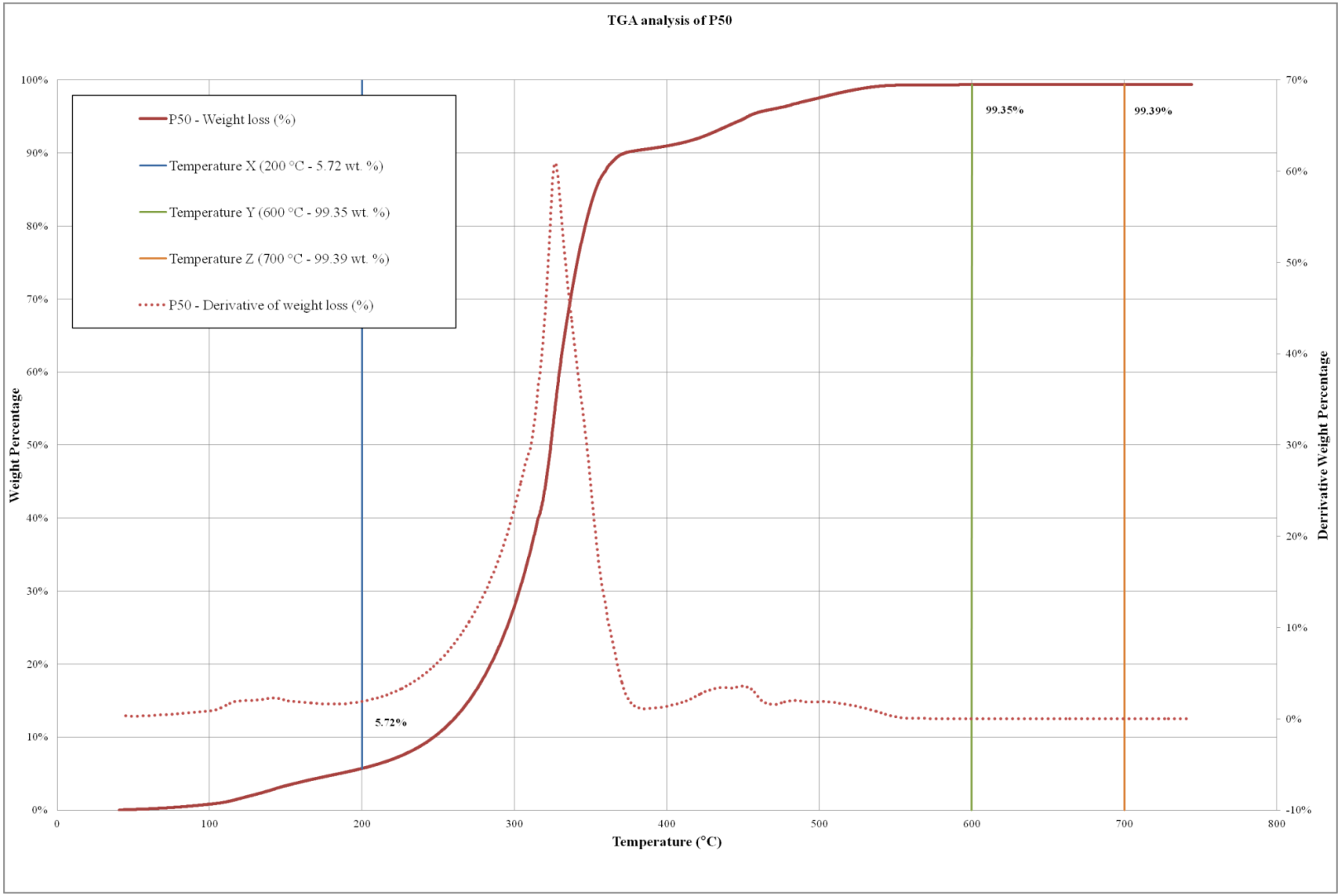

Figure 10-8: TGA analysis of P50

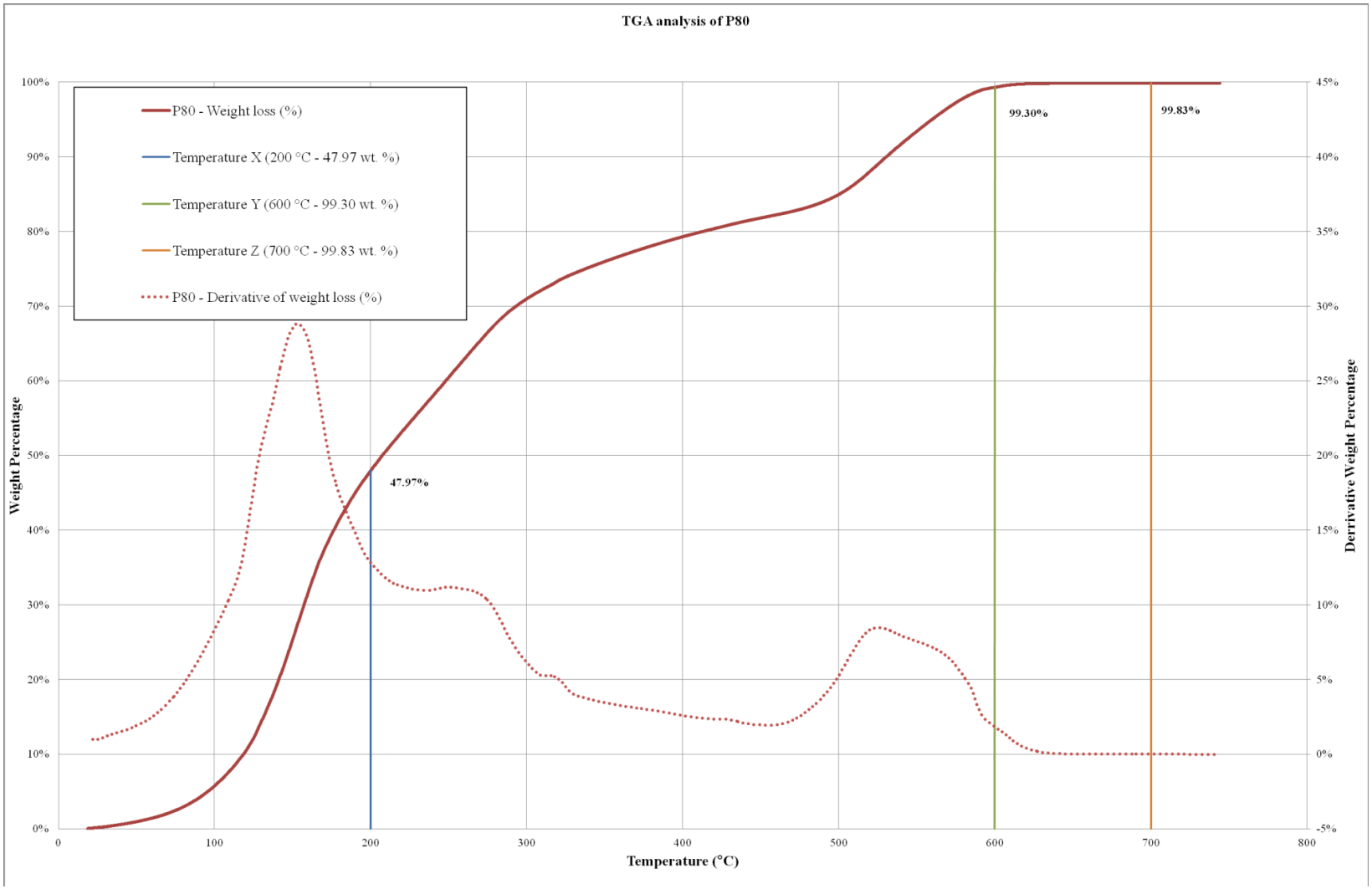

Figure 10-9: TGA analysis of P80

10.3 Chamber and stack temperatures

Figure 10-10 and Figure 10-11 represent the raw data for chamber and stack temperature measurements using the portable RDXL4SD 4-chanel Omega data logger.

Note that the stack temperature measurement in Figure 10-10 is higher from 11:00 to 12:00. This is because the probe was placed in the upper section of the stack and then moved to the bottom of the stack for the rest of the trial. Throughout the trial shown in Figure 10-11, the stack probe is placed at the bottom of the stack.

From 14:30 to 15:15 in Figure 10-10, the stack temperature measurement is between 10 and 20 °C because the probe was removed from the stack to leave room for the port to be used for other forms of stack analysis.

Due to the furnace stopping to reheat the fuel every so often, the chamber and stack temperature measurements jump from 200 – 400 °C when the furnace is running to 50 – 100 °C when the burner has stopped and the fuel is being preheated.

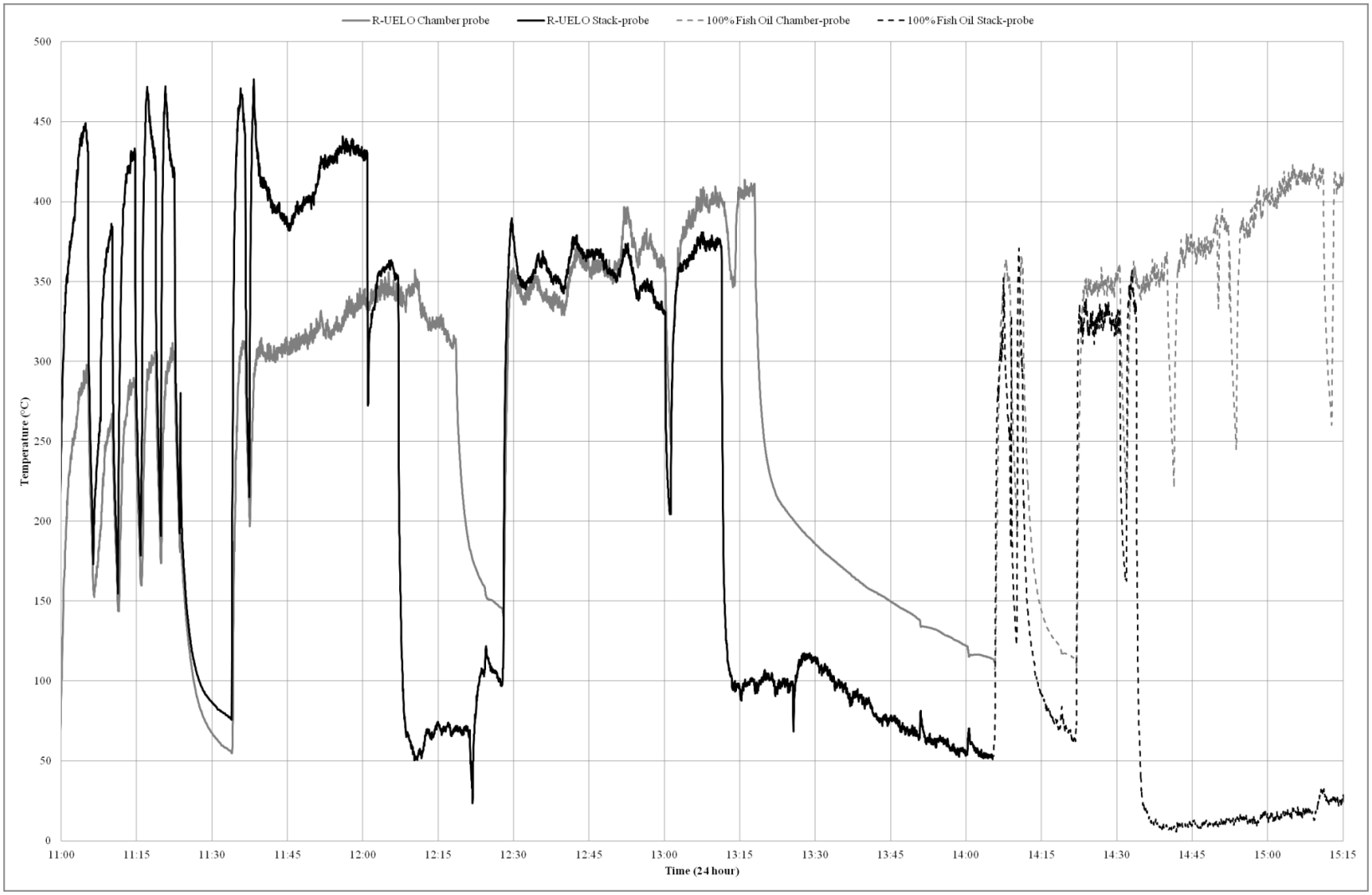

Figure 10-10: Temperature measurements for combustion of R-UELO and 100% fish oil

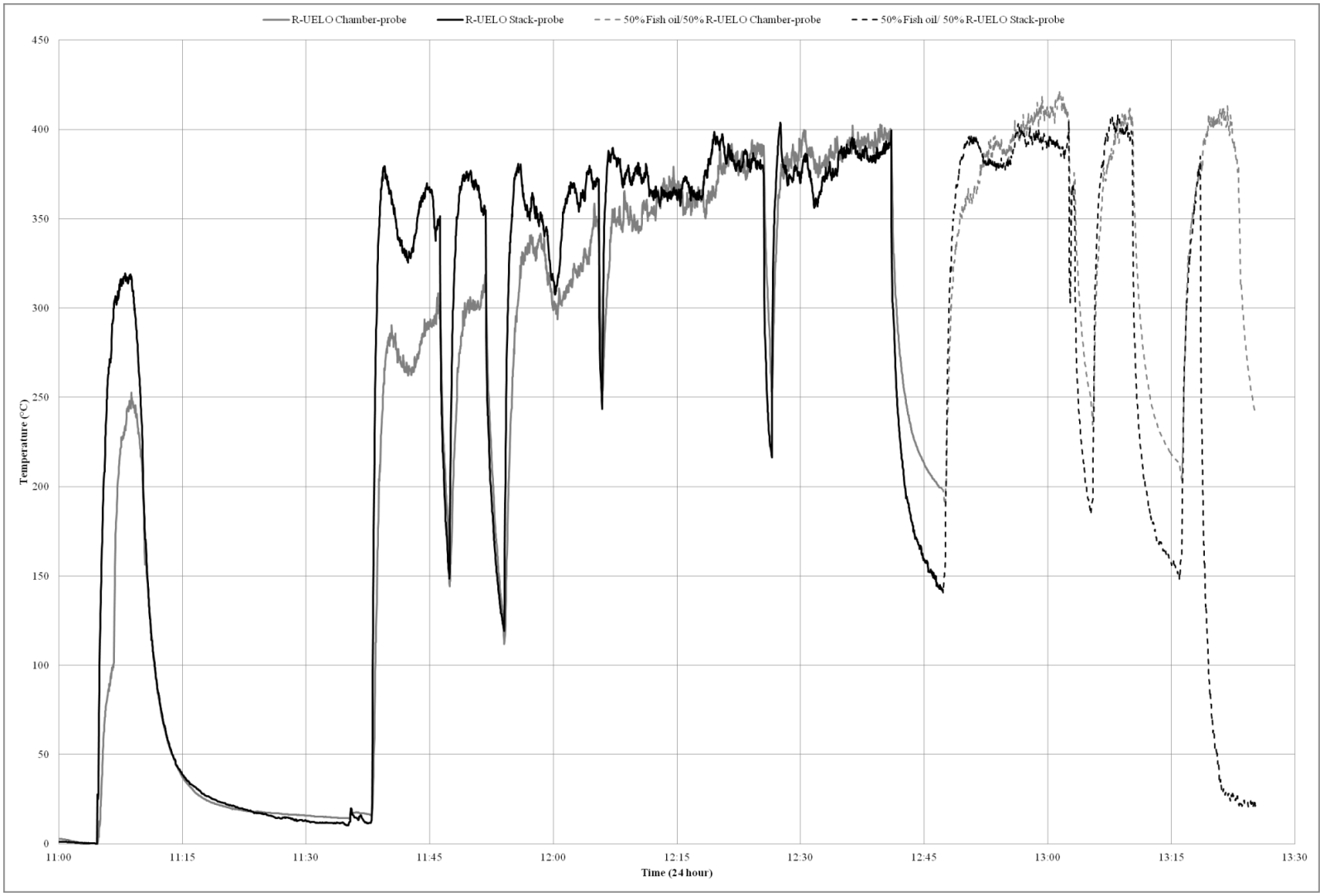

Figure 10-11: Temperature measurements for combustion of R-UELO and 50% R-UELO/fish oil

10.4 Adiabatic flame temperature calculation

Elemental analysis of R-UELO and fish oil is shown in the table below.

Fuel	Carbon (wt. %)	Hydrogen (wt. %)	Oxygen (wt. %)
R-UELO	84.3	13.9	1.1
Fish oil	77.6	11.3	11.2

A simplified stoichiometric reaction is used to represent combustion

$$C + O_2 = CO_2 \rightarrow 12.01\ kg\ C + 32\ kg\ O_2 = 44.01\ kg\ CO_2$$

$$2H_2 + O_2 = 2H_2O \rightarrow 2.016\ kg\ H_2 + 16\ kg\ O_2 = 18.016\ kg\ H_2O$$

Assume nitrogen is unreactive and combustion follows the simplified equations above with a basis of 1 kg of fuel per hour.

$$O_2 = O_2\ used\ for\ CO_2 + O_2\ used\ for\ H_2O - O_2\ in\ fuel$$

$$CO_2 = CO_2\ produced$$

$$H_2O = H_2O\ produced$$

$$N_2 = 76.77\ wt.\%\ of\ N_2\ per\ 23.23\ wt.\%\ O_2$$

Fuel	kg O_2/ kg fuel	kg CO_2/ kg fuel	kg H_2O/ kg fuel	kg N_2/ kg fuel	kg air/ kg fuel
R-UELO	3.34	3.09	1.24	11.04	14.38
Fish oil	2.85	2.84	1.01	9.43	12.28

For R-UELO, heat capacity is estimated from the heat capacity of virgin engine lubricating oil. For fish oil, the heat capacity is estimated to be 1.3. Heat capacities are calculated using NIST-JANAF Thermochemical Tables, Fourth Edition J. Physical

Chemicstry Reference Data in NIST Chemistry WebBook, NIST Standard Reference Database Number 69.

(260 - 400 K)	Cp [R-UELO] =	0.004167 * T + 0.665
(260 - 400 K)	Cp [fish oil] =	1.30
(100 - 700 K)	Cp [O2] =	31.32234 + -20.23531*T + 57.86644*T^2 + -36.50624*T^3 + -0.007374/T^2
(1200 - 6000 K)	Cp [CO2] =	58.16639 + 2.720074*T + -0.492289*T^2 + 0.038844*T^3 + -6.447293/T^2
(500 - 1700 K)	Cp [H2O] =	30.09200 + 6.832514*T + 6.793435*T^2 + -2.534480*T^3 + 0.082139/T^2
(100 - 500 K)	Cp [N2] =	28.98641 + 1.853978*T + -9.647459*T^2 + 16.63537*T^3 + 0.000117/T^2
(500 - 2000 K)	Cp [N2] =	19.50583 + 19.88705*T + -8.598535*T^2 + 1.369784*T^3 + 0.527601/T^2

Heat of reactants is calculated at a pre-heat temperature of 55 °C or 328.15 K.

$$Heat\ of\ Reactants = (T_1 - T_{ref})\ \times \sum (mass \times C_p)\ of\ reactants$$

	R-UELO	Fish oil
Heat of reactants (kJ)	495.68	411.90

Heat of products is the sum of heat of reactants and heat of combustion of the products. It is also equal to the sum of the heat of each component at the flame temperature or T2.

$$Heat\ of\ Products = Heat\ of\ combustion + Heat\ of\ Reactants$$

$$Heat\ of\ Products = (T_2 - T_1)\ \times \sum (mass \times C_p)\ of\ products$$

Calculating for T_2 gives the adiabatic flame temperature for the given fuel.

	R-UELO	Fish oil
Adiabatic flame temperature (°C)	2102	1994

10.5 Theoretical combustion calculations

Elemental analysis of R-UELO and fish oil is shown in the table below.

Fuel	Carbon (wt. %)	Hydrogen (wt. %)	Oxygen (wt. %)
Diesel	86.2	13.8	0.0
R-UELO	84.3	13.9	1.1
Fish oil	77.6	11.3	11.2

A simplified stoichiometric reaction is used to represent combustion

$$C + O_2 = CO_2 \rightarrow 12.01\ kg\ C + 32\ kg\ O_2 = 44.01\ kg\ CO_2$$

$$2H_2 + O_2 = 2H_2O \rightarrow 2.016\ kg\ H_2 + 16\ kg\ O_2 = 18.016\ kg\ H_2O$$

Assume Nitrogen is unreactive and combustion follows the simplified equations above.

$$O_2 = O_2\ used\ for\ CO_2 + O_2\ used\ for\ H_2O - O_2\ in\ fuel$$

$$CO_2 = CO_2\ produced$$

$$H_2O = H_2O\ produced$$

$$N_2 = 76.77\ wt.\%\ of\ N_2\ per\ 23.23\ wt.\%\ O_2$$

Fuel	kg O_2/ kg fuel	kg CO_2/ kg fuel	kg H_2O/ kg fuel	kg N_2/ kg fuel	kg air/ kg fuel
Diesel	3.39	3.16	1.23	11.20	14.59
R-UELO	3.34	3.09	1.24	11.04	14.38
Fish oil	2.85	2.84	1.01	9.43	12.28

HHV measured in the bomb calorimeter and an enthalpy of vaporization of water at 50 °C (2,382 kJ/kg) is used to calculate LHV for each fuel.

Fuel	HHV (kJ/kg)	LHV (kJ/kg)
Diesel	43,000	40,041
R-UELO	45,394	42,435
Fish oil	36,763	34,358

Fuel flow rates are measured during experiments and are taken from Table 7-9.

10.5.1 Combustion calculations with 0% excess air (stoichiometric)

Fuel	Fuel flow (kg/hr)	Air flow (kg/hr)	Total (kg/hr)
Diesel	2.4	35.0	37.4
R-UELO	2.7	38.8	41.5
Fish oil	3.9	47.9	51.8

Flow rates of components in the exhaust gas are calculated from stoichimetric ratios

Fuel	Exhaust O_2 (kg/hr)	Exhaust CO_2 (kg/hr)	Exhaust H_2O (kg/hr)	Exhaust N_2 (kg/hr)
Diesel	0.0	7.6	3.0	26.9
R-UELO	0.0	8.3	3.4	29.8
Fish oil	0.0	11.1	3.9	36.8

Assuming 0.03 kg of moisture per kg of air supply, final is calculated.

Diesel	kg/hr	kmole/hr	vol. % of wet gas	vol. % of dry gas
O_2	0.0	0.00	0.0	0.0
CO_2	7.6	0.17	12.7	15.2
H_2O	4.0	0.22	16.6	-
N_2	26.9	0.96	70.9	84.8
Total	**38.48**	**1.35**	**100**	**100**

R-UELO	kg/hr	kmole/hr	vol. % of wet gas	vol. % of dry gas
O_2	0.0	0.00	0.0	0.0
CO_2	8.3	0.19	12.6	15.1
H_2O	4.5	0.25	16.7	-
N_2	29.8	1.06	70.7	84.9
Total	**42.66**	**1.50**	**100**	**100**

Fish oil	kg/hr	kmole/hr	vol. % of wet gas	vol. % of dry gas
O_2	0.0	0.00	0.0	0.0
CO_2	11.1	0.25	13.5	16.1
H_2O	5.4	0.30	16.0	-
N_2	36.8	1.31	70.5	83.9
Total	**53.2**	**1.86**	**100**	**100**

10.5.2 Combustion calculations with 15% excess air

Fuel	Fuel flow (kg/hr)	Air flow (kg/hr)	Total (kg/hr)
Diesel	2.4	40.3	42.7
R-UELO	2.7	44.6	47.3
Fish oil	3.9	55.1	59.0

Flow rates of components in the exhaust gas are calculated from stoichiometric ratios.

Fuel	Exhaust O_2 (kg/hr)	Exhaust CO_2 (kg/hr)	Exhaust H_2O (kg/hr)	Exhaust N_2 (kg/hr)
Diesel	1.2	7.6	3.0	30.9
R-UELO	1.4	8.3	3.4	34.3
Fish oil	1.7	11.1	3.9	42.3

Assuming 0.03 kg of moisture per kg of air supply, final composition is calculated.

Diesel	kg/hr	kmole/hr	vol. % of wet gas	vol. % of dry gas
O_2	1.2	0.04	2.5	2.9
CO_2	7.6	0.17	11.2	13.1
H_2O	4.2	0.23	15.0	-
N_2	30.9	1.10	71.4	84.0
Total	**43.9**	**1.31**	**100**	**100**

R-UELO	kg/hr	kmole/hr	vol. % of wet gas	vol. % of dry gas
O_2	1.4	0.04	2.5	2.9
CO_2	8.3	0.19	11.1	13.0
H_2O	4.7	0.26	15.2	-
N_2	34.3	1.22	71.3	84.1
Total	**48.7**	**1.72**	**100**	**100**

Fish oil	kg/hr	kmole/hr	vol. % of wet gas	vol. % of dry gas
O_2	1.7	0.05	2.5	2.9
CO_2	11.1	0.25	11.9	13.9
H_2O	5.6	0.31	14.6	-
N_2	42.3	1.51	71.1	83.2
Total	**60.6**	**2.12**	**100**	**100**

10.6 Micro GC results

Table 10-4: Micro GC EZChrom Software integration results

		Channel 1 - 10m PPU Heated Injector					Channel 2 - 8m 5CB Heated Injector				
Sample	Date & Time	Ret.Time (s)	Area	Area %	Height	Height %	Ret.Time (s)	Area	Area %	Height	Height %
Diesel_0	12/5/2017	TOTAL	110715323	100	105868834	100	TOTAL	106353769	100	195443591	100
	4:16:01 PM	28.07	109018317	98.47	104459966	98.67	20.75	104627938	98.38	192862488	98.68
		40.34	1697006	1.53	1408868	1.33	22.07	157278	0.15	265900	0.14
							26.65	1568553	1.47	2315203	1.18
Diesel_1	12/5/2017	TOTAL	365978444	100	336959584	100	TOTAL	273868054	99.99	868305671	99.99
	4:12:37 PM	27.88	364728369	99.66	336003233	99.72	20.51	103166814	37.67	429966402	49.52
		40.52	1250075	0.34	956351	0.28	20.82	169236395	61.79	436276480	50.24
							22.06	357781	0.13	476981	0.05
							26.71	1107064	0.4	1585808	0.18
Diesel_2	12/6/2017	TOTAL	325804975	100	303866295	100	TOTAL	241835889	100	750492345	100
	4:48:00 PM	27.99	324593878	99.63	302903895	99.68	20.45	77432128	32.02	370928836	49.42
		40.44	1211097	0.37	962400	0.32	20.79	163159154	67.47	377718784	50.33
							22.01	178922	0.07	276620	0.04
							26.61	1065685	0.44	1568105	0.21
Diesel_3	12/8/2017	TOTAL	324244647	100	303286232	100	TOTAL	242615087	100	750910170	100
	11:17:29 AM	28.03	321963831	99.3	301416005	99.38	20.47	78206788	32.23	370419638	49.33
		40.3	2280816	0.7	1870227	0.62	20.81	162252376	66.88	377303634	50.25
							22.06	226234	0.09	333583	0.04
							26.57	1929689	0.8	2853315	0.38
R-UELO_1	1/8/2018	TOTAL	357895785	100	329420709	100	TOTAL	278787273	100.01	862541644	100
	11:32:20 AM	27.92	356640861	99.65	328451364	99.71	20.59	92909555	33.33	426167950	49.41
		40.55	1254924	0.35	969345	0.29	20.91	182118102	65.33	431971716	50.08
							22.03	1801154	0.65	2681696	0.31
							26.84	1958462	0.7	1720282	0.2
R-UELO_2	1/8/2018	TOTAL	358727432	100	331099777	100	TOTAL	275122342	100	858847948	100
	3:16:58 PM	27.95	357453198	99.64	330015612	99.67	20.57	90256156	32.81	424451651	49.42
		40.57	1274234	0.36	1084165	0.33	20.88	181178317	65.85	429949715	50.06
							22.02	1799155	0.65	2658841	0.31
							26.81	1888714	0.69	1787741	0.21
50/50_1	1/19/2018	TOTAL	334606111	100.01	325099564	100	TOTAL	258437144	100	804484470	100.01
	4:31:27 PM	28.06	292800484	87.51	290182815	89.26	20.45	75212600	29.1	370558135	46.06
		29.53	40643898	12.15	33993825	10.46	20.76	147759200	57.17	376626185	46.82
		40.6	1161729	0.35	922924	0.28	21.79	34309827	13.28	55729050	6.93
							26.64	1155517	0.45	1571100	0.2
50/50_2	1/19/2018	TOTAL	334985158	100	324615640	99.99	TOTAL	257443270	100	801683206	100.01
	5:47:43 PM	28.04	295362909	88.17	291130432	89.68	20.42	75634819	29.38	370828097	46.26
		29.41	38383844	11.46	32509487	10.01	20.74	148392194	57.64	376569259	46.97
		40.57	1238405	0.37	975721	0.3	21.77	32258996	12.53	52635846	6.57
							26.6	1157261	0.45	1650004	0.21
50/50_3	1/19/2018	TOTAL	334992088	100	325421105	100	TOTAL	258827832	100	804100043	100
	5:42:33 PM	28	293728567	87.68	290670783	89.32	20.39	76752174	29.65	370825922	46.12
		29.38	40073702	11.96	33808304	10.39	20.71	147083117	56.83	376639690	46.84
		40.52	1189819	0.36	942018	0.29	21.73	33851969	13.08	55035010	6.84
							26.57	1140572	0.44	1599421	0.2
Fish oil_0	1/18/2018	TOTAL	329678233	100	319356871	100	TOTAL	253340680	100	774604124	99.99
	10:00:11 AM	28	306133091	92.86	293587095	91.93	20.33	76320068	30.13	370433269	47.82
		29.04	20607758	6.25	23245990	7.28	20.65	158479602	62.56	376938948	48.66
		35.43	1249560	0.38	1125565	0.35	21.77	14577037	5.75	22929326	2.96
		40.46	1367419	0.41	1109333	0.35	22.99	1187496	0.47	1810026	0.23
		47.35	320405	0.1	288888	0.09	26.55	2360664	0.93	1964550	0.25
							33.04	133264	0.05	178684	0.02
							37.88	282549	0.11	349321	0.05
Fish oil_1	1/18/2018	TOTAL	335556859	99.99	327445370	99.99	TOTAL	260681600	100	813658547	99.99
	10:14:08 AM	28.01	285789551	85.17	286001588	87.34	20.33	72381677	27.77	371123695	45.61
		29.28	47190462	14.06	39299766	12	20.64	146713060	56.28	376419499	46.26
		35.5	652509	0.19	579681	0.18	21.64	38665988	14.83	62677518	7.7
		40.47	1773661	0.53	1421316	0.43	22.96	579802	0.22	835143	0.1
		47.45	150676	0.04	143019	0.04	26.48	2202865	0.85	2422292	0.3
							37.89	138208	0.05	180400	0.02

Table 10-4 above shows the EZChrom software integration results from the Agilent Micro GC analysis. Results highlighted in red are considered outliers and results highlighted in green correspond to the printed chromatographs. The diesel emission sample “Diesel_0” is considered an outlier because the total area and total height measured was much less than any other sample. The fish oil emission sample “Fish oil_0” is considered an outlier because the second peak is partially co-eluted with the first peak.

Figure 10-12 to Figure 10-19 show large-scale chromatographs produced from the Agilent Micro GC.

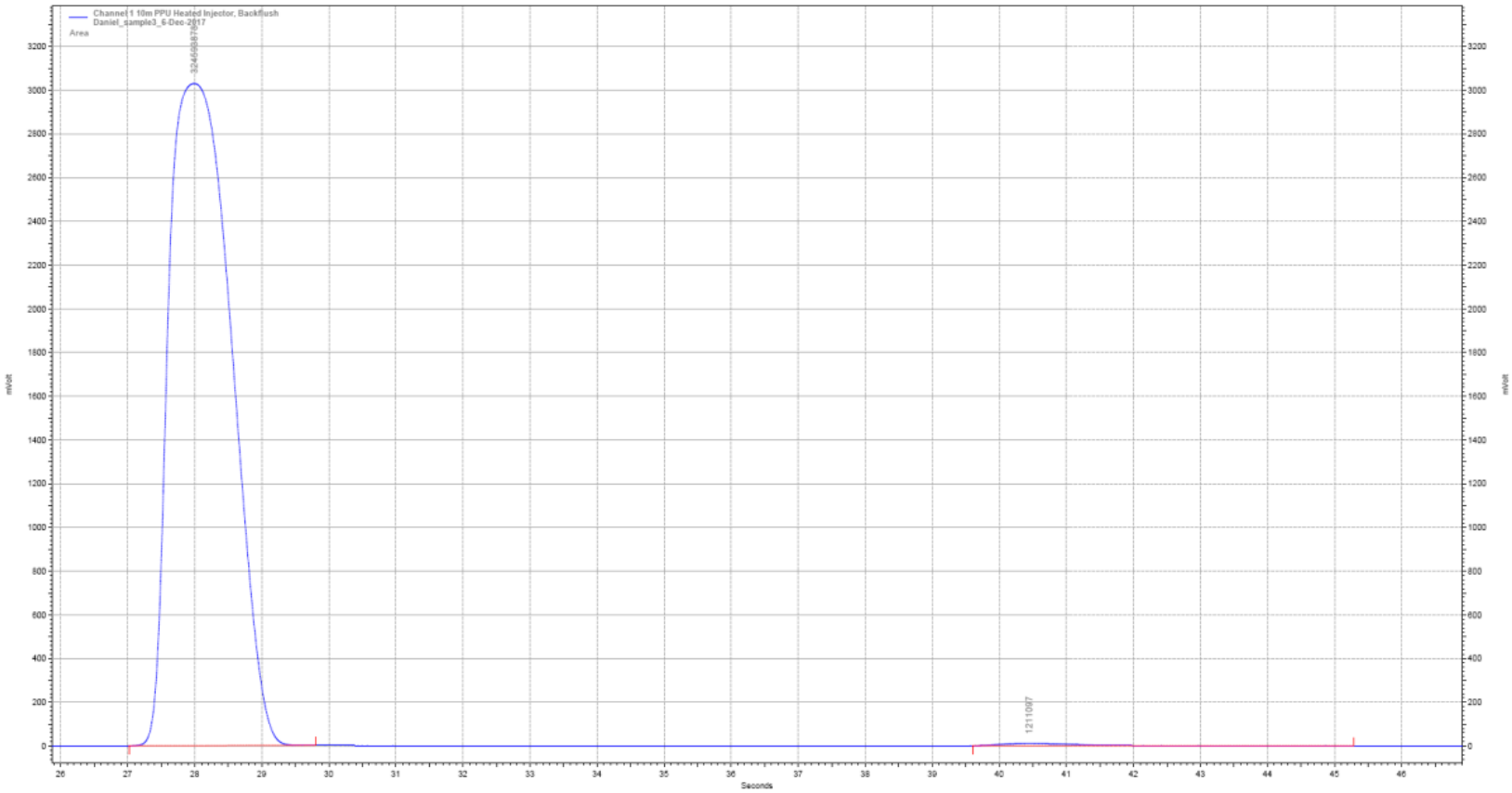

Figure 10-12: Column 1 results for diesel fuel

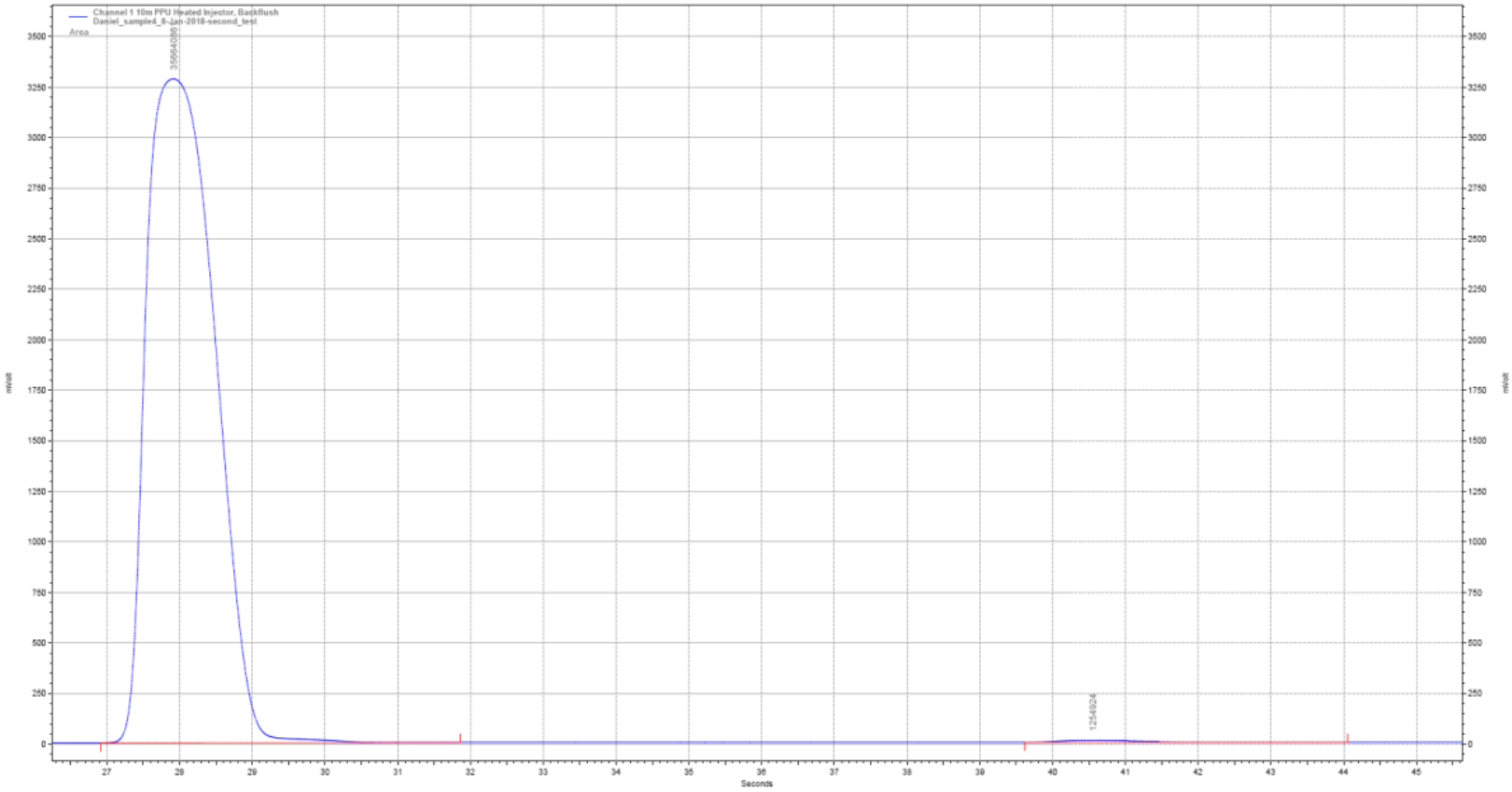

Figure 10-13: Column 1 results for R-UELO

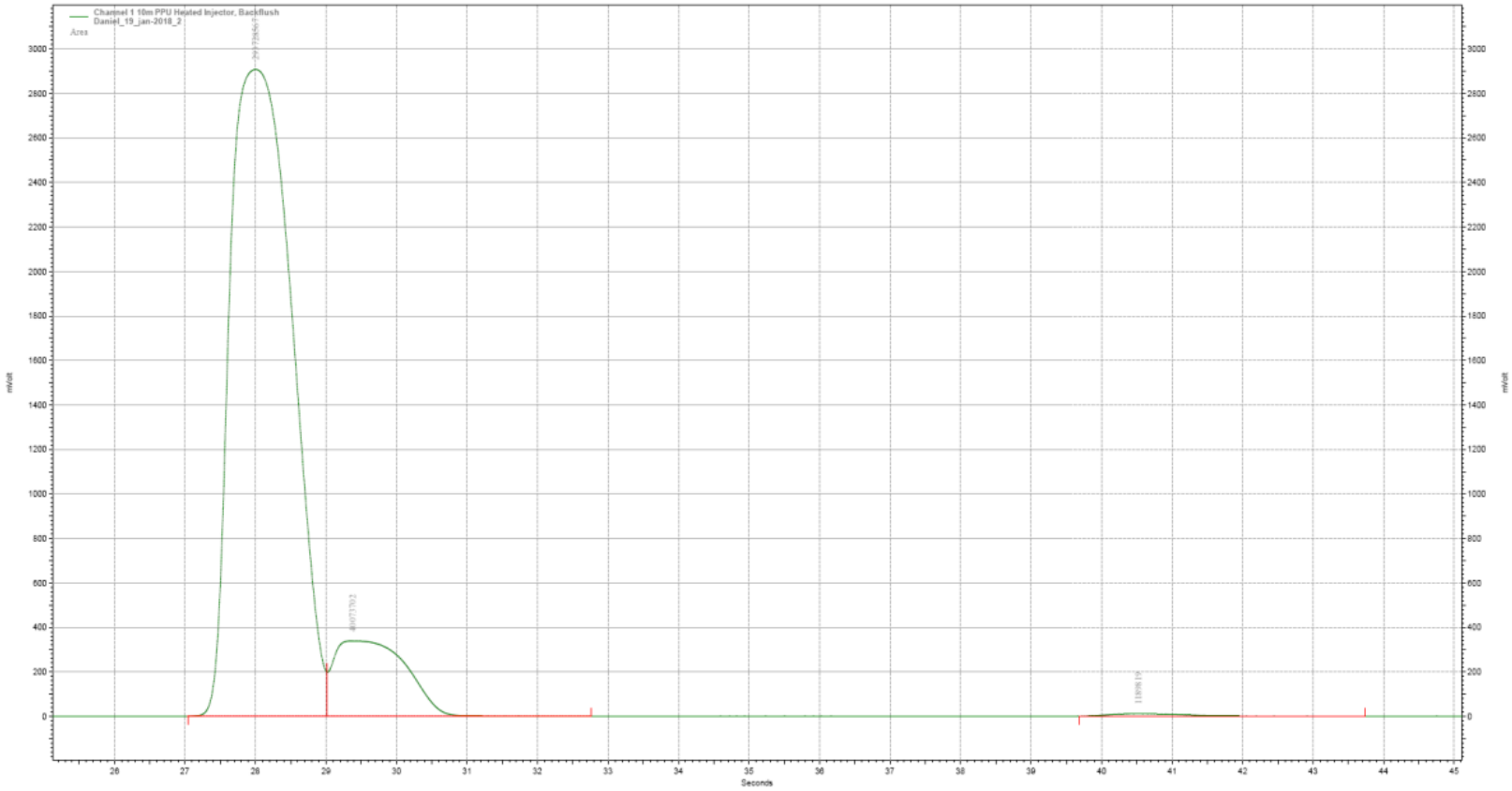

Figure 10-14: Column 1 results for 50/50% R-UELO/fish oil blend

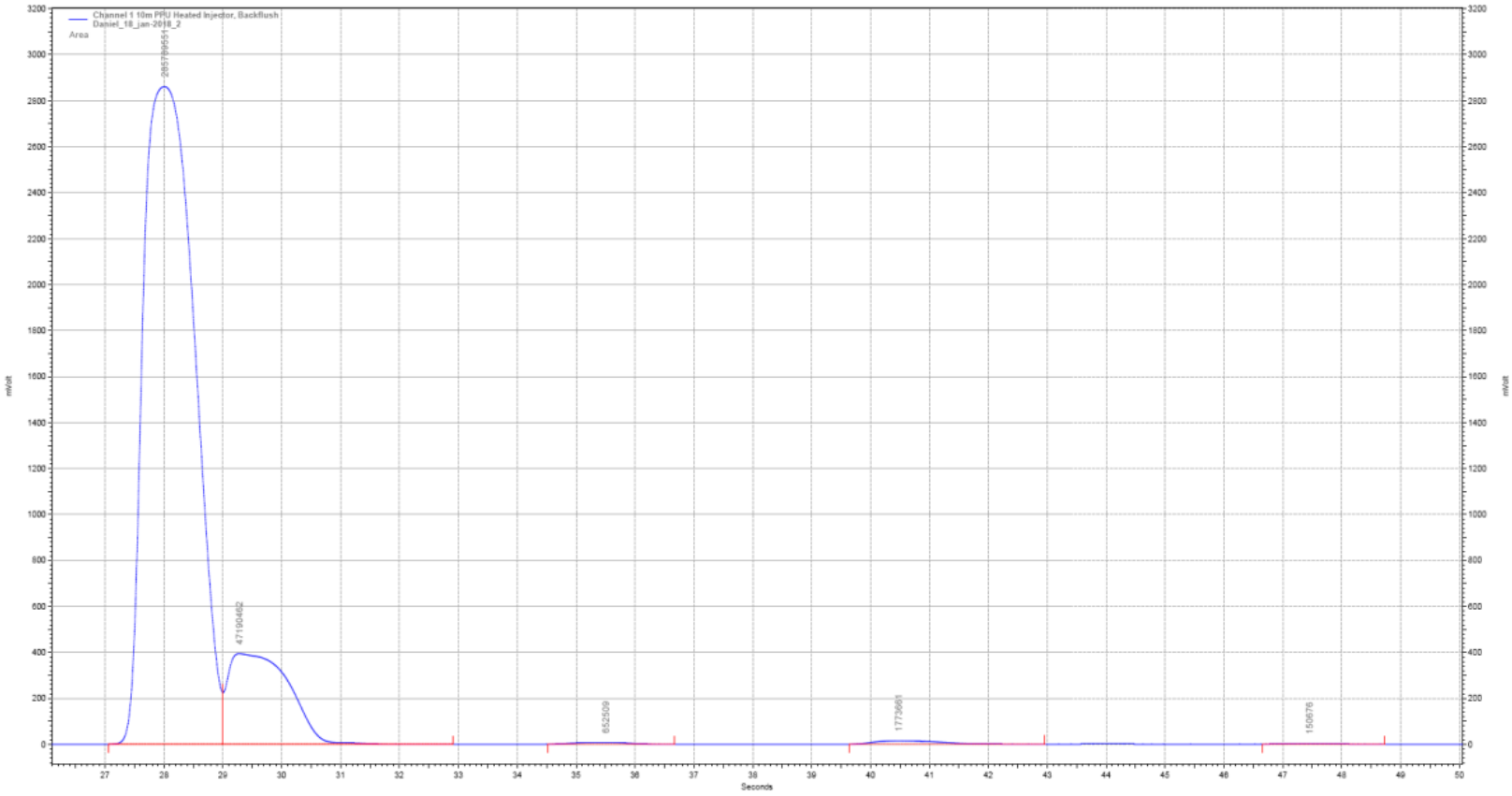

Figure 10-15: Column 1 results for 100% fish oil

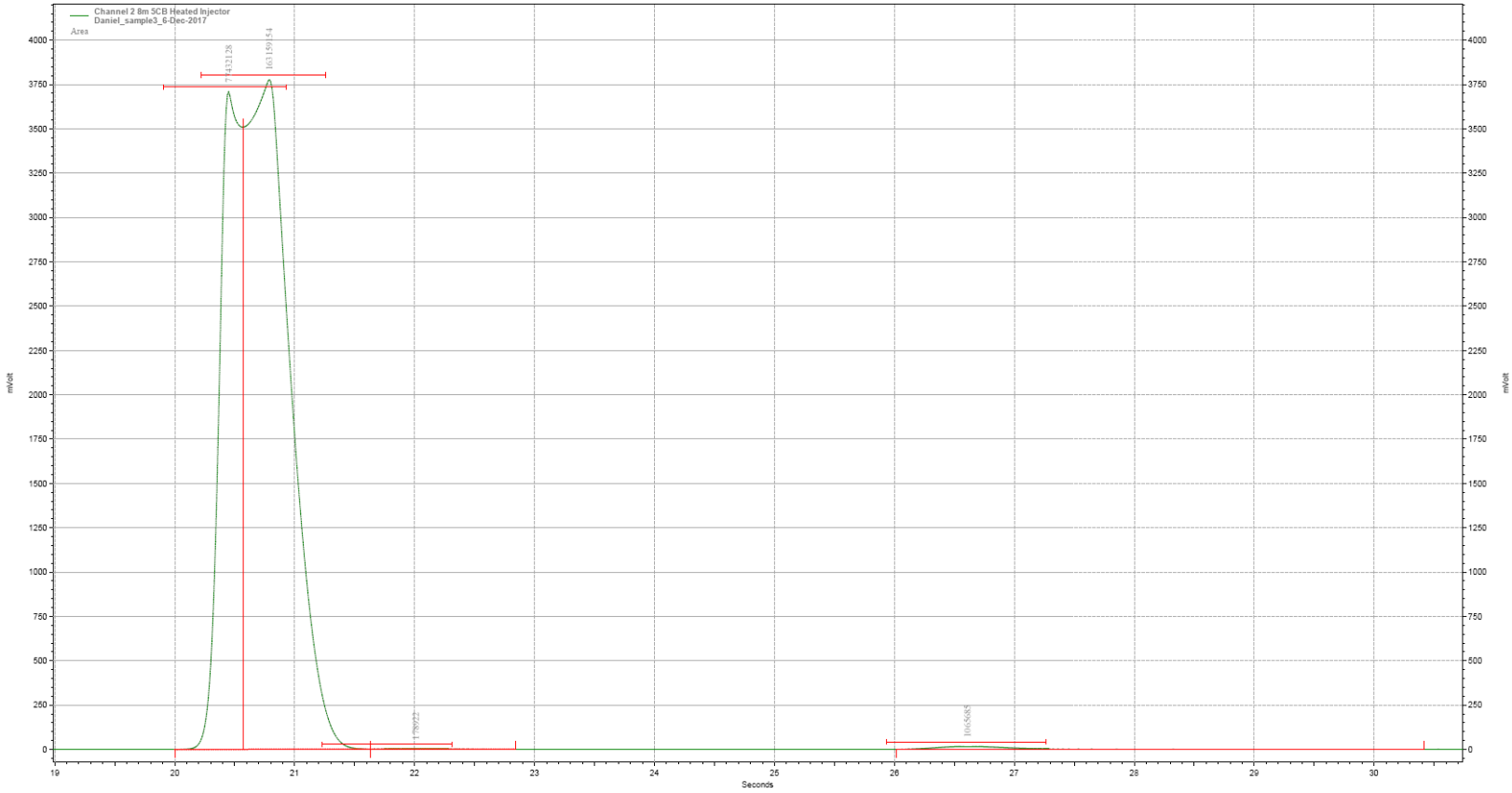

Figure 10-16: Column 2 results for diesel fuel

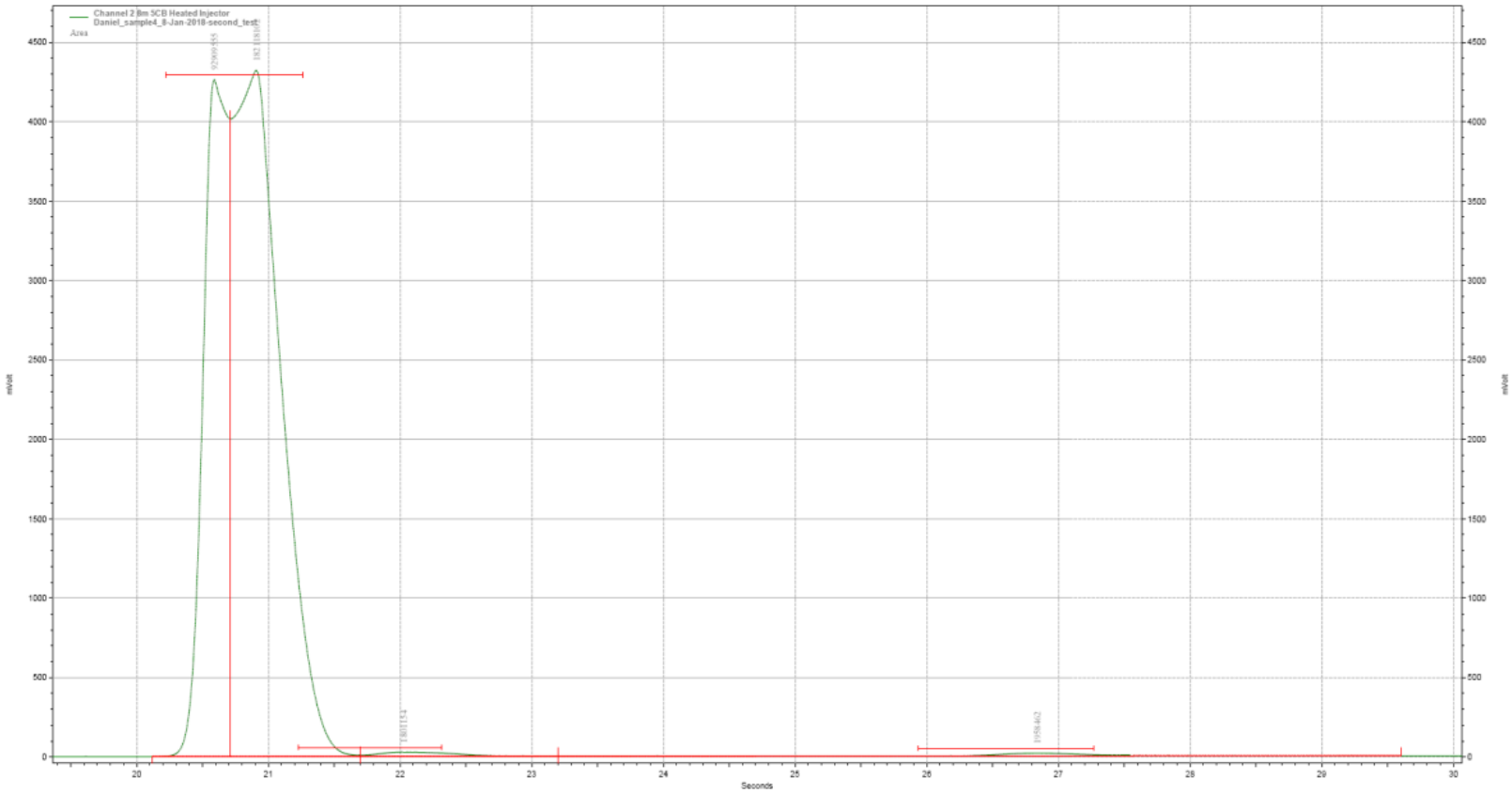

Figure 10-17: Column 2 results for R-UELO

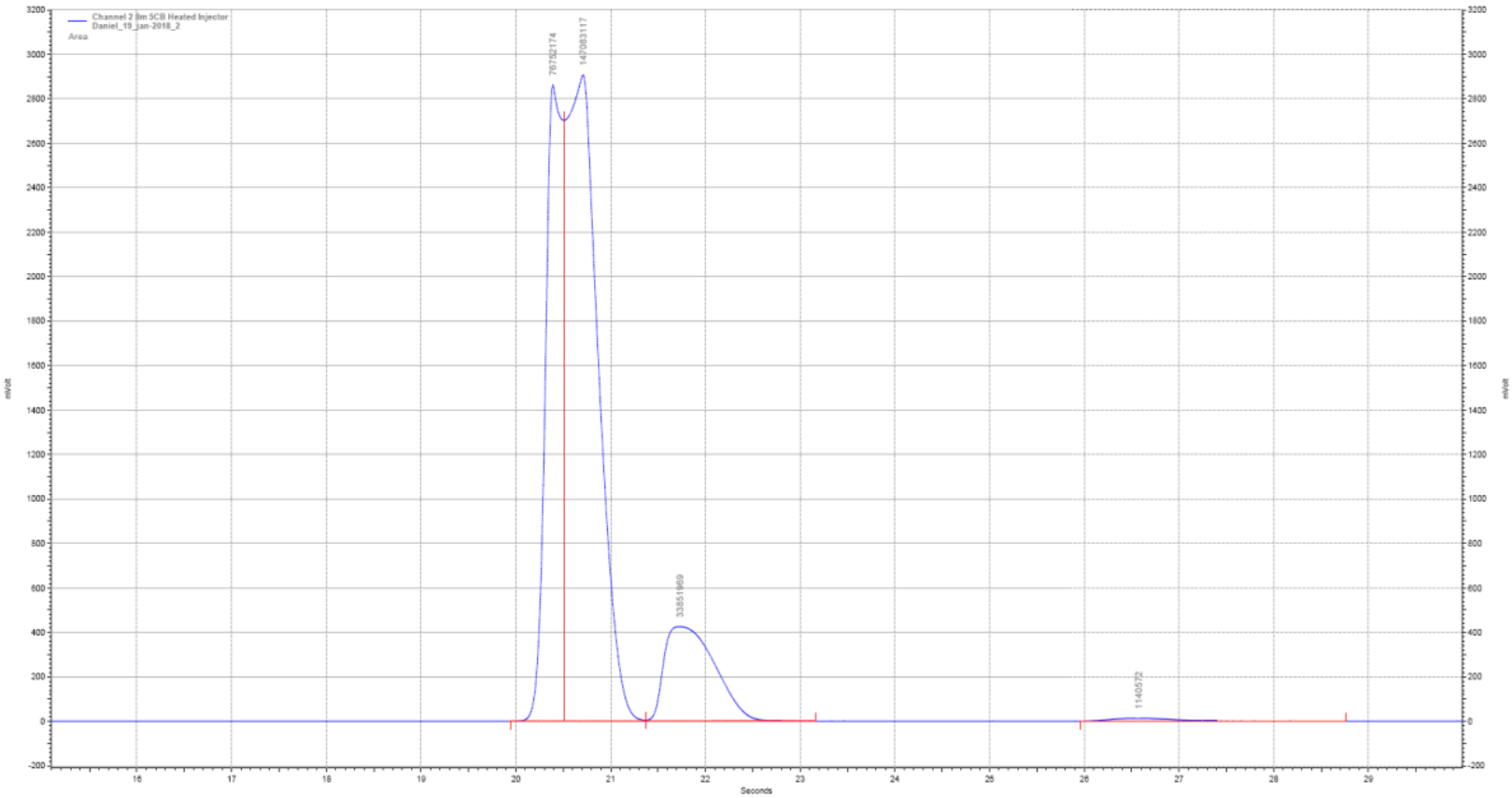

Figure 10-18: Column 2 results for 50/50% R-UELO/fish oil blend

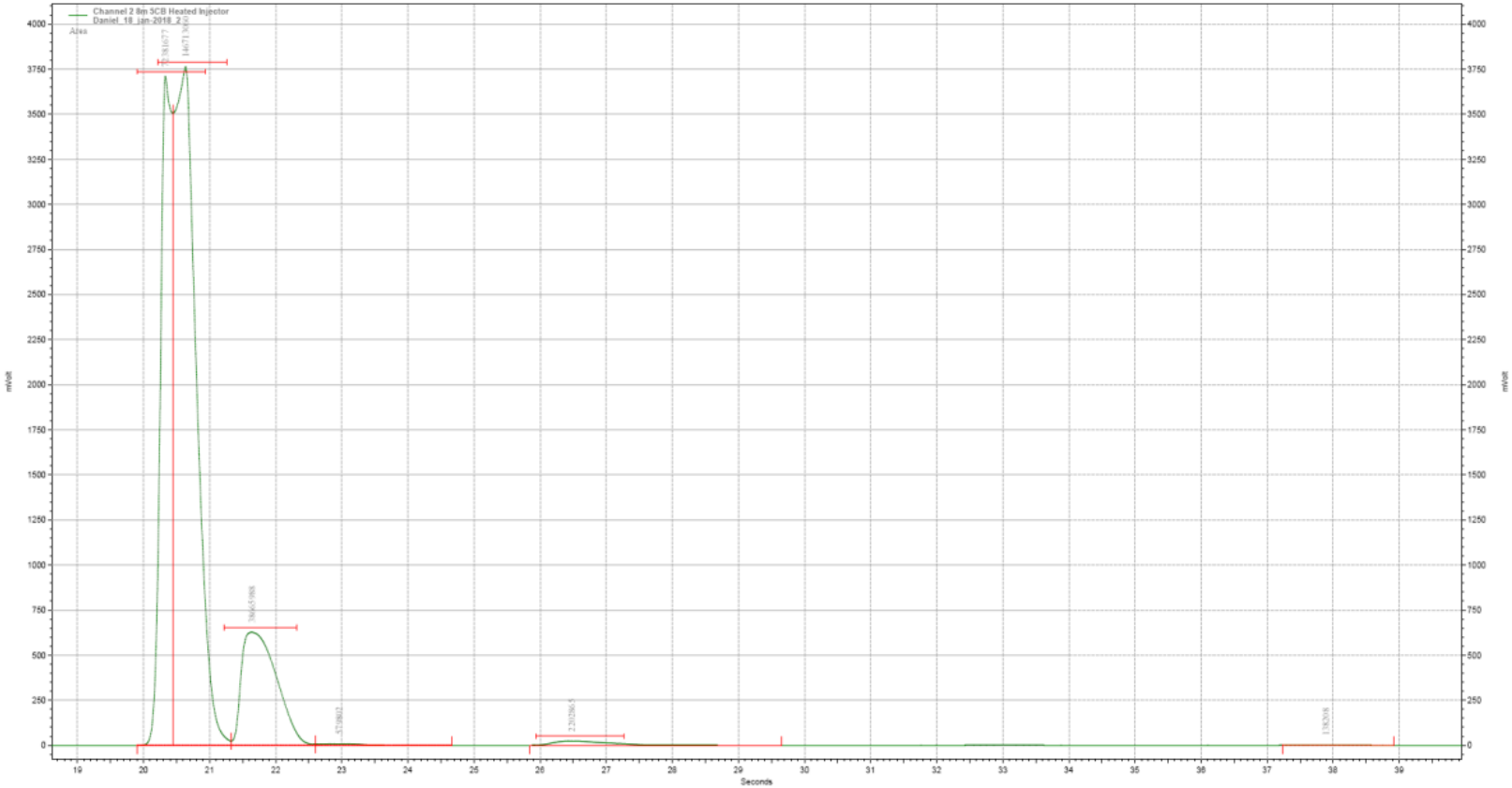

Figure 10-19: Column 2 results for 100% fish oil